Università degli Studi di Padova
Dipartimento di Fisica & Astronomia G. Galilei Corso di laurea in Fisica

Tesi di Laurea Magistrale

Spectra of random matrices

Relatore:
Prof. Amos Maritan

Controrelatore:
Prof. Antonio Trovato

Laureando: Silvia Martina
Matricola N: 1061574

Anno Accademico 2016-2017

Contents

Abstract

The recent interest of the scientific community about the properties of networks is based on the possibility to study complex real world systems by renouncing the exact knowledge of the nature of system itself. This approach allows to model the system, for example, as a large collection of agents linked together in pairs to form a network. The networks are very studied in different scientific fields and, particularly, in the ecological one, in order to understand the dynamics of the evolution related to a community composed by different species interacting with each other.
A random matrix can incorporate many information according to the type of the system. By using the graph's theory, it is possible to extrapolate information about the matrix and, therefore, about the system considered.
The statistical features of the eigenvalues of large random matrices have been the focus of wide interest in mathematics and physics[1]. This thesis is mainly focused on the study of the spectral density of sparse random matrices. Symmetric random matrices and non-Hermitian matrices have been considered in this work, paying attention to both the analytical and numerical approach of the eigenvalues distribution calculation.
There are different mathematical methods used to analyze ensembles of random matrices with a particular underlying symmetry. It is well-known that the spectral density of random matrices ensembles will converge, as the matrix dimension grows, to a precise limit. One example is Girko elliptic law [2].
The introduction of the sparsity is one of the factors that complicate enormously the mathematical analysis and new techniques for the calculation of the spectral density are welcome. The cavity method is a new approach presented to extend our knowledge about large-scale statistical behavior of eigenvalues of random sparse Hermitian and non-Hermitian matrices. Therefore, the cavity method provides a specific analysis related to the study about how the modularity structure influences the stability in the ecological communities.

Abstract

Il recente interesse della comunità scientifica riguardo le proprietà dei networks è basato sulla possibilità di studiare sistemi complessi del mondo reale rinunciando all'esatta conoscenza della natura del sistema stesso. Questo approccio permette di modellizzare il sistema, per esempio, come una grande collezioni di agenti connessi in coppie per formare un network. I networks sono molto studiati in differenti campi scientifici e ,particolarmente, in quello ecologico, per capire the dinamiche di evoluzione relative ad una comunità composta da specie differenti che interagiscono tra di loro.
Una matrice random può incorporare molte informazioni a seconda del tipo di sistema. Attraverso l'uso della teoria dei grafi, è possibile estrapolare infomazioni sulla matrice e quindi sul sistema considerato.
Le caratteristiche statistiche degli autovalori di grandi matrici random sono state il centro di un ampio interesse in matematica e fisica [1]. Questa tesi è principalmente focalizzata sullo studio della densità spettrale di matrici random sparse. Matrici random simmetriche e non-Hermitiane sono state considerate in questo lavoro, ponendo l'attenzione sia sull'approccio analitico sia su quello numerico del calcolo della distribuzione degli autovalori.
Ci sono differenti metodi matematici usati per analizzare ensembles di matrici random con una particolare simmetria sottostante. E' ben noto che la densità spettrale di ensembles di matrici random convergerà, quando la dimensione della matrice cresce, ad un limite preciso. Un esempio è la legge ellittica di Girko [2].
L'introduzione della sparsità è uno dei fattori che complica enormemente l'analisi matematica e nuove tecniche per il calcolo della densità spettrale sono accolte.
Il metodo di cavità è un nuovo approccio presentato per estendere la nostra conoscenza riguardo il comportamento statistico su larga scala degli autovalori di matrici random sparse Hermitiane e non-Hermitiane.
Inoltre, il metodo di cavità fornisce un'analisi specifica relativa allo studio riguardo a come la struttura modulare influenza la stabilità nelle comunità ecologiche.

Chapter 1

Introduction

In 1972 May proved that sufficiently large ecological network, resting at a feasible equilibrium point, have a probability of persisting close to zero: arbitrarily small perturbations of the population densities would drive the system away from equilibrium [3] [4]. The study of May has been focused on the network in which species interact at random [3] [4][5]. The tools of Random Matrix Theory (RMT) [6] [7] has been exploited to extend the May's work to more complex cases in which particular features of natural system would violate May's simple assumptions and how these violations would translate into stabilizing or destabilizing mechanism.
The birth of the modern RMT is due to the work of Eugene Wigner in physics [8] and the mathematical area has grown strongly over the last fifty years. The reason of the wide interest, within the scientific communities, about this field is the applicability of RMT to many different real systems. For example, the biological systems are typically very large and inherently complex : the basic parameters used to describe parts of the cells and its mechanism, individuals and populations in ecosystem are all affected by environmental and demographic stochasticity and the variations across space and time.
Therefore the RMT is ideally suited to study the fundamental behavior of large biological system with network structure. In particular an important open question is to understand how the topological structure of a network influences its stability and in general which mechanisms define the stability and the instability of an ecological system.
The concept of local asymptotic stability, developed inside the modeling of ecological communities as a continuous-time dynamical system, is described by a set of autonomous (i.e. which do not explicitly contain the time variable) ordinary differential equations for each density of population $X_i(t)$. Each equation about the time evolution of $X_i(t)$ is related to the growth rate of a population of the entire ecological community:

$$\frac{dX_i(t)}{dt} = f_i(\mathbf{X}(t)) \tag{1.1}$$

where the vector $\mathbf{X}(t)$ is the vector of all population densities and f_i is a function relating the growth rate of population i to the density of the S populations.
The system is at equilibrium point if:

$$\frac{dX_i(t)}{dt}\Big|_{\mathbf{X}^*} = f_i(\mathbf{X}^*) = 0 \tag{1.2}$$

for all i. In this condition the system will remain at equilibrium until it is not perturbed. The equilibrium is said to be stable if all infinitesimal perturbations are dampened and locally

unstable if there is an infinitesimal perturbation after which the system never goes back to the equilibrium. The analysis of the stability is performed by linearization of the system at equilibrium point. For this scope, the Jacobian matrix J is introduced. It is associated to each system whose elements J_{ij} are defined as:

$$J_{ij}(\mathbf{X}) = \frac{\partial f_i(\mathbf{X}(t))}{\partial X_j} \tag{1.3}$$

and evaluating these at the equilibrium point, the so-called *community matrix* M is obtained [5], defined as:

$$M_{ij} = J_{ij}\Big|_{\mathbf{X}^*} = \frac{\partial f_i}{\partial x_j}(\mathbf{X}(t))\Big|_{\mathbf{X}^*}. \tag{1.4}$$

The entry M_{ij} is a measure of how a slight increase in the population j influences the growth rate of the population i. The eigenvalues of M give information about the stability of the underlying equilibrium point: if all eigenvalues have negative real parts then the equilibrium is stable, while if some eigenvalues has positive real part, the equilibrium is unstable, because in the directions of the corresponding eigenvectors the system is driven away from the equilibrium.
Because this analysis is based on linearization, the results hold only locally and it is not saying about global stability. Another limit is that the stability does not necessary imply lack of persistence: population could coexist thanks to limit cycles or chaotic attractors, which typically are originated from unstable equilibrium points.
To establish if a system is stable or not, it is enough to find the real part of the *rightmost* eigenvalue(s) (which will be denoted as $\Re(\lambda_1)$). In order to follow this approach it is necessary to know exactly the functions $f_i(\mathbf{X}(t))$ as well as to calculate precisely the equilibrium $\mathbf{X}^*$. This means that any different set of equations, and each equilibrium state of the same system would lead to a different community matrix.
The May's insight was to consider directly the community matrix, modeled as a large random matrix and to attempt estimating the real part of its rightmost eigenvalue based on the characteristics of the random matrix.
In his study, May did not specify the details of the distribution but only its mean and its variance. This choice becomes exact in the large S limit as these are the only important quantities needed to have information about eigenvalues distribution [9]. This propriety is known as *universality*.
May set all the diagonal elements $M_{ii} = -1$, the off-diagonal elements equal to 0 with probability $1 - C$ and he drew them independently from a distribution with mean 0 and variance σ^2, with probability C. For such matrices, May established that the eigenvalues all have negative real parts with very high probability whenever:

$$\sigma\sqrt{SC} < 1 \tag{1.5}$$

and the equilibrium is stable (unstable) with high probability when the inequality is met (is not met). If the diagonal elements are fixed at $-d < 0$ (necessary condition for a species to be self-regulating) the inequality has d on the right-hand side.
The "stability criterion" has been also derived for famous type of ensembles using RMT [10]. One of the most studied cases in this context is the "circular law". This law considers a S X S matrix $\mathbf{M}$, whose entries are independent and identically distributed random variables with mean zero e variance one. Then, the empirical spectral distribution of $\mathbf{M}/\sqrt{S}$ converges

to the uniform distribution on the unit disk as $S \to \infty$. Hence, for sufficiently large S, all the eigenvalues of $\mathbf{M}$ are approximately uniformly distributed in the disk in the complex plane centered at (0,0) and with radius $\sqrt{S}$, so that $\Re(\lambda_1) \approx \sqrt{S}$.
In order to derive the May's result the assumptions of the circular law have been relaxed. When the variance is different from one the only effect is the re-scaling for the radius of the disk: it is multiplied by an additional factor of $\sqrt{\sigma^2}$ compared to the unit variance case. The introduction of a probability (C) of having entries different from zero changes the radius with other additional factor equal to $\sqrt{C}$. Finally, subtracting a constant from the diagonal elements, the shape of the distribution of the eigenvalues does not change but its position is shifted horizontally (the center of the disk is moved to value $-d$).
These considerations are sufficient to recover May's result, imposing that for stability it is necessary to have negative real part $\Re(\lambda_1) < 0$.
In natural systems it is not expected that the positive effects of the resource on the consumers exactly offset the negative effects of consumers on resources. Then it is appropriate to consider a nonzero mean for the off-diagonal entries. In this case it is expected that one eigenvalue corresponds to the expectation of the row sum, i.e.

$$\mathbb{E}\Big[\sum_j M_{ij}\Big] = -d + (S-1)\mathbb{E}[M_{ij}] = -d + (S-1)E \tag{1.6}$$

where $E = C\mu$ (μ is the mean of the distribution from which the off-diagonal coefficient has sampled with probability C).
The other $S-1$ eigenvalues are still closely approximated by a uniform distribution on a disk. The center of the disk is given by the mean of the other $S-1$ eigenvalues and is equal to $-(d+E)$. To estimate its radius it has been calculated the variance of the off-diagonal elements of $\mathbf{M}$, which is:

$$V = \mathrm{Var}[M_{ij}] = \mathbb{E}[M_{ij}^2] - E^2 = C(\sigma^2 + \mu^2) - C^2\mu^2 = C(\sigma^2 + (1-C)\mu^2). \tag{1.7}$$

The radius is estimated $\sqrt{SV}$.
To consider all possible scenarios, one can write a criterion for stability that takes into account both the eigenvalues corresponding to the row sum and the rightmost eigenvalue on the disk. It is the following:

$$\max\{\sqrt{SV} - E, (S-1)E\} < d. \tag{1.8}$$

However, in ecological network pairs of species have well-defined interactions such as predator-prey, mutualistic and competitive. In these cases M_{ij} is not independent from M_{ji}. To express this dependence, it is a good idea to sample directly the coefficients in pairs from a bivariate distribution.
The elliptic law is the result obtained by this generalization of the circular law and its statement is as follows. Take a S X S matrix $\mathbf{M}$, whose off-diagonal coefficients are independently sampled in pairs from a bivariate distribution with zero marginal means, unit marginal variances and correlation ρ (i.e. $\rho = \mathbb{E}[M_{ij}M_{ji}]$). Then, as $S \to \infty$, the eigenvalue distribution of $\mathbf{M}/\sqrt{S}$ converges to the uniform distribution on an ellipse centered at (0,0) with horizontal semi-axis of length $1+\rho$ and vertical semi-axis of length $1-\rho$. This law shows an useful analogy with two-dimensional classical electrostatics.
Just as for the circular law, the elliptic law can be extended to the same more general cases. Following the same strategy illustrated above about the relevant statistic for the off-diagonal

coefficients, it has been found that the ellipse is centered at $-d-E$, and has horizontal semi-axis $\sqrt{SV}(1+\rho)$. The variance is the same as the previous case. The correlation ρ is related to the parameter of the bivariate distribution of mean $\boldsymbol{\mu}$ and covariance matrix $\boldsymbol{\Sigma}$:

$$\boldsymbol{\mu} = \begin{bmatrix} \mu \\ \mu \end{bmatrix}, \quad \boldsymbol{\Sigma} = \begin{bmatrix} \sigma^2 & \tilde{\rho}\sigma^2 \\ \tilde{\rho}\sigma^2 & \sigma^2 \end{bmatrix}$$

by the relation:

$$\rho = \frac{\mathbb{E}[M_{ij}M_{ji}] - \mathbb{E}^2[M_{ij}]}{\mathrm{Var}[M_{ij}]} = \frac{\tilde{\rho}\sigma^2 + (1-C)\mu^2}{\sigma^2 + (1-C)\mu^2}. \tag{1.9}$$

Finally, the criterion for stability becomes [11]:

$$\max\{\sqrt{SV}(1+\rho) - E, (S-1)E\} < d. \tag{1.10}$$

In the ecological field, one of the most important issue is to understand how the distribution of $\mathbf{X}^*$ affects the stability for different type of community matrix. In fact the particular shape of the distribution of species abundances influences the location of rightmost eigenvalue. The previous studied models correspond to the most famous and simple types of ecological system modeling the equilibrium point. In general, the community matrix $\mathbf{M}$ has particular features according to the model used to describe the evolution of the species. The elliptic law fails to predict the location of the leading eigenvalue in more realistic cases. One of these concerns the species that can be divided into subsets such that within-subset connections are much more frequent than between-subset connections. This partition subdivides the entire community in "modules". The presence of modules must leave a mark in the eigenvalue distribution.
A considerable contribution to extend the elliptic law to the case of very sparse (the matrix has many entries equal to zero) and structured matrix is provided by the cavity method. It is a valid support to study eigenvalues distribution analytically and in some particular case permits to obtain information about how the stability is influenced by the parameters used to build the random structured matrix.
The plain of the thesis is the following. In the first chapter of this thesis it is introduced the mathematical tools and the numerical simulations developed to explain how the cavity approach is used to obtain the spectral density of sparse symmetric random matrices [12]. The set of recursive equations, which characterize the cavity method, has been solved numerically employing a simple iterative approach known as belief propagation.
The second one extends the cavity method to the more complex case of sparse non-Hermitian random matrices [13] and the approach has been verified through a numerical analysis for some types of ensemble.
In the last chapter an application to the ecological community is shown. In particular a quaternionic parameterization of the cavity method has been used. It allows to analyze analytically the effect of a structured matrix, with two subsystems of the same size, on the stability. The results are in good agreement with the numerical simulations and underline that a given structure is stabilizing or destabilizing according to the specific conditions.

Chapter 2

Spectral density of sparse symmetric random matrices

2.1 Introduction

One of the most well-studied ensemble is the Gaussian ensemble of real symmetric matrices. In this case the average spectral density of the eigenvalues is given by the Wigner semicircle law [1][14][15].
In this chapter it is explained how it is possible to derive the spectral density of sparse symmetric random matrices by comparing it with interacting particles in statistical mechanics. In this analogy, the number of particles is equal to the size of the considered matrix. Each particle is located on one of the nodes of a weighted graph and they are connected according to the coefficients of the matrix. Associated to the particles are stochastic variables which can be interpreted as the non-deterministic effect of the interaction of a single particle with the others. Following this approach the spectral density can be written as the sum of the variances imaginary part of the relative distributions.
The cavity methods final result is a set of equations that can be interpreted as a belief-propagation algorithm on single instances. This algorithm can then be easily implemented. In this work has been demonstrated under the fully-connected limit that the method gives an exact result when the size of the graph goes to infinity and the average connectance tends to the size of the matrices.

2.2 Cavity approach to the spectral density

It has been considered an ensemble $\mathcal{M}$ of $N \times N$ symmetric matrices. Every matrix has a set of eigenvalues noted as $\{\lambda_i^A\}_{i=1,\dots,N}$. The empirical spectral density is defined as:

$$\rho_A(\lambda) = \frac{1}{N}\sum_{i=1}^{N}\delta(\lambda - \lambda_i^A) \tag{2.1}$$

where δ is a Dirac delta. For Hermitian matrices, the spectral density represents a probability measure over the real plane. However, if the eigenvalues of A are confined to a certain subset then it can be treated as a measure on that subset.
Since A is extracted by some random matrices ensemble, the empirical spectral density is a random probability measure. The objective of this analysis is to totally characterize the

empirical spectral densities of random matrices from the ensemble, particularly in the limit $N \to \infty$.
For some ensembles, the answer is well-known. For a real symmetric $N \times N$ matrix A, its spectral density can be modified with the following technique as was shown by Edwards and Jones[15].
If to λ is added a small negative immaginary part $-i\epsilon$, then the Sokhotsky-Plemelj theorem can be used to write the following expression:

$$\lim_{\epsilon \to 0^+} \frac{1}{\lambda - \lambda_i^A - i\epsilon} = \mathcal{P}\Big(\frac{1}{\lambda - \lambda_i^A}\Big) + i\pi\delta(\lambda - \lambda_i^A) \tag{2.2}$$

where $\mathcal{P}$ detones the Cauchy principal value. This leads to:

$$\rho_A(\lambda) = \lim_{\epsilon \to 0^+} \frac{1}{\pi N} \sum_{i=1}^{N} \mathrm{Im}(\lambda - \lambda_i^A - i\epsilon)^{-1} = \lim_{\epsilon \to 0^+} \frac{1}{\pi N} \mathrm{Im}\mathrm{Tr}\Big(\frac{1}{(\lambda - i\epsilon)\mathbf{1} - A}\Big). \tag{2.3}$$

Considering that:

$$\det((\lambda - i\epsilon)\mathbf{1} - A) = \prod_{k=i}^{N} (\lambda - i\epsilon - \lambda_i^A) \tag{2.4}$$

and:

$$\frac{\partial}{\partial\lambda}[\ln\det((\lambda - i\epsilon)\mathbf{1} - A)] = \sum_{i=1}^{N} \frac{1}{\lambda - i\epsilon - \lambda_i^A} = \mathrm{Tr}\Big(\frac{1}{(\lambda - i\epsilon)\mathbf{1} - A}\Big) \tag{2.5}$$

finally can be obtained:

$$\rho_A(\lambda) = \lim_{\epsilon \to 0^+} \frac{1}{\pi N} \mathrm{Im}\frac{\partial}{\partial\lambda}[\ln\det((\lambda - i\epsilon)\mathbf{1} - A)] = \lim_{\epsilon \to 0^+} \frac{-2}{\pi N} \mathrm{Im}\frac{\partial}{\partial\lambda}[\ln\det{}^{-\frac{1}{2}}((\lambda - i\epsilon)\mathbf{1} - A)] \tag{2.6}$$

Defining $z = \lambda - i\epsilon$, the determinant of a symmetric matrix may be represented by multiple Fresnel integral:

$$\det{}^{-\frac{1}{2}}(z\mathbf{1} - A) = \left(\frac{e^{i\frac{\pi}{4}}}{\pi^{\frac{1}{2}}}\right)^N \int_{-\infty}^{+\infty} \prod dx_i \exp\Big(-i \sum_{i,j=1}^{N} x_i (z\mathbf{1} - A)_{ij} x_j\Big) \tag{2.7}$$

Details of the proof of this relation can be found in Appendix A.

By making a variable substitution we get rid of the imaginary unit. In the general case this type of integrals do not converge. In order to ensure convergence, the interval of integration can be written as $[-a \cdot \infty, +a \cdot \infty]$, where $a^2 = i$ and z has a negative imaginary part. This choice of the boundary is crucial to obtain the non-compact symmetry group for localization, but it is not important for the density of the states.
Fortunately, with this substitution of the integration interval a partition function in z emerges:

$$\mathcal{Z}_A(z) = \int \prod_{i=1}^{N} \frac{dx_i}{\sqrt{2\pi}} \exp\Big(-\frac{1}{2} \sum_{i,j=1}^{N} x_i (z\mathbf{1} - A)_{ij} x_j\Big) \tag{2.8}$$

It can then be introduced a Gibbs-Boltzmann probability distribution of $\boldsymbol{x}$:

$$P_A(\boldsymbol{x}) = \frac{1}{\mathcal{Z}_A(z)} e^{-\mathcal{H}_A(\boldsymbol{x},z)} \tag{2.9}$$

with:

$$\mathcal{H}_A(\boldsymbol{x},z) = \frac{1}{2} \sum_{(i,j)\in\mathcal{G}_A}^{N} x_i (z\mathbf{1} - A)_{ij} x_j \tag{2.10}$$

2.3 The technique

The issue to obtain the spectral density $\rho_A(\lambda)$ is converted into a statistical mechanics problem of N interacting particles $\boldsymbol{x}$=(x_1,...,x_N) on a graph $\mathcal{G}_A$ with effective Hamiltonian 2.10.
As the size of the graph grow, the cavity method seeks to exploit the topological structure of the underlying network in order to extract some statistical information to quantify aspects of its structure. This approach allows to rewrite the spectral density as follows:

$$\rho_A(\lambda) = -\lim_{\epsilon\to 0^+} \frac{2}{\pi N} \mathrm{Im}\left(\frac{\mathcal{Z}'_A(z)}{\mathcal{Z}_A(z)}\right)_{z=\lambda-i\epsilon} = \lim_{\epsilon\to 0^+} \frac{1}{\pi N} \sum_{i=1}^{N} \mathrm{Im}[< x_i^2 >_z]_{z=\lambda-i\epsilon} \tag{2.11}$$

where $< ... >_z$ denotes the average over distribution 2.9. As shown in 2.11, the understanding of the spectral density of random matrices can be extended by considering the local marginals $P_i(x_i)$ from Gibbs-Boltzmann distribution $P_A(\boldsymbol{x})$ instead of considering the averaged spectral density $\rho_A(\lambda)$. The marginal distribution of x_i is the probability distribution $P_A(\boldsymbol{x})$ integrated over the other N-1 variables.
In this vision the dynamical variables reside on the vertices of a graph and interact in pairs according to the edges of the graph. For any pairs of particles the weight of interaction is defined by A_{ij} when $A_{ij} \neq 0$.
The cavity method offers a way to calculate $P_i(x_i)$.

The cavity method

It has been considered in a general way a vector of spins $\boldsymbol{\sigma}$, which represents the dynamical variables associated to the particles in the vertices of a graph $\mathcal{G}_A = (V, E)$. The Joint Probability Density Function (JPDF) P($\boldsymbol{\sigma}$) can be factorized into terms $\{\psi_{ij}\}$, which are associated to the edges of $\mathcal{G}_A$, and $\{\phi_i\}$, associated to the vertices of the graph. The JPDF is then supposed to be of the form:

$$P(\boldsymbol{\sigma}) = \frac{1}{\mathcal{Z}} \prod_{(i,j)\in E} \psi_{ij}(\sigma_i, \sigma_j) \prod_{i\in V} \phi_i(\sigma_i), \tag{2.12}$$

where the state of each node i is denoted by σ_i.

From this original system it is possible to consider a system where the node i is removed. To do so, we then define $G^{(i)} = (V^{(i)}, E^{(i)})$ the subgraph of $\mathcal{G}_A$ obtained by the removal of vertex i, the so-called cavity graph (Fig. 2.1).

The JPDF of spins on this cavity graph is given by:

$$P^{(i)}(\boldsymbol{\sigma}^{(i)}) = \frac{1}{\mathcal{Z}^{(i)}} \prod_{(j,k)\in E^{(i)}} \psi_{jk}(\sigma_j, \sigma_k) \prod_{j\in V^{(i)}} \phi_j(\sigma_j) \tag{2.13}$$

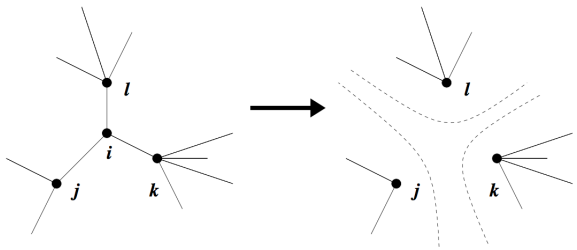

Figure 2.1: Part of a treelike graph $\mathcal{G}_A$ showing the neighborhood of node i. After the removal of this node, the resulting graph $\mathcal{G}_A^{(i)}$ is composed by three indipendent branches headed by sites j,k and l.

where $\boldsymbol{\sigma}^{(i)}$ is the spin vector with the i^{th} component removed.
The single-spin marginals are obtained by integrating on the variables which occupy the neighbouring vertices of i. For this reason, with $P_{\partial i}^{(i)}(\boldsymbol{\sigma}_{\partial i})$ we indicate the joint probability marginal distribution of spins on the cavity graph whose vertices are described above.
In this way, we obtain:

$$P_i(\sigma_i) = \frac{1}{\mathcal{Z}_i} \int \Big[\prod_{j\in\partial i} d\sigma_j\Big] P_{\partial i}^{(i)}(\boldsymbol{\sigma}_{\partial i})\Big(\phi_i(\sigma_i) \prod_{j\in\partial i} \psi_{ij}(\sigma_i,\sigma_j)\Big), \tag{2.14}$$

where $\mathcal{Z}_i = \mathcal{Z}/\mathcal{Z}^{(i)}$.
A common feature of many interesting random graph ensemble is the tree-like structure in the large limit of N. The main idea of the cavity approach is to exploit this underlying framework in order to approximately compute the distributions $P_{\partial i}^{(i)}(\boldsymbol{\sigma}_{\partial i})$ and therefore, give an approximation to the true marginal distribution at any given vertex.

At this point, it has been calculated $P_i^{(j)}(\sigma_i)$ of the spin at the vertex i in the graph $G^{(j)}$ for some $i \in V$ and $j \in \partial i$. Removing the vertex j from equation 2.14, we obtain:

$$P_i^{(j)}(\sigma_i) = \frac{1}{\mathcal{Z}_i^{(j)}} \int \Big[\prod_{l\in\partial i/\ j} d\sigma_l\Big] P_{\partial i/\ j}^{(i)(j)}(\boldsymbol{\sigma}_{\partial i/\ j})\Big(\phi_i(\sigma_i) \prod_{l\in\partial i/\ j} \psi_{il}(\sigma_i,\sigma_l)\Big), \tag{2.15}$$

where $\mathcal{Z}_i^{(j)} = \mathcal{Z}^{(i)}/\mathcal{Z}^{(i)(j)}$. Assuming that $\mathcal{G}_A$ is a tree, the removal of a vertex in the graph consequently makes each vertex in $\partial i/\ j$ to belong to a different connected component of the cavity graph $G^{(i)}$. It is possible, therefore, to conclude that:

$$P_{\partial i/\ j}^{(i)(j)}(\boldsymbol{\sigma}_{\partial i/\ j}) = \prod_{l\in\partial i/\ j} P_l^{(i)}(\sigma_l) \tag{2.16}$$

and, thus, 2.15 has been semplified significantly to:

$$P_i^{(j)}(\sigma_i) = \frac{1}{\mathcal{Z}_i^{(j)}} \phi_i(\sigma_i) \prod_{l\in\partial i/\ j} \Big(\int d\sigma_l P_l^{(i)}(\sigma_l)\psi_{il}(\sigma_i,\sigma_l)\Big) \tag{2.17}$$

in the same way, 2.14 becomes:

$$P_i(\sigma_i) = \frac{1}{\mathcal{Z}_i} \phi_i(\sigma_i) \prod_{j\in\partial i} \Big(\int d\sigma_j P_j^{(i)}(\sigma_j)\psi_{ij}(\sigma_i,\sigma_j)\Big). \tag{2.18}$$

So we have $2|E|$ equations in 2.17 for a system on a graph $\mathcal{G}_A = (E, V)$, which represent a set of self-consistent relations for cavity distributions $\{P_i^{(j)}\}$. The solution of these equations can potentially be very difficult and depends on the possibility to parameterize the cavity distributions with a finite set of parameters.
In principle, the cavity approach can be applied for any graph, tree or not, but the degree of approximation and the time of convergence strongly depend on the type of ensemble. In particular, the solution is influenced by the degree of interactions of the spins in the cavity graph and by how their presences affect the marginal distributions at a given vertex.
Once the system is solved, the marginal distributions may be calculated using 2.18.
It is well-known the validity of the method for large random graphs drawn from a tree-like ensemble (in which short loop are rare). In the next section it will be shown a similar case for an ensemble of symmetric locally treelike sparse matrices.

2.4 Treelike symmetric matrices

In the case of symmetric locally treelike sparse matrices the cavity distributions are easy to derive, which is not generally true. Therefore, for this kind of system the set of cavity equations to be solved $\{P_i^{(j)}\}$ can be written as:

$$P_i^{(j)}(x_i) = \frac{e^{-zx_i^2/2}}{\mathcal{Z}_i^{(j)}} \int d\boldsymbol{x}_{\partial i/\ j} \exp\left(x_i \sum_{l \in \partial i/\ j} A_{il} x_l\right) \prod_{l \in \partial i/\ j} P_l^{(i)}(x_l) \tag{2.19}$$

for all i=1,...,N and for all $j \in \partial i$. Once the cavity distributions are known, the marginal distributions $P_i(x_i)$ of the original system $\mathcal{G}_A$ are given by:

$$P_i(x_i) = \frac{e^{-zx_i^2/2}}{\mathcal{Z}_i} \int d\boldsymbol{x}_{\partial i} \exp\left(x_i \sum_{l \in \partial i} A_{il} x_l\right) \prod_{l \in \partial i} P_l^{(i)}(x_l) \tag{2.20}$$

for all i=1,...,N. The set of equations [**?**] is self-consistently solved by assuming to have a Gaussian cavity distribution written as follow:

$$P_l^{(i)}(x) = \frac{1}{\sqrt{2\pi\Delta_l^{(i)}}} e^{-(1/2\Delta_l^{(i)})x^2} \tag{2.21}$$

Replacing this form into the set, the system of the associated cavity variances $\Delta_j^{(i)}$(z) can be obtained:

$$\Delta_i^{(j)}(z) = \frac{1}{z - \sum_{l \in \partial i/\ j} A_{il}^2 \Delta_l^{(i)}(z)} \tag{2.22}$$

for all i=1,..,N and for all $j \in \partial i$. The derivation of this relation is shown in Appendix B. In the very same way, it can be assumed also a Gaussian behaviour for the marginal distributions $P_i(x_i)$, and their variances Δ_i can be written as a function of the cavity variances [**?**]:

$$\Delta_i(z) = \frac{1}{z - \sum_{l \in \partial i} A_{il}^2 \Delta_l^{(i)}(z)}. \tag{2.23}$$

Finally using 2.11 the spectral density is obtained:

$$\rho_A(\lambda) = \lim_{\epsilon \to 0^+} \frac{1}{\pi N} \sum_{i=1}^{N} \mathrm{Im}[\Delta_i(z)]_{z=\lambda - i\epsilon} \tag{2.24}$$

In the end, the problem of computing an approximation to the spectral density is reduced to solve the system 2.22. To find the solutions the equations must be iterated until convergence is reached. One computational methods used to this purpose is the belief propagation algorithm.

2.5 Numerical result and comparison

In order to solve the large system of cavity equations numerically, it can be used a simple iterative approach, known as belief propagation algorithm. In this context the number $\Delta_i^{(j)}$ is considered as a message sent from vertex i to vertex j. These messages contain the "influence" that one variable exerts on another. The scheme of implementation of belief propagation is as follow: starting with an arbitrary list of initial guesses $\{\Delta_i^{(j)}[1]\}_{i \in V, j \in \partial i}$, one repeatedly applies the update equation:

$$\Delta_i^{(j)}[n] = \left(z - \sum_{l \in \partial i / \ j} \Delta_l^{(i)}[n-1] A_{il}^2 \right)^{-1} \tag{2.25}$$

until the convergence is reached. A fixed point $\{\Delta_i^{(j)}\}_{i \in V, j \in \partial i}$ is obtained, such that:

$$\Delta_i^{(j)} = \Delta_i^{(j)}[n] = \Delta_i^{(j)}[n-1] \tag{2.26}$$

In the case of a treelike graph, the belief propagation algorithm will compute the exact marginal variances in a finite number of steps equal to the diameter of the tree. Choosing a Poissonian graph each entry A_{ij} of the N x N matrix A is drawn from:

$$P(A_{ij}) = \frac{c}{N} \pi(A_{ij}) + (1 - \frac{c}{N}) \delta(A_{ij}) \tag{2.27}$$

where c is the average connectivity, and $\pi(x)$ is the distribution of nonzero edge weights. As a first example we consider the bimodal distribution:

$$\pi(A_{ij}) = \frac{1}{2} \delta(A_{ij} - 1) + \frac{1}{2} \delta(A_{ij} + 1) \tag{2.28}$$

The language used for the implementation of the iterative equations, in this work, is Python. The complete code for the analysis is reported in Appendix D.
IN order to compare the spectral density computed with the method to the one obtained from a direct diagonalization of the matrices, a regularised form of the empirical spectral density has been used. This allows to have Lorentzian peaks instead of Dirac's delta.
Must be noted that an equivalent regularised form for non-hermitian matrices is not possible to obtain through standard operations.

For a fixed $N \times N$ matrix X, the resolvent R is defined by:

$$R(z;X) = (X - z)^{-1} \tag{2.29}$$

The resolvent is a functional and is defined for all complex numbers z outside of the spectrum of X. The Green's function associated to the resolvent is its normalised trace:

$$G(z;X) = \frac{1}{N} Tr R(z;X) \tag{2.30}$$

The Green's function is also related to the spectral density of X by the formula:

$$G(z;X) = \int \frac{1}{\mu - z} \rho(\mu;X)\, d\mu \tag{2.31}$$

This expression is known as Stieltjes trasform of the density ρ. For a Hermitian X, it can be possible to verify the following properties:

1. The Green's function is a closed analytic map on $\mathfrak{C}^+ = \{z : \text{Im } z > 0\}$.

2. The empirical spectral density can be recovered from the Green's function by the inverse Stieltjes transform:

$$\rho_\epsilon(\lambda;X) = \lim_{\epsilon \to 0} \frac{1}{\pi} \text{Im}\, G(\lambda + i\epsilon; X) \tag{2.32}$$

3. Neglecting the limit $\epsilon \to 0$ the equation 2.32 becomes a Chauchy probability density with width parameter ϵ:

$$\begin{aligned} \rho_\epsilon(\lambda;X) &= \frac{1}{\pi} \text{Im}\, G(\lambda + i\epsilon; X) \\ &= \frac{1}{\pi} \int \frac{\epsilon}{\epsilon^2 + (\lambda - \mu)^2} \rho(\mu;X)\, d\mu \end{aligned} \tag{2.33}$$

Using the basic definition 2.1 the empirical spectral density can be written as:

$$\rho_\epsilon(\lambda;X) = \frac{1}{\pi N} \sum_{i=1}^{N} \frac{\epsilon}{\epsilon^2 + |\lambda_i^{(X)} - \lambda|^2}. \tag{2.34}$$

This last equation has been used to have a regularised spectral density to compare with the one obtained from the cavity method. One of the results for the above case is shown in figure 2.2 which illustrate how the increase of the ensemble's matrices number yields the empirical spectral density to be closer to the one obtained by the cavity's method.
The results obtained with this approach are an improvement in respect to the approximation scheme of the spectral density used in the absence of more powerful mathematical tools, as the effective medium approximation (EMA), or the single defect approximation (SDA)[16]-[17].

The Lorentzian peaks width as shown in figure 2.2 is given by the small value of ϵ which is present both in the cavity equations and the analitycal form for the spectral density. These peaks are an approximation of the Dirac's δ which are characteristic of the spectrum of this type of ensembles [18][19].

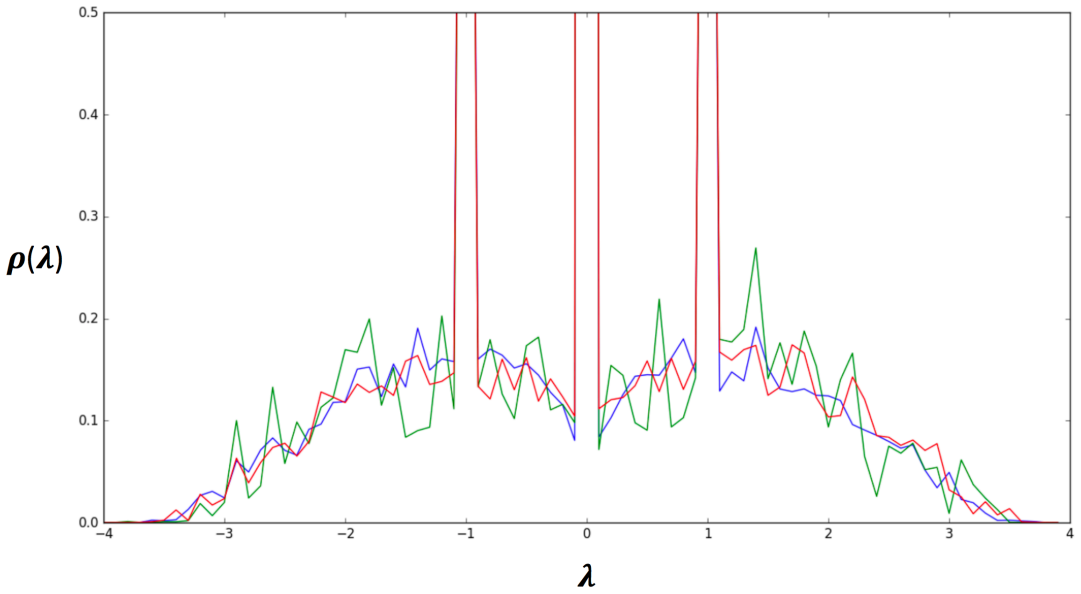

Figure 2.2: Along the horizontal axis the values of λ are placed. In green: the regularised empirical spectral density $\rho_\epsilon(\lambda;\mathrm{A})$ of a Poissonian random graph of size N=100 with c=2 at ϵ=0.005, averaged over 20 samples. In red: same empirical spectral density but averaged over 100 samples. In blue: the result of the spectral density solved by belief propagation, leaving a small value of ϵ in the cavity equations, which implies approximating Dirac 's δ by Lorentzian peaks.

It is evident that the parameter ϵ used to obtain a regularised function for the spectral density is in a close relation with the one used in the cavity method. For a better understanding, the regularised spectral density can be compared with the histogram built with the eigenvalues gotten by direct diagonalization (the same used to obtain ρ_ϵ). The result is shown in fig.2.3 and the figure on the left has been obtained by setting the bins of the histogram equal to ϵ. It is noticeable that the ρ_ϵ^{reg} is a good analitycal function of ρ_ϵ^{bin}, since the deviations are relative to the tallest bins because the height of the peaks is associated to the number of the eigenvalues that fall in a range equal to ϵ and the ϵ itself.

The analisys confirmed the validity of the comparison between the spectral density obtained by the cavity method and the regularised empirical spectral density.

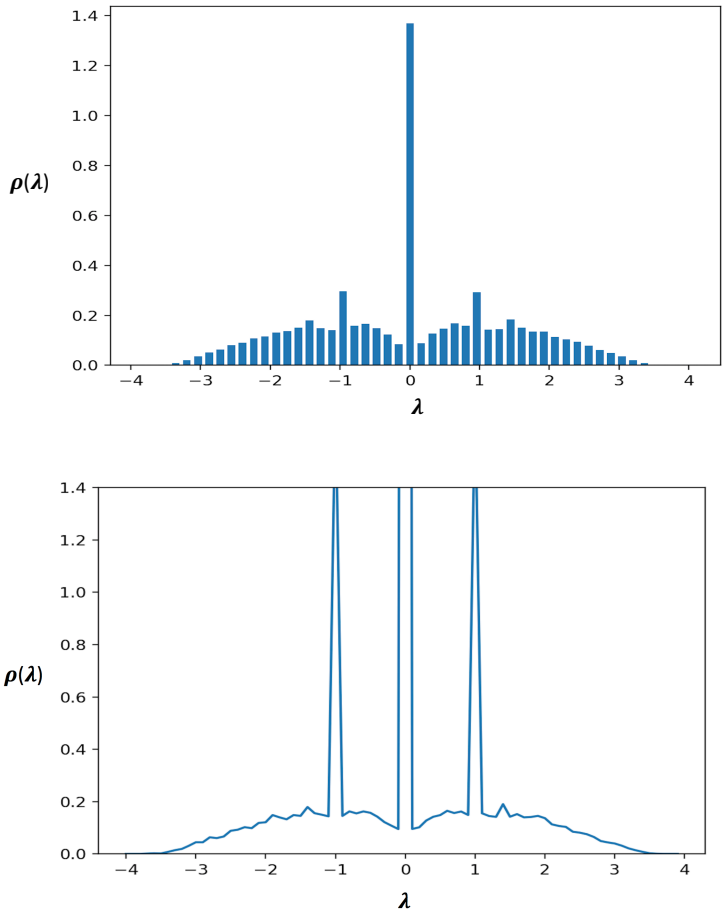

Figure 2.3: Comparison between ρ_ϵ^{reg} and ρ_ϵ^{bin}. Both obtained considering matrices of size 100 with c=2 and the result is averaged over 1000 matrices. The bin size has been chosen equal to 0.1.

2.6 Large-c limit: The Wigner semicircle law

In this section the cavity method approach will be verified by studying the set of equations 2.22 and 2.23 in the full-connected limit. In the last section the studied ensembles have been built by choosing every nonzero element on the basis of a given probability. This probability depends on the parameter c, which represents the average number of nodes to which a single node is connected. By defining with k_i the number of nodes close to the i-node, the average connectivity c (also called sparsity parameter) is:

$$c = \frac{1}{N}\sum_i k_i \tag{2.35}$$

The full-connected limit can be done by performing first the limit $k_i \to c$ and then $c \to \infty$ under the assumption that the graph is already "infinitely" large. A second option would be to first perform the limit $c \to N$ and then $N \to \infty$. In a full-connected graph ($c = N$) the cavity equations are still valid but the reason for the decorrelation is statistical rather than topological. Before demonstrating the relation between the cavity equations in the

full-connected limit, we remind the well known Wigner semicircle Law:

Theorem 1 (Wigner's Law)**.** *Let $\{A_N\}$ be a sequence of $N \times N$ random matrices such that for each N the entries of A_N are indipendent random variables of unit variance, draw from symmetric distributions with bounded moments. Then for fixed λ,*

$$\lim_{N\to\infty} \mathbb{E}\rho(\lambda; A_N/\sqrt{N}) = \frac{1}{2\pi}\sqrt{4-\lambda^2}\mathbb{I}_{[-2,2]}(\lambda). \tag{2.36}$$

The Wigner's Law shows a statistical result for a specific class of matrices. Therefore, it can be thought of as the analogue of the central limit theorem, in which an ever increasing number of random variables of an unknown type combine to produce a known deterministic limit.
The entries of the matrix A have been taken as $A_{ij} = J_{ij}/\sqrt{c}$, where $J_{ij}(= J_{ji})$ is a Gaussian variable with zero mean and variance J^2. For large c the equations 2.22 and 2.23 show that $\Delta_i^{(j)}(z) = \Delta_i(z) + \mathcal{O}(c^{-1})$. So, in this limit it can be obtained:

$$\lim_{c\to\infty} \sum_{l\in\partial i} A_{il}^2 \Delta_l^{(i)} = \lim_{c\to\infty} \frac{1}{c} \sum_{l\in\partial i} J_{il}^2 \Delta_l^{(i)} = J^2\Delta \tag{2.37}$$

where:

$$\Delta = \lim_{c\to\infty} \frac{1}{c} \sum_{l\in\partial i} \Delta_l. \tag{2.38}$$

The Eq. 2.23 provides the relation:

$$\Delta = \frac{1}{z - J^2\Delta} \tag{2.39}$$

which gives a ρ_A different from zero in the interval $[-2J; 2J]$ and equal to:

$$\rho_A(\lambda) = \frac{1}{2\pi J^2}\sqrt{4J^2 - \lambda^2}. \tag{2.40}$$

In figure 2.4 is reported a numerical result of the average distribution of the eigenvalues for a Gaussian symmetric ensemble and its expectation value according to the Wigner's Law.

To verify the method implementation and to study, numerically, how the average spectral density of an ensemble composed by sparse random matrices tends to the fully-connected law when $c, N \to \infty$, we performed some calculations for Gaussian ensembles where the c parameter increases.

Figure 2.5 show the results of the calculations and it is immediate to observe that as c increases the central peak in $\lambda = 0$ lowers and the form of the spectral distribution approaches the Wigner's Law. Therefore, each figure has been realized considering Gaussian distributions with mean zero and variance $1/c$ for the random entries of the matrices different from zero with probability c/N. The size of the matrices is not very large ($N = 20$) and the ensemble is composed by only 10 matrices for the spectral density obtained with the cavity method (blue line), while the result of the regularised empirical spectral density (orange line) is obtained by averaging over 1000 matrices.
An important consideration, concerning figure 2.2 and figure 2.5, is that the statistical fluctations are dominant in the empirical spectral density. In order to have a good comparison between the two methods it has been considered a large number of matrices for the eigenvalues obtained from the standard diagonalization algorithm in Python.
The results obtained show that the cavity method can be efficiently used in the statistical

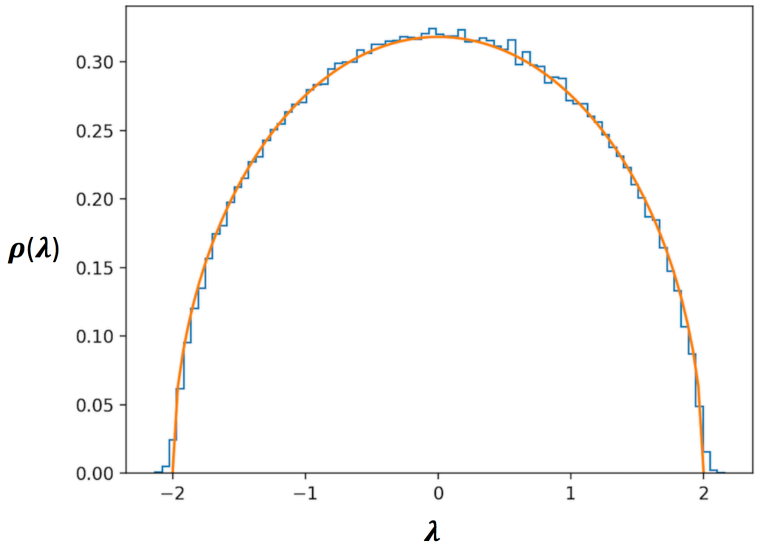

Figure 2.4: The figure illustrates the comparison between Wigner's Law and the normalized histogram of the eigenvalues obtained from an ensemble of 2000 symmetric matrices of size 100 where the entries are extracted by a Gaussian distribution with $\mu = 0$ and $J = 1/N$.

limit $N \to \infty$ for the sparse random matrices built in different ways even if relatively small matrices (N=20) have been used. Another consideration about figure 2.5 is that the computational time of the code which implements the cavity method, for the same matricial size, increases by increasing the value of the average connectivity parameter c. This is expected because the method is based on a treelike network structure for any size of the matrix, but when the size is big enough and the connectivity is not low the method leads to an exact result but in an indefinite time.

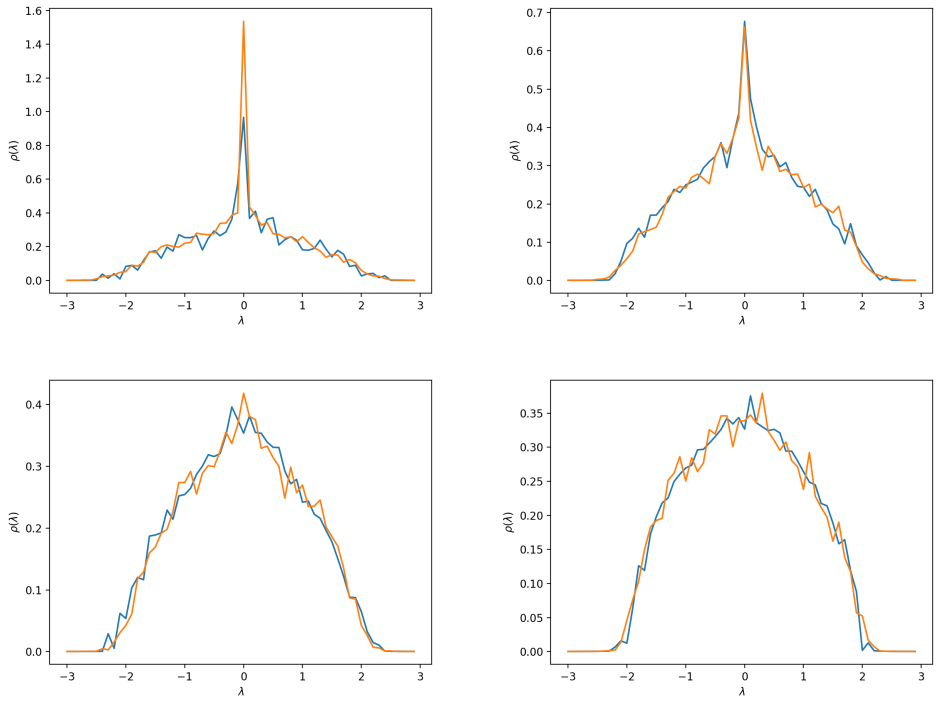

Figure 2.5: The figures have been obtained by generating symmetric matrices with N=20 and their coefficients have been taken different from zero with probability c/N and drawn by a Gaussian distribution with zero mean and variance $1/c$. Moving from left to right and from top to bottom, c assumes value: 5,7,10 and 15. The blue line is the result for the cavity method averaged over 10 matrices while the orange line is the spectral density obtained by exact numerical diagonalization and averaged over 1000 samples.

2.7 Conclusion

In this chapter it has been examined the spectral density of ensembles of sparse random symmetric matrices. The generalization of the applicability of the cavity method to Hermitian matrices is performed replacing in the eq. 2.22 and in eq. 2.23 the elements A_{il}^2 with $|A_{il}|^2$. This work has been inspired by Edwards and Jones [15] and following their work the purpose of obtaining the spectral density has been moved to the study of a system of interacting particles on a sparse graph, which was then analyzed by the cavity approach. In this framework a set of coupled cavity equations has been derived and then interpreted as a belief-propagation algorithm on single instances, which has then been easily implemented. Finally, the spectral density has been obtained from the recursive equations for the cavity distributions, parametrized by their variances.
It has been demostrated that the method can be a valid approach with new theoretical and practical advantages: it offers an alternative and maybe an easier processing to (re)derive the spectral density compared to previous works based on approximative schemes, as well as an improvement on the agreement with numerical diagonalization.
It has been shown, also, that the Dirac's δ, which is typical of the spectrum associated to a particular ensemble, may be approximated by Lorentzian peaks [20]. In previous works the averaged spectral density was obtained by using the replica approach, or in [21][22] by using

supersymmetric methods. It is well known that cavity and replica methods are equivalent, for instance, for diluted spin glasses [23]. For this type of interacting systems, with continuous dynamical variables, one expects an infinite number of cavity fields to parametrize the cavity distribution and so it is necessary to perform a series of approximations in order to apply the cavity method [24] [16] [25][17].
On the other hand, for general sparse matrices (low and moderate values of c) this replica method fails to provide an accurate description of the spectral density. With this work has, instead, been demonstrated that for Gaussian cavity distributions, the problem can be solved exactly by self-consistently determining their variances.

Chapter 3

Cavity method for the Non-Hermitian case

In this chapter it is shown the extension of the analysis performed on the spectral density of the random Non-Hermitian (asymmetric for real numbers) matrices ensemble reintroducing the concept of both the circular and elliptical law.
In the first section the elliptic law is studied using the analogy between the spectral density and electrostatic density. Using the correlation between the two densities, it is possible to derive the spectral density of asymmetric matrices starting from an electrostatic potential [26] and extend our knowledge to a broader context.
In the later sections it is presented a technique to extend the cavity method to *sparse* Non-Hermitian matrices compared to the specific approach to *sparse* Hermitian matrices introduced in the previous chapter. In the latter, the spectral density can be written in terms of (convergent) Gaussian integrals as well as an N-independent regularization through a unique Green function, where N is the size of the matrix. Moreover, the analytic form of the Green function allows to freely swap between the limit $\mathrm{N} \to \infty$ and the limit $\epsilon \to 0$ hence obtaining the spectral density as the Green function's limit evaluated away from the real numbers axis.
A similar analysis cannot be applied to Non-Hermitian matrices because of the presence of complex eigenvalues invalidating equation 2.32. However, the 'Hermetization' technique allows to use an alternative formalism to tackle the problem as well as obtaining a simple closed set of equations whose solutions characterize the spectral density of a given ensemble of matrices in the statistical limit of $N \to \infty$.

3.1 Random Asymmetric Matrices

The study of the distribution of eigenvalues of an ensemble of large real asymmetric matrices has been performed using matrices with entries J_{ij} having a Gaussian distribution with zero mean and correlations defined as:

$$[J_{ij}^2]_J = 1/N, \quad [J_{ij}J_{ji}]_J = \tau/N$$

for $i \neq j$ and $-1 \leq \tau \leq 1$ where τ defines the degree of correlation among the symmetric elements of a single matrix and the brackets $[...]_J$ denote the ensemble average. The limit case $\tau = 1$ corresponds to an ensemble of symmetric matrices while $\tau = -1$ to the anti-symmetric matrices. It is worth noticing that the fully asymmetric ensemble where the elements J_{ij}

and J_{ji} are completely independent can be recovered for the $\tau = 0$ case.
It is well known that the average density of eigenvalues (ω) when $\omega = x + iy$ in the limit $N \to \infty$ is given by:

$$\rho(\omega) = \begin{cases} (\pi ab)^{-1}, & \text{if} \quad (x/a)^2 + (y/b)^2 \leq 1 \\ 0, & \text{otherwise;} \end{cases} \tag{3.1}$$

where $a = 1 + \tau$ and $b = 1 - \tau$. In other words, the average density of eigenvalues for this ensemble is uniform within an ellipse, in the complex plane, centred on zero with semi-axes a (along the real direction) and b (along the imaginary direction). For $\tau = 0$ the ellipse degenerates into a unit circle (circular law).
It is possible to see from fig. 3.1, the strong agreement between the numerical diagonalization

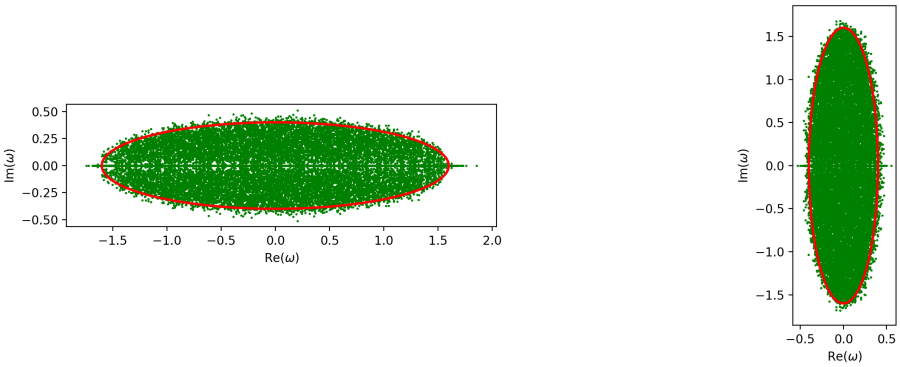

Figure 3.1: Numerical results for the distribution of 200 eigeinvalues ω for N=100. The left figure is obtained for $\tau = \frac{3}{5}$ while the right figure for $\tau = -\frac{3}{5}$. The red line shows the ellipse predicted by Eq. 3.1.

and the analytical predictions for large values of N apart from minor deviations near the real axes where the observed density of states is higher than the average density. It can be demonstrated that this non uniformity is due to the finite-size of the value N and the effect decreases as the size increases ultimately vanishing as $N \to \infty$. As a matter of fact, when N is finite, the repulsion level of the eigenstates near the real axis becomes lower than the average repulsion level [26].
Associated with the matrix $\mathbf{J}$, it is feasible to define the Green function as:

$$G(\omega) = \frac{1}{N}\Big[\mathrm{Tr}\frac{1}{\mathbf{1}\omega - \mathbf{J}}\Big]_J \tag{3.2}$$

where $\mathbf{1}$ is the identity matrix. This function is defined for all complex numbers ω, except for the eigenvalues of $\mathbf{J}$. By choosing a particular set of eigenvectors, it is possible to rewrite eq. 3.2 to provide a better understanding of the analogy between the spectral and electrostatic density. $\mathbf{r}^\alpha$ and $\mathbf{l}_\alpha$ are the right and left eigenvectors of the matrix $\mathbf{J}$ respectively, which satisfy the following relations:

$$\mathbf{J}\mathbf{r}^\alpha = \lambda_\alpha \mathbf{r}^\alpha$$
$$\mathbf{l}_\alpha \mathbf{J} = \lambda_\alpha \mathbf{l}_\alpha$$

for each $\alpha = 1, ...N$. If the following orthonormalization proprieties:

$$\mathbf{l}_\alpha \cdot \mathbf{r}^\beta = \delta_\alpha^\beta \quad \text{with} \quad \alpha, \beta = 1, ..., N \tag{3.3}$$

$$\sum_{\alpha=1}^{N} l_\alpha^i l_j^\alpha = \delta_j^i \tag{3.4}$$

$$\sum_{\alpha=1}^{N} r_\alpha^i r_j^\alpha = \delta_j^i \tag{3.5}$$

are satisfied, the elements J_{ij} can be written as:

$$J_{ij} = \sum_{\alpha=1}^{N} l_i^\alpha r_{\alpha_j} \lambda_\alpha \tag{3.6}$$

Then the elements of a function which depends by $\mathbf{J}$ can be written as:

$$(f(\mathbf{J}))_{ij} \equiv \sum_{\alpha=1}^{N} l_i^\alpha r_{\alpha_j} f(\lambda_\alpha) \tag{3.7}$$

and its trace as:

$$\mathrm{Tr}(f(\mathbf{J})) = \sum_{i,\alpha} l_i^\alpha r_{\alpha_i} f(\lambda_\alpha) = \sum_\alpha f(\lambda_\alpha) = \sum_\alpha \int \delta^2(\lambda - \lambda_\alpha) f(\lambda) d^2\lambda = N \int d^2\lambda \rho(\lambda) f(\lambda) \tag{3.8}$$

where it has been used the definition of spectral density in the complex field. As the Green function (eq. 3.2) is defined by the trace of a matrix depending by $\mathbf{J}$, the previous passages lead to the new equation:

$$G(\omega) = \frac{1}{N}\Big[\sum_\lambda \frac{1}{\omega - \lambda}\Big]_J = \int d^2\lambda \frac{\rho(\lambda)}{\omega - \lambda}. \tag{3.9}$$

The Green function has now become an integral over the eigenvalues λ of a second function which depends on the average density of the eigenvalues of $\mathbf{J}$ in the complex plane. This expression clearly suggests a possible analogy with a two-dimensional classical electrostatic field. In order to show this relation, the eq. 3.9 can be integrated around a region $\mathfrak{R}$ which contains the eigenvalues λ, assuming that no eigenvalues lie on the border $\partial\mathfrak{R}$:

$$\int_{\partial\mathfrak{R}} \frac{d\omega}{2\pi i} G(\omega) = \frac{1}{N}\Big[\sum_\lambda \int_{\partial\mathfrak{R}} \frac{d\omega}{2\pi i} \frac{1}{\omega - \lambda}\Big]_J = \frac{1}{N}\Big[\sum_{\lambda \in \mathfrak{R}} 1\Big]_J = \int_{\mathfrak{R}} d^2\omega \rho(\omega). \tag{3.10}$$

The integration has used the residue theorem to evaluate the line integral of the analytic function $f(\omega) = \frac{1}{\omega - \lambda}$ over the closed curve $\partial\mathfrak{R}$.
In order to solve the line integral it is necessary to choose a convenient parametrization of the curve in the complex plane. The coordinates of the curve's points are functions of a new variable τ, therefore, the points on the border of $\mathfrak{R}$ assume the following form: $\omega(\tau) = x(\tau) + iy(\tau)$ where $\frac{d\vec{\omega}(\tau)}{i} = dy(\tau) - i\, dx(\tau) = \hat{n}|d\vec{r}|$ with $|d\vec{r}| = \sqrt{\dot{x}(\tau)^2 + \dot{y}(\tau)^2} d\tau \equiv dl$ as the infinitesimal length of the curve and $\hat{n}$ as the unitary vector normal to the curve $\partial\mathfrak{R}$. The new integral can be resolved by applying the Gauss theorem using a vector field defined as the product between an arbitrary constant vector field $\vec{a}$ and the scalar field $G(\omega)$. By

applying the divergence propriety to the vector field: $\nabla \cdot (G\vec{\boldsymbol{a}}) = \vec{\boldsymbol{a}} \cdot (\vec{\nabla} G)$, the integral of the vector field $\vec{\boldsymbol{J}} \equiv G\vec{\boldsymbol{a}}$ over the region $\mathfrak{R}$ can be written as:

$$\int_{\mathfrak{R}} d^2\omega \quad \nabla \cdot \vec{\boldsymbol{J}} = \int_{\partial\mathfrak{R}} dl \quad \hat{n} \cdot \vec{\boldsymbol{J}} \Longrightarrow \int_{\mathfrak{R}} d^2\omega \quad \left(\frac{\partial G}{\partial x} + i\frac{\partial G}{\partial y}\right) = \int_{\partial\mathfrak{R}} \frac{d\omega}{i} \quad G \tag{3.11}$$

where the last passage is allowed because $\vec{\boldsymbol{a}}$ is chosen arbitrarily. Exploiting the relation expressed in eq. 3.10, it is possible to obtain the following relation:

$$\int_{\mathfrak{R}} d^2\omega \quad \left(\frac{\partial G}{\partial x} + i\frac{\partial G}{\partial y}\right) = 2\pi \int_{\mathfrak{R}} d^2\omega \quad \rho(\omega). \tag{3.12}$$

Equating the functions being integrated and considering that the right-hand side of eq. 3.12 is defined over real values because of the definition of spectral density, the following equations can be obtained:

$$\frac{\partial \mathrm{Re}G}{\partial x} - \frac{\partial \mathrm{Im}G}{\partial y} = 2\pi\rho \tag{3.13}$$

$$\frac{\partial \mathrm{Im}G}{\partial x} + \frac{\partial \mathrm{Re}G}{\partial y} = 0. \tag{3.14}$$

Thanks to a clever redefinition of the Green function in terms of the electric field $\vec{E}$:

$$E_x \equiv 2\mathrm{Re}G \quad , \quad E_y \equiv -2\mathrm{Im}G \tag{3.15}$$

the eq. 3.13 becomes the Gauss' law relating the distribution of an electric charge to the resulting electric field, while eq. 3.14 becomes $\vec{\nabla} \times \vec{E} = 0$. The last consequence permits to associate a scalar potential Φ to the electric field $\vec{E}$ satisfying the following relations:

$$2\mathrm{Re}G = -\frac{\partial \Phi}{\partial x}, \quad -2\mathrm{Im}G = -\frac{\partial \Phi}{\partial y} \tag{3.16}$$

where Φ obeys the Poisson's equation:

$$\nabla^2\Phi = -\vec{\nabla} \cdot \vec{E} = -4\pi\rho. \tag{3.17}$$

In order to evaluate $\rho(\omega)$ it is necessary to know $G(\omega)$ in the region where ρ is not zero, however, $G(\omega)$ is defined outside this region and in general it is not possible to estimate it by analytic evaluation from outside the region. This fact can be explained in the language of electrostatics: the charge distribution is not completely determined by the value of the electric field outside the charged region. For this reason, it is possible to show that $G(\omega)$ cannot be calculated even using perturbative methods outside the region where $\rho = 0$.
Expanding eq. 3.9 as a power series of $\mathbf{J}$,

$$G(\omega) = \frac{1}{N}\sum_i \Big[\frac{1}{\omega} + \frac{\lambda_i}{\omega^2} + \frac{\lambda_i^2}{\omega^3} + ...\Big]_J = \frac{1}{\omega}\Big[1 + \frac{\sum_i J_{ii}}{N\omega} + \frac{\sum_{ij} J_{ij}J_{ji}}{N\omega^2} + ...\Big]_J, \tag{3.18}$$

where for the fully asymmetric case in which $[J_{ij}J_{ji}]_J = 0$, the expansion yields $G(\omega) = 1/\omega$ in the limit $N \to \infty$, to all orders in $\mathbf{J}$. This result, however, is not valid on all complex plane. In fact eq. 3.1 implies that for $\tau = 0$, $G(\omega)$ becomes:

$$G(\omega) = \frac{1}{\pi}\int_{|\lambda|\leq 1} \frac{d^2\lambda}{\omega - \lambda}. \tag{3.19}$$

Following the electrostatic analogy, it is possible to consider the components of the electric field and G(ω) with components equal to its real and imaginary part, in the complex plane:

$$E(\omega) = 2G(\omega)^*. \tag{3.20}$$

Rearranging $G(\omega)$ as follows:

$$G(\omega) = \frac{1}{\pi}\int_{|\lambda|\leq 1} d^2\lambda \frac{(\omega-\lambda)^*}{|\omega-\lambda|^2} \tag{3.21}$$

it is straightforward to associate the electric field **E** in the complex plane to the integral over a charged region:

$$E(\omega) = \frac{2}{\pi}\int_{|\lambda|\leq 1} d^2\lambda \frac{\omega-\lambda}{|\omega-\lambda|^2}. \tag{3.22}$$

This expression is clearly similar to that of the electric field evaluated at a point ω in the bi-dimensional space generated by the presence of uniformly distributed electrical charges when the Gauss Law is valid. By applying these considerations, the integral becomes:

$$\int_S \vec{E}\cdot\vec{n} = 2\pi Q \quad \text{in convenient units} \tag{3.23}$$

where S is a 1-D sphere, $\vec{n}$ is the unitary vector normal to S and Q is the total charge enclosed by S.
If $|\omega| \geq 1$ the electric field becomes:

$$|E(\omega)|\ 2\ \pi\ |\omega| = 2\ \pi\ \frac{2}{\pi}\ \pi \Longrightarrow E(\omega) = 2\frac{\omega}{|\omega|^2} \quad \text{hence} \quad G(\omega) = \frac{1}{\omega} \tag{3.24}$$

while, when $|\omega| \leq 1$ the electric field in $\vec{\omega}$ is due to the contribution of the charge inside the circle of radius ω:

$$|E(\omega)|\ 2\ \pi\ |\omega| = 2\ \pi\ \frac{2}{\pi}\ \pi|\omega|^2 \Longrightarrow E(\omega) = 2\omega \quad \text{hence} \quad G(\omega) = \omega^* \tag{3.25}$$

The result of eq. 3.24, $1/\omega$, which decreases as the inverse of the distance, corresponds to the two-dimensional Coulomb law, while the result of eq. 3.25, ω^*, corresponds to a linear electric field inside an homogeneously charged disk. These results have clearly demonstrated that the perturbative method, which assumes the possibility of expressing **J** as a power series (see eq. 3.18), is not valid inside the disk but only in the region where $\rho = 0$ and where $G(\omega)$ is an analytic function. It should also be noted that for symmetric matrices the *charge* Q is concentrated on a line and therefore analytic derivation can be used to obtain $G(\omega)$ and $\rho(\omega)$ over the entire complex plane [14].

In conclusion, for λ along the real axis (where the eigenvalues of Hermitian matrices are confined), the Green function is analytic and its imaginary part gives a smooth and N-independent regularization of the spectral density (as it has been demonstrated in 2.33). But if the matrix is non-Hermitian, the eigenvalues invade the complex plane and the Green function provides no such regularization. In order to evaluate the analytical form of the spectral density of sparse Non-Hermitian random matrices, it is imperative to find a new approach in order to apply the same analogy used for the Hermitian case, or some related artefact as the electrostatic potential introduced in [2]. The goal is to write the spectral density in a way that allows to obtain a convergent Fresnel integral as with the case of Hermitian matrices.

3.2 Hermitization

Hermitization is a process introduced by Feinberg and Zee [27][28] in which they worked with matrices of double the size of the ones initially defined. A similar approach has been introduced by Janik, Nowak, and collaborators [29] proposing a similar block structure extension technique. They have obtained a generalization of the Green function with a quaternionic structure yielding many interesting results, including a specific application concerning the study of ecological communities as it has been shown in Chapter 4.

It has been considered an ensemble $\mathcal{M}$ of $N \times N$ complex, sparse non-Hermitian random matrices. If A is a non-Hermitian matrix, its eigenvalues are complex. For a point $z = x + iy$ in the complex plane, the spectral density of A at z is:

$$\rho_A(z,\bar{z}) = \frac{1}{N}\sum_{i=1}^{N}\delta(x - \mathrm{Re}\lambda_i^A)\delta(y - \mathrm{Im}\lambda_i^A) \tag{3.26}$$

The spectral density can be also written as[1]:

$$\rho_A(z,\bar{z}) = \frac{1}{\pi N}\lim_{\kappa\to 0}\partial_{\bar{z}}\partial_z \ln\det\widehat{H} \tag{3.27}$$

where $\widehat{H}$ is a $2N \times 2N$ Hermitian matrix:

$$\widehat{H} \equiv \widehat{H}(z,\bar{z};\kappa) = \begin{pmatrix} \kappa\mathbf{1}_N & A - z\mathbf{1}_N \\ A^\dagger - \bar{z}\mathbf{1}_N & \kappa\mathbf{1}_N \end{pmatrix} \tag{3.28}$$

and $\mathbf{1}_N$ is the identity matrix $N \times N$. The $\widehat{H}$ matrix is the one originally introduced by Feinberg and Zee.
The eq. 3.27 can be written as:

$$\rho_A(x,y) = \frac{-1}{\pi N}\lim_{\kappa\to 0}\frac{1}{4}\left(\frac{\partial}{\partial x} + i\frac{\partial}{\partial y}\right)\left(\frac{\partial}{\partial x} - i\frac{\partial}{\partial y}\right)\ln\det\widehat{H} = \frac{-1}{4\pi N}\lim_{\kappa\to 0}\nabla^2\ln\det\widehat{H}. \tag{3.29}$$

To solve eq. 3.29 it has been used the work of Sylvester for block matrices [30] that can be explained as follows. Let X be a block matrix consisting of four $N \times N$ blocks, i.e. A, B, C and D, arranged in the following way:

$$\mathbf{X} = \begin{pmatrix} A & B \\ C & D \end{pmatrix}.$$

If A and D are proportional to the identity matrix $\mathbf{1}_N$, because of the decomposition of the determinant of the matrix X using Shur's complements, the formula gives:

$$\det\mathbf{X} = \det(\kappa^2\mathbf{1}_N - BC). \tag{3.30}$$

Therefore, $\widehat{H}$, working in the limit $\kappa = 0$, becomes:

$$\det\widehat{H}(x,y) = (-1)^N\det[(A - z\mathbf{1}_N)(A^\dagger - \bar{z}\mathbf{1}_N)].$$

[1]It has been used the notation conventions $\partial_z = \frac{1}{2}\left(\frac{\partial}{\partial x} - i\frac{\partial}{\partial y}\right)$, $\partial_{\bar{z}} = \frac{1}{2}\left(\frac{\partial}{\partial x} + i\frac{\partial}{\partial y}\right)$

It is now possible to introduce another non-Hermitian matrix H, which leads to the same spectral density of eq. 3.28, later on used to apply the cavity method:

$$H \equiv H(z, \bar{z}, \kappa) = \begin{pmatrix} \kappa \mathbf{1}_N & i(z\mathbf{1}_N - A) \\ i(z\mathbf{1}_N - A)^\dagger & \kappa \mathbf{1}_N \end{pmatrix}. \tag{3.31}$$

The equivalence between the two matrices can be observed using the following relation:

$$\ln \det \widehat{H} = \ln(-1)^N + \ln \det H = i\pi N + \ln \det H \qquad \text{for} \quad \kappa = 0 \tag{3.32}$$

and considering that applying ∇^2 to eq. 3.32 both $\widehat{H}$ and H yield the same results. By substituting H with $\widehat{H}$ in eq. 3.29 the problem has shifted to proving the following relation:

$$\rho_A(x, y) = \frac{-1}{4\pi N} \nabla^2 \ln \det[(A - z\mathbf{1}_N)(A^\dagger - \bar{z}\mathbf{1}_N)] \tag{3.33}$$

where it has been changed the action of ∇^2 with the limit $\kappa \to 0$ permitted by the analytic nature of the equation.[2]
Using the identity:

$$\ln \det V = \mathrm{Tr} \ln V$$

eq. 3.33 reduces to:

$$\begin{aligned} \rho_A(x, y) &= \frac{-1}{4\pi N} \nabla^2 \sum_i^N [\ln(\lambda_i - z) + \ln(\bar{\lambda_i} - \bar{z})] = \frac{-1}{4\pi N} \nabla^2 \sum_i^N \ln|\lambda_i - z|^2 \\ &= \frac{1}{4\pi N} \nabla^2 \sum_i^N \ln[(x_i - x)^2 + (y_i - y)^2], \end{aligned} \tag{3.34}$$

where x_i and y_i are the real and imaginary part of λ_i respectively. To solve eq. 3.34, it is needed to compute:

$$\nabla^2 \ln(x^2 + y^2).$$

without considering the divergence at $\begin{pmatrix} x \\ y \end{pmatrix} = \begin{pmatrix} 0 \\ 0 \end{pmatrix}$. In order to avoid this divergence, the parameter ϵ is introduced and the expression is regularized as follows:

$$\nabla^2 \ln(x^2 + y^2 + \epsilon) = \frac{4\epsilon}{(x^2 + y^2 + \epsilon)^2}. \tag{3.35}$$

This expression leads to two different conclusions:

1. If $\begin{pmatrix} x \\ y \end{pmatrix} \neq \begin{pmatrix} 0 \\ 0 \end{pmatrix}$ and $\epsilon \to 0$ the result is null.
2. If $\begin{pmatrix} x \\ y \end{pmatrix} = \begin{pmatrix} 0 \\ 0 \end{pmatrix}$ the function assumes the value $\frac{4}{\epsilon}$, and for $\epsilon \to 0$ the result diverges.

Therefore it is expected that the weak convergence of conclusion 2 leads to a distribution of this form:

[2] The presence of the parameter κ is important to ensure the convergence of the integrals when the technique of the cavity method will be used in the following sections where the change will not be allowed in a rigours way.

$$\mathrm{C}\ \delta(x)\delta(y).$$

Matching the integrals on $\mathbb{R}^2$ of eq. 3.35 and of the delta functions in the limit $\epsilon = 0$, produces a value for the constant C of 4π. Applying all these information, the following relation is obtained:

$$\nabla^2 \ln(x^2+y^2) = 4\pi\delta(x)\delta(y) \Longrightarrow (\text{eq. } 3.34) = \frac{1}{N}\sum_i^N \delta(x_i - x)\delta(y_i - y) = \rho_A(x,y) \tag{3.36}$$

At this point it is straightforward to confirm the interpretation of ρ_A in the context of electrostatics in two dimensions: $\rho_A(z,\bar{z})$ in eq. 3.27 can be interpreted as the density of the electrical charges, all equal to $1/N$, placed at the position $\vec{r}_i = \begin{pmatrix} x_i \\ y_i \end{pmatrix}$ in the bi-dimensional space. Furthermore, it has been clarified the correctness of the *Hermitization* process that has allowed to confirm the analogy of the spectral density with the one for the electrical charges considered in the previous section.

3.3 Preparation

Analogously to the Hermitian case, this section analyses the case of a disordered system which is treatable by statistical mechanics as a multitude of interacting particles.[3] Considering eq. 3.27 it is noticeable that all the eigenvalues of H, assuming that κ is positive, have a strictly positive real part. Introducing $2N$ complex integration variables organized into N-vectors $\boldsymbol{\phi}$ and $\boldsymbol{\chi}$, it is possible to write the inverse of the determinant of H as a convergent Fresnel integral:[4]

$$\frac{1}{\det[H(z;\bar{z};\kappa)]} = \left(\frac{1}{\pi}\right)^{2N} \int \exp\left\{ -(\boldsymbol{\phi}^\dagger \quad \boldsymbol{\chi}^\dagger) H(z;\bar{z};\kappa) \begin{pmatrix} \boldsymbol{\phi} \\ \boldsymbol{\chi} \end{pmatrix} \right\} d\boldsymbol{\phi} d\boldsymbol{\chi}. \tag{3.37}$$

where $d\boldsymbol{\phi} = \prod_{i=1}^N d\mathrm{Re}\phi_i d\mathrm{Im}\phi_i$ and $d\boldsymbol{\chi} = \prod_{i=1}^N d\mathrm{Re}\chi_i d\mathrm{Im}\chi_i$.
The form of the matrix H has been allowed to arrange the bi-linear form $2N \times 2N$ in the exponential as a sum of N terms rearranging the $2N$ variables in N pairs of complex variables:

$$\psi_i = \begin{pmatrix} u_i \\ v_i \end{pmatrix}, \qquad \text{i=1,...,N}$$

introducing the *Hamiltonian*

$$\mathcal{H}(\boldsymbol{\psi}, z;\bar{z};\kappa) = \sum_i^N \psi_i^\dagger [\kappa \mathbf{1}_2 + i(x\sigma_x - y\sigma_y)]\psi_i - i\sum_{i,j=1}^N \psi_i^\dagger (A_{ij}^h \sigma_x - A_{ij}^s \sigma_y)\psi_j, \tag{3.38}$$

where σ_x and σ_y are the usual Pauli matrices and A^h and A^s are Hermitian matrices which allows to rewrite A as $A = A^h + iA^s$. Now, introducing a *distribution* P:

$$P(\boldsymbol{\psi}) = \frac{1}{\mathcal{Z}} e^{-\mathcal{H}(\boldsymbol{\psi},z;\bar{z};\kappa)} \tag{3.39}$$

[3] It is important to stress that this analogy has been made only to better understand the implication of the cavity method and has no physical equivalent with a many-body interacting system.

[4] Note that κ is associated with the real part of the eigenvalues of H and this guarantees the convergence of the integral.

and the definition of *average* $< ... >$:

$$< ... >= \int \mathcal{D}\boldsymbol{\psi} P(\boldsymbol{\psi})(...), \tag{3.40}$$

where $\mathcal{Z}$ is a normalizing constant, it is possible to clearly present the analogy of the system to statistical mechanics.[5] Ultimately, the spectral density of eq. 3.27 can be written as[6]:

$$\rho_A(z;\bar{z}) = \lim_{\kappa\to 0} \frac{1}{\pi N} \sum_{l=1}^{N} -i\partial_{\bar{z}} < \psi_l^{\dagger} \sigma^{+} \psi_l >, \tag{3.41}$$

where $\sigma^{+} = (\sigma_x + i\sigma_y)/2$.
In order to evaluate these averages, it is sufficient to consider the local marginals $P_i(\psi_i)$ and calculate them by applying the cavity method.
The regularised spectral density of a non-Hermitian matrix, as defined by:[7]

$$\rho_A^{\kappa}(x,y) = \frac{-1}{4\pi N} \nabla^2 \ln \det[(A - z\mathbf{1}_N)(A^{\dagger} - \bar{z}\mathbf{1}_N) + \kappa^2 \mathbf{1}_N], \tag{3.42}$$

is not so easily exploited to obtain rigorous results for the unregularized density as in the Hermitian case. Although it is certainly true that for any fixed, finite size matrix A the following relation is valid:

$$\rho_A(x,y) = \lim_{\kappa\to 0} \rho_A^{\kappa}(x,y),$$

there is in general no simple convolution identity such as eq. 2.34. Even when the regularized spectral density of random matrix ensemble is known for $N \to \infty$, the unregularized density is not straightforward to obtain.
Simply put, if the matrices involved are not normal, there may be parts of the complex plane far from the spectrum where the Green function is very large. In practical terms, this causes great difficulty in justifying the swapping between the $N \to \infty$ and $\kappa \to 0$ limits [31]. The general approach has been used to justify the exchange of the limits taking into account the necessity to prove bounds on the least singular values of the matrices involved, though this method has the drawback that it must be completed on an ad-hoc basis for each ensemble. Under particular type of random perturbations it is possible to offer a remarkable relation between the regularized spectral density of a non-Hermitian matrix and the mean spectral density of the same matrix.

3.4 Treelike Matrices

Treelike sparse matrices have been considered to find the marginal probability necessary to obtain the final spectral density. As in the Hermitian case, it has been associated a directed graph $\mathcal{G}_A$ with the matrix A and the feature *treelike* is assumed if short loops are rare. The interaction of variables ψ_i and ψ_j have been moved to the edges between i and j. In this analogy if the element A_{ij} or A_{ji} is not null, then the pair of vertices (i,j) are neighbors, ∂_i

[5] Because the integration measure is complex, it is clearly not a real stochastic measure, however, many of the mathematical derivations remain valid allowing the probabilistic analogy.

[6] it is obtained by eq. 3.27 remembering that the determinant of H is proporzional to the partition function $\mathcal{Z}$.

[7] The parameter $\kappa > 0$ is necessary to keep the argument of the logarithm strictly positive in this relation.

indicates the set of all neighbors of i, k_i denotes the number of neighbors of i (the degree of i) and $c = N^{-1}\sum_i k_i$ defines the average degree.
In the hypothesis that A is treelike, the elimination of a vertex of the graph associated to the variable ψ_i changes the marginal distributions of the neighboring variables ψ_l ($l \in \partial_i$), which is denoted by $P_l^{(i)}(\psi_l)$. Therefore, the joint distribution of the neighbors of the vertex i is now factorized as:

$$P^{(i)}(\{\psi_l\}_{l\in\partial i}) = \prod_{l\in\partial i} P_l^{(i)}(\psi_l). \tag{3.43}$$

This approximation is exact on trees and graphs which remain treelike in the limit $N \to \infty$. The cavity marginals $\{P_i^{(j)}\}$ obey simple recursive relations

$$P_i^{(j)}(\psi_i) = \frac{e^{-\mathcal{H}_i}}{Z_i^{(j)}} \int \mathcal{D}(\boldsymbol{\psi}_{\partial i/j}) e^{-\sum_{l\in\partial i/j}\mathcal{H}_{il}} \prod_{l\in\partial i/j} P_l^{(i)}(\psi_l) \tag{3.44}$$

where $Z_i^{(j)}$ is a normalizing constant. The Hamiltonian in eq. 3.38 has been separated in a contribution of single variables $\mathcal{H}_i$ and a contribution associated to pairs of variables $\mathcal{H}_{ij}$. Once the cavity distributions are known, the actual marginal distribution of vertex i can be recovered by the combination of those of the neighbors through the following relation:

$$P_i(\psi_i) = \frac{e^{-\mathcal{H}_i}}{Z_i} \int \mathcal{D}(\boldsymbol{\psi}_{\partial i}) e^{-\sum_{l\in\partial i}\mathcal{H}_{il}} \prod_{l\in\partial i} P_l^{(i)}(\psi_l). \tag{3.45}$$

The set of recursive equations in eq.3.44 is self-consistently solved by distributions of a bivariate Gaussian type. Then for all $i = 1, ..., N$ and all $j \in \partial i$ the distribution $P_i^{(j)}$ can be written as:

$$P_i^{(j)}(\psi_i) = \frac{1}{Z_i^{(j)}} \exp(-\psi_i^\dagger [\mathcal{C}_i^{(j)}]^{-1} \psi_i) \tag{3.46}$$

where $\mathcal{C}_i^{(j)}$ is a 2×2 matrix. Inserting this form in eq. 3.44, it can be obtained a set of recursive equations for the matrices $\{\mathcal{C}_i^{(j)}\}$. Thus, the system in eq. 3.44 has now become:

$$e^{-\psi_i^\dagger \left[\mathcal{C}_i^{(j)}\right]^{-1}\psi_i} =$$
$$e^{-\mathcal{H}_i} \int \mathcal{D}(\boldsymbol{\psi}_{\partial i/j}) \exp^{-\sum_{l\in\partial i/j}[-i\psi_i^\dagger(A^h_{il}\sigma_x - A^s_{il}\sigma_y)\psi_l - i\psi_l^\dagger(A^h_{li}\sigma_x - A^s_{li}\sigma_y)\psi_i]} \prod_{l\in\partial i/\ j} \frac{1}{Z_l^{(i)}} e^{-\sum_{l\in\partial i/j}\psi_l^\dagger \left[\mathcal{C}_l^{(i)}\right]^{-1}\psi_l} \tag{3.47}$$

In order to solve the previous equation, it has been necessary to apply a series of variables' changes. By fixing the indices l and i, the exponential shows two bilinear forms with a matrix which is a combination of Pauli matrices. It is also important to stress that it has been done a unitary transformation to diagonalize the matrix $[\mathcal{C}_l^{(i)}]^{-1}$ and defined

$$B = A^h_{il}\sigma_x - A^s_{il}\sigma_y$$
$$B' = A^h_{li}\sigma_x - A^s_{li}\sigma_y.$$

to simplify the integral of eq. 3.47. The new variables $\phi_l = U_l^{-1}\psi_l$ allow to rewrite eq. 3.47 as follow:

$$\int \prod_{l\in\partial i/\ j} \frac{\mathcal{D}\phi_l}{Z_l^{(i)}} \exp\left[+i\psi_i^\dagger B U_l \phi_l + i\phi_l^\dagger U_l^\dagger B'\psi_i - \phi_l^\dagger U_l^\dagger [\mathcal{C}_l^{(i)}]^{-1} U_l \phi_l\right] \tag{3.48}$$

The next step has required to define two new variables:

$$J_i = \psi_i^\dagger B$$
$$J_i' = B'\psi_i$$

and use a different notation for the diagonal matrix, $D_l^{(i)} \equiv U_l^\dagger [\mathcal{C}_l^{(i)}]^{-1} U_l$. The relation which connect J_i and J_i' is:

$$J_i' = J_i^\dagger.$$

because $B' = B^\dagger$. The variable ϕ_l incorporates two complex variables which have been called u_l and v_l. Then eq. 3.48 has been written as:

$$\int \prod_{l\in\partial i/\ j} \frac{\mathcal{D}\phi_l}{Z_l^{(i)}} e^{\sum_\alpha [iJ'^\dagger_{i\alpha} U^l_{\alpha 1} u_l + iJ'^\dagger_{i\alpha} U^l_{\alpha 2} v_l + iu_l^* U^{l\dagger}_{1\alpha} J'_{i\alpha} + iv_l^* U^{l\dagger}_{2\alpha} J'_{i\alpha} - d^{(i)}_{l1}|u_l|^2 - d^{(i)}_{l2}|v_l|^2]} \tag{3.49}$$

where the numbers $d_{l1}^{(i)}$ and $d_{l2}^{(i)}$ are the diagonal elements of $D_l^{(i)}$. The quantities in the exponential now shows the following relations:

$$b^* = [\textstyle\sum_\alpha U^{l\dagger}_{1\alpha} J'_{i\alpha}]^* = \sum_\alpha J'^\dagger_{i\alpha} U^l_{\alpha 1}$$
$$c^* = [\textstyle\sum_\alpha U^{l\dagger}_{2\alpha} J'_{i\alpha}]^* = \sum_\alpha J'^\dagger_{i\alpha} U^l_{\alpha 2}.$$

which have been exploited to rearrange eq. 3.49:

$$\int \prod_{l\in\partial i/\ j} \frac{du_l dv_l du_l^* dv_l^*}{4Z_l^{(i)}} \exp\left\{ -d^{(i)}_{l1}\left(|u_l|^2 - i\frac{b^*}{d^{(i)}_{l1}} u_l - i\frac{b}{d^{(i)}_{l1}} u_l^* \right) - d^{(i)}_{l2}\left(|v_l|^2 - i\frac{c^*}{d^{(i)}_{l2}} v_l - i\frac{c}{d^{(i)}_{l2}} v_l^* \right) \right\}. \tag{3.50}$$

Since the integrals in the variables (u_l, u_l^*) and (v_l, v_l^*) are similar, it has been possible to limit the analysis to only one of them still retaining the validity of the method. Changing variables and replacing the real and imaginary part:

$$u_l^R = \tfrac{1}{\sqrt{2}}(u_l + u_l^*)$$
$$u_l^I = \tfrac{-i}{\sqrt{2}}(u_l - u_l^*).$$

it has been possible to obtain the following relation:

$$\int \prod_{l\in\partial i/\ j} \frac{du_l^R du_l^I}{4Z_l^{(i)}} \exp\left(-\tfrac{d^{(i)}_{l1}}{2} u^2_{lR} + i\tfrac{b^*}{\sqrt{2}} u_l^R + i\tfrac{b}{\sqrt{2}} u_l^R \right) \exp\left(-\tfrac{d^{(i)}_{l1}}{2} u^2_{lI} - \tfrac{b^*}{\sqrt{2}} u_l^I + \tfrac{b}{\sqrt{2}} u_l^I \right) =$$

$$\int \prod_{l\in\partial i/\ j} \frac{du_l^R du_l^I}{4Z_l^{(i)}} e^{\left(-\tfrac{d^{(i)}_{l1}}{2} u^2_{lR} + i\sqrt{2}(Re\, b) u_l^R - \tfrac{d^{(i)}_{l1}}{2} u^2_{lI} + i\sqrt{2}(Im\, b) u_l^I \right)}.$$

Thanks to the Hubbard-Stratonovich formula:

$$\int_{-\infty}^{+\infty} e^{-\frac{1}{2}ax^2 + iJx} dx = \left(\frac{2\pi}{a}\right)^{1/2} e^{-\frac{J^2}{2a}}$$

it has been possible to compute the integral of eq. 3.50:

$$\prod_{l\in\partial i/\ j} \frac{1}{4Z_l^{(i)}} \left(\frac{2\pi}{d^{(i)}_{l1}}\right)\left(\frac{2\pi}{d^{(i)}_{l2}}\right) e^{-\frac{|b|^2}{d^{(i)}_{l1}} - \frac{|c|^2}{d^{(i)}_{l2}}} = \prod_{l\in\partial i/\ j} e^{-\sum_{\alpha,\beta} J'^\dagger_\alpha U^l_{\alpha 1} \left(\frac{1}{d^{(i)}_{l1}}\right) U^{l\dagger}_{1\beta} J'_\beta - \sum_{\gamma,\delta} J'^\dagger_\gamma U^l_{\gamma 2} \left(\frac{1}{d^{(i)}_{l2}}\right) U^{l\dagger}_{2\delta} J'_\delta}$$

$$= \prod_{l\in\partial i/\ j} e^{-J'^\dagger U^l \begin{pmatrix} \frac{1}{d^{(i)}_{l1}} & 0 \\ 0 & \frac{1}{d^{(i)}_{l2}} \end{pmatrix} U^{l\dagger} J'} \tag{3.51}$$

It is important to stress that the following relation has been extensively used:

$$Z_l^{(i)} = \frac{\pi^2}{\det\left[\mathcal{C}_l^{(i)}\right]^{-1}}$$

Realisign that the matrix in the exponential is the inverse matrix of $D_l^{(i)}$, it has been possible to write:

$$\left[D_l^{(i)}\right]^{-1} = \left[U_l^\dagger \left(\mathcal{C}_l^{(i)}\right)^{-1} U_l\right]^{-1} = U_l^\dagger \mathcal{C}_l^{(i)} U_l.$$

and through this relation, eq. 4.8 has now become:

$$\prod_{l\in\partial i/\ j} e^{J'^\dagger_\alpha U^l_{\alpha\beta} U^{l\dagger}_{\beta\sigma} [\mathcal{C}_l^{(i)}]_{\sigma\lambda} U^l_{\lambda\delta} U^{l\dagger}_{\delta\gamma} J'_\gamma} = \prod_{l\in\partial i/\ j} e^{J'^\dagger_\sigma [\mathcal{C}_l^{(i)}]_{\sigma\lambda} J'_\lambda} \tag{3.52}$$

Finally, the recursive equations in eq. 3.44 have become a set of recursive equations for the matrices $\mathcal{C}_i^{(j)}$:

$$\mathcal{C}_i^{(j)} = \left[\kappa \mathbf{1}_2 + i(x\sigma_x - y\sigma_y) + F\left(\mathcal{C}^{(i)}_{\partial i/j}\right)\right]^{-1} \tag{3.53}$$

for all $i = 1, .., N$ and all $j \in \partial i$, where F is the matrix field :

$$F\left(\mathcal{C}^{(i)}_{\partial i/j}\right) = \sum_{l\in\partial i/j} (A^h_{il}\sigma_x - A^s_{il}\sigma_y)\mathcal{C}_l^{(i)}(A^h_{li}\sigma_x - A^s_{li}\sigma_y). \tag{3.54}$$

Eq. 3.45 has now given the "true" covariance matrices:

$$C_i = \left[\kappa \mathbf{1}_2 + i(x\sigma_x - y\sigma_y) + F\left(C^{(i)}_{\partial i}\right)\right]^{-1} \tag{3.55}$$

for all $i = 1, .., N$.
Performing the inverse of H in block form, it has been possible to hypothesize a tentative form for the structure of the matrices $\{C_i^{(j)}\}$:

$$C_i^{(j)} \equiv \begin{pmatrix} a_i^{(j)} & i\bar{b}_i^{(j)} \\ ib_i^{(j)} & d_i^{(j)} \end{pmatrix} \qquad \begin{matrix} a_i^{(j)}, d_i^{(j)} \in \mathbb{R}^+ \\ b_i^{(j)} \in \mathbb{C} \end{matrix}.$$

This form allows to obtain the spectral density in terms of the function $b_i \equiv b_i(z, \bar{z}, \kappa)$ as the mean value of eq. 3.41 has been computed using techniques of Quantum Field Theory [32]. By inserting different sources in the partition function Z_l and exploiting the following relation:

$$Z_l = \int \mathcal{D}\boldsymbol{\psi} \exp^{-\psi_l^\dagger [C_l^{-1}]\psi_l + \psi_l^\dagger J + J^\dagger \psi_l} = (\det C_l)\ \exp^{J^\dagger C_l J}$$

the mean value $< \psi^\dagger_{l\alpha}\psi_{l\beta} >$ has been computed as:

$$\frac{\partial^2}{\partial J_\alpha \partial J^\dagger_\beta} \ln Z_l \bigg|_{J=0=J^\dagger} = -C_l^{\beta\alpha}. \tag{3.56}$$

Considering the specific case of $< \psi_{l1}\psi_{l2} >$, the result for the spectral density has become:

$$\rho_A(z, \bar{z}) = -\frac{1}{\pi N} \lim_{\kappa\to 0} \sum_{i=1}^{N} \partial_{\bar{z}} b_i(z, \bar{z}, \kappa). \tag{3.57}$$

In order to compute the spectral density it is now necessary to deal with the partial derivatives $\partial_{\bar{z}}$, therefore, it is crucial to formulate a set of recursive equations for the partial derivatives of the covariance matrices $\{\partial_{\bar{z}}\mathcal{C}_i^{(j)}\}$. Using the set of relations in eq. 3.44, it has been possible to obtain:[8]

$$\partial_{\bar{z}}\mathcal{C}_i^{(j)} = -\mathcal{C}_i^{(j)}\left[\begin{pmatrix} 0 & 0 \\ i & 0 \end{pmatrix} + F(\partial_{\bar{z}}\mathcal{C}^{(i)}_{\partial i/\ j})\right]\mathcal{C}_i^{(j)}. \tag{3.58}$$

In a similar way, considering the equation 3.55, the derivative of the "true" covariance matrix at i is given by:

$$\partial_{\bar{z}}\mathcal{C}_i = -\mathcal{C}_i\left[\begin{pmatrix} 0 & 0 \\ i & 0 \end{pmatrix} + F(\partial_{\bar{z}}\mathcal{C}^{(i)}_{\partial i})\right]\mathcal{C}_i. \tag{3.59}$$

To synthesize the entire procedure, it can be said that the eq. 3.44 and eq. 3.58 represent the principal results associated to the application of the cavity method to a random non-Hermitian matrix A, which has an underlying network structure that can be considered treelike when many of its entries are equal to zero. The absence of loops guarantees the convergence of these equations in a short time, i.e. in a number of steps equal to the diameter of the tree, because the method has been built on a graph that share this feature. This ascertainment does not prevent the application of the method to graphs which are not trees, however, in this case it is necessary to halt the iterations when a pre-determined level of convergence has been reached.
In a more practical way, one iterates both sets of equations until the convergence is obtained and once the cavity covariance matrices and their derivatives for each node and neighbors are known, the "true" marginals are then recovered by eq. 3.55 and eq. 3.59 for each vertex. Finally the spectral density is obtained by the use of eq. 3.57.

3.5 The fully connected limit - Girko's Elliptic Law

To verify the correctness of the cavity approach also for ensembles with non-Hermitian random matrices, it has been derived the generalized Girko's law of Ref. [26]. A matrix A which obeys this law is characterized by having its elements A_{ij} drawn by a Gaussian distribution with zero mean and a correlation between the symmetrical elements, i.e. $\mathbb{E}(A_{ij}) = 0$ and $\mathbb{E}(A_{ij}A_{ji}) = \tau/N$. The parameter $\tau \in [0, 1]$ controls the degree of hermiticity: for $\tau = 1$, A is completely Hermitian and obeys Wigner's Law, whereas, for $\tau = 0$ A is maximally non-Hermitian. With these information it is possible to rewrite the matrix A in terms of statistically independent Hermitian matrices A^h and A^s in the following form:

$$A_{ij} = \sqrt{\frac{1+\tau}{2}}A^h_{ij} + i\sqrt{\frac{1-\tau}{2}}A^s_{ij}, \tag{3.60}$$

where the entries of A^h and A^s are random variables satisfying:

$$\mathbb{E}(|A^h_{ij}|^2) = \mathbb{E}(|A^s_{ij}|^2) = 1/N.$$

for each i and j. As in the fully connected limit for the previous chapter, it has been taken $c \to N$ and $N \to \infty$ which imply $C_i^{(j)} = C_i + O(1/c)$. Under these assumptions and

[8] It has been used the common relation for the derivative of the inverse matrix of A : $\partial_{\bar{z}}(A^{-1}) = -A^{-1}(\partial_{\bar{z}}A)A^{-1}$

considering eq. 3.44, it is straightforward to obtain an equation for the mean single-spin variance matrix $\mathbf{\Delta}$:[9]

$$\mathbf{\Delta}^{-1} = i(x\sigma_x - y\sigma_y) + \frac{1}{2}(1+\tau)\sigma_x\mathbf{\Delta}\sigma_x + \frac{1}{2}(1-\tau)\sigma_y\mathbf{\Delta}\sigma_y. \tag{3.61}$$

A possible form for $\mathbf{\Delta}$, which can solve the previous relation, corresponds to the usual structure of the covariance matrix:

$$\begin{pmatrix} a & i\bar{b} \\ ib & d \end{pmatrix}.$$

Therefore, the equation for $\mathbf{\Delta}$ can be equivalently written as a system of equations for a, b and d:

$$\begin{cases} ad - \tau b^2 - xb - iyb = 1 \\ iax - ay + ia\bar{b} + i\tau ab = 0 \\ ixd + dy + id(b + \tau\bar{b}) = 0 \end{cases}$$

When $d \neq 0$ the relation provides the following solutions:

$$\begin{cases} a = d = \sqrt{1 - \left(\frac{x}{1+\tau}\right)^2 - \left(\frac{y}{1-\tau}\right)^2} \\ b = \frac{-x}{1+\tau} + i\frac{y}{1-\tau} \end{cases}$$

which are defined inside the ellipse of equation $\left(\frac{x}{1+\tau}\right)^2 + \left(\frac{y}{1-\tau}\right)^2 < 1$.
When $d = 0$ and $a \neq 0$ the system does not have a unique solution for b as function of z and $\bar{z}$. Instead for $a = d = 0$ only the first equation of the system has to be solved and, by assuming $b = \beta(x - iy)$, two equations can be obtained for the real and imaginary part of the first equation:

$$\begin{cases} \tau\beta^2(x^2 - y^2) + \beta(x^2 - y^2) + 1 = 0 \\ \beta^2 = 0 \end{cases}$$

which, solving in $\bar{z}$, produces:

$$(\partial_{\bar{z}}\beta)\bar{z} + \beta = 0. \tag{3.62}$$

From these results and eq. 3.57, the spectral density can be easily found to be:

$$\rho_A(z, \bar{z}) = -\frac{1}{\pi}\partial_{\bar{z}} b(z, \bar{z}) = \begin{cases} \frac{1}{\pi(1-\tau^2)} & \text{when } \left(\frac{x}{1+\tau}\right)^2 + \left(\frac{y}{1-\tau}\right)^2 < 1 \\ 0 & \text{otherwise} \end{cases}$$

This exactly reproduces the Girko's Elliptic Law. It is relevant to point out that when $\tau = 0$ all correlations among the entries of the matrix A vanish and the Circular Law is retrieve as a special case of the Girko's Law.

[9] The parameter κ has been set to zero in order to simplify the analysis although still retaining the full validity of the method.

3.6 Numerical results

In order to prove the validity of this approach for ensembles of sparse random Non-Hermitian matrices, the cavity method has been used to analyze two different cases: (i) symmetrically connected Poissonian random graphs with average connectivity c and with asymmetric Gaussian edge with zero mean and variance $1/c$ and (ii) asymmetrically connected Poissonian graphs with edge weights drawn uniformly from a circle of radius $1/\sqrt{c}$. In fig. 3.2a it is shown the result for a given matrix built according to (i) and obtained using the belief propagation algorithm. Eq. 3.44 and eq. 3.58 have been iterated together until reaching the convergence and then the spectral density has been computed using eq. 3.55, eq. 3.59 and eq. 3.57.
It has been used "small" matrices of $S = 40$ size and the spectral density has been obtained averaging over 20 samples. 900 points have been used to build the bi-dimensional surface of fig. 3.2a. In fig.3.2b is shown the two-dimensional histogram for the eigenvalues obtained by direct diagonalization of a certain number of matrices with size $S = 40$. The histogram has been divided by the number of samples and the height of each bin specifies the average number of the associated eigenvalues. In the figure at the top left can be seen the histogram associated to the eigenvalues of 20 matrices. It is emphasized the presence of the central bin in (0,0) with a mean number of eigenvalues equal to the value of the peak obtained by the cavity method at the same point. At the top right of the same figure, it is shown the same histogram but the color map has been set to a lower set of values in order to enhance the small difference in the number of eigenvalues associated to each bi-dimensional bin. This figure shows how the histogram which should reconstruct the spectral density associated to a single matrix, in the statistical limit with S very large, is characterized by having many statistical fluctuations. It is also possible to point out that the support of the spectral distribution obtained by the cavity method coincides with the collocation of the eigenvalues extracted by the numerical diagonalization but shows that their changes over the distribution are not clear.
Subsequently, it has been considered an ensemble of 1000 matrices of size $S = 40$ to build the histogram of the averaged eigenvalues. Looking at the bottom of fig.3.2b, it is evident that the statistical fluctuations are far less dominant and the histogram of the averaged eigenvalues is comparable with the spectral density obtained by the cavity method. The comparison is very positive and shows excellent agreement between the two simulations. On a different note, this type of ensemble (with a certain sparsity parameter) clearly shows the high location of eigenvalues for the bi-dimensional bins associated with the real part of the eigenvalues equal to zero. This feature has been explained in the section 1.1 as an effect of the finite size of the matrices.

Considering the type of ensemble as (ii), it has been implemented matrices of size $S = 20$ with unitary weights and average connectivity $c = 2$. The results of the cavity method has been averaged over 50 samples. In fig. 3.3a is shown the comparison between the results obtained by the implementation of the cavity method and the bi-dimensional histogram of the eigenvalues extracted by the direct diagonalization. The central peak is well reconstructed as it is evident in the top left of fig. 3.3a. In order to enhance the contrast of the lower section of the histogram, fig. 3.3a (bottom) shows the same graph limiting the peak's height to a maximum value of 2. The same ensemble has been used to obtain the bi-dimensional histogram shown in fig. 3.3b (top right) limiting the values to a maximum 0.10 value. Similarly

to case (i), the results of the discrete distribution associated with the computed eigenvalues have not shown clearly the trend of the variation of the (discrete) spectral density.
However, increasing the statistic by averaging over 1000 matrices, the behavior of the discrete distribution becomes more evident as well as comparable with the spectral density obtained by the cavity method. The central bin has a significant high value and the resolution of the eigenvalues distribution shows a clearer contrast when considering the color map up to a maximum value 0.10. The high density of the eigenvalues with real part equal to zero is an effect of the finite size of the matrices which is not evident in the cavity approach results.
The Python code implemented for this analysis is reported in Appendix D.
It is possible to notice that the ensembles of both cases satisfy the conditions for Girko's law in the limit $c \to \infty$. However, it is evident from fig. 3.2 and fig. 3.3, for finite c, that the spectral densities are dramatically different among each other and deviate from the limiting case of Girko's law.

3.7 Conclusion

In this section it has been answered the question of determining the mean spectral density of an ensemble of sparse non-Hermitian random matrices. The cavity method has been used to this aim following the same steps used for the Hermitian case. In fact, the problem of considering non-Hermitian matrices has only complicated the mathematical tools necessary to obtain a Gaussian integral which is a fundamental part of obtaining a correct spectral density evaluation.
The cavity method implemented by belief propagation leads to a fast convergence of the mean spectral density for matrices of a given size whose results are in good agreement with those obtained by direct diagonalization.
In the case of dense matrices (both Hermitian and non-Hermitian), past studies who have used techniques of supersymmetry and replica analysis have found noticeable success, however, applied to sparse matrices, these approaches have not been so fruitful, leading to a set of saddle-point equations which have resisted computational solution for over 17 years. In the study of ensemble average, the cavity and replica methods are known to be equivalent and the solutions obtained are common to all approaches and can also be derived through a careful treatment of the aforementioned saddle-point equations.
The power of the methods is evident for the good analytic form of the mean spectral density in comparison to the histogram of the eigenvalues obtained computationally.
In the following chapter it is shown how to exploit this approach in order to obtain some direct information about the spectral distribution dependent on the characteristics of the random matrices. The analytic results of the cavity method permit to understand how the location of the rightmost eigenvalue(s) is influenced by the assumed values of the parameters which characterize the structure of the random matrix.

a)

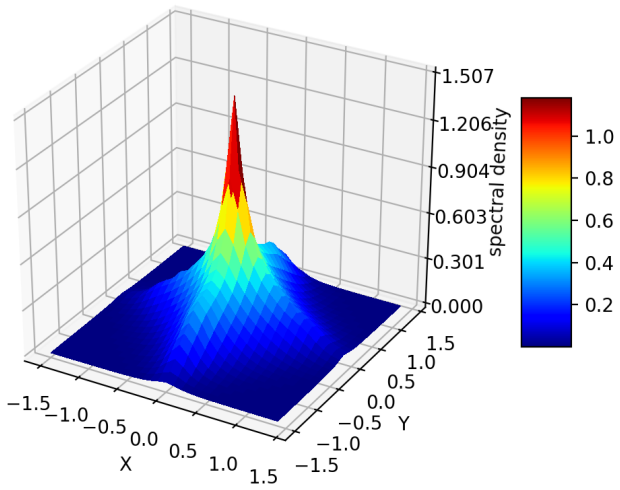

b)

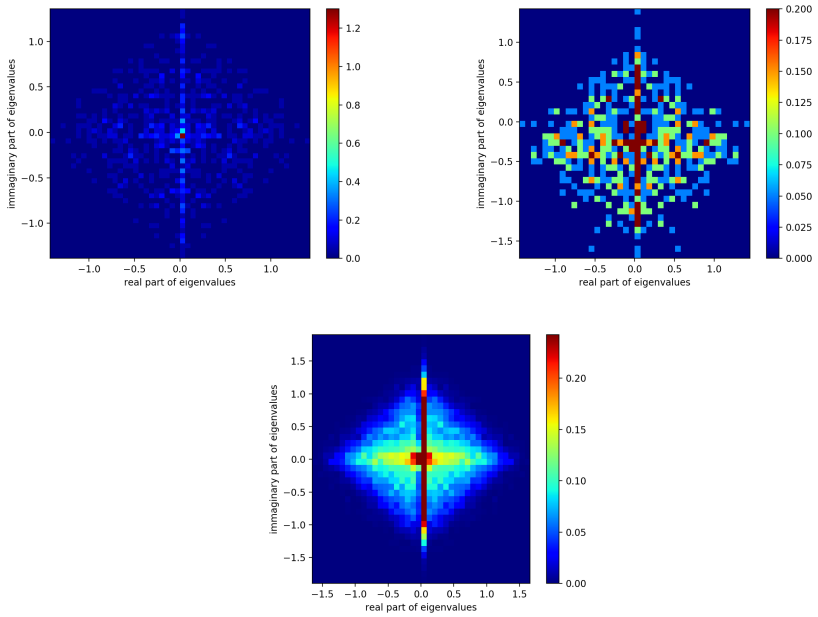

Figure 3.2: Fig.a shows the result obtained by the cavity approach for the spectral density of symmetric Poissonian graphs of size $S = 40$ with asymmetric Gaussian edge weights (with zero mean and variance $1/c$) averaged over 20 samples. The X axis is relative to the real part of the eigenvalues and the Y axis to its imaginary part. Fig.b represents a sequence of bi-dimensional histograms created with the eigenvalues obtained by numerical diagonalization. The top left figure shows that the central bin has the same height as the value of the peak in fig.a. The top right figure underlines the preponderant statistical fluctuations for a small relative ensemble of matrices used to obtain the distribution of averaged eigenvalues (equal to that used to average the spectral density obtained by each matrix). The bottom figure represents the results obtained considering an ensemble of 1000 matrices clearly depicting a good accordance with fig.a.

a)

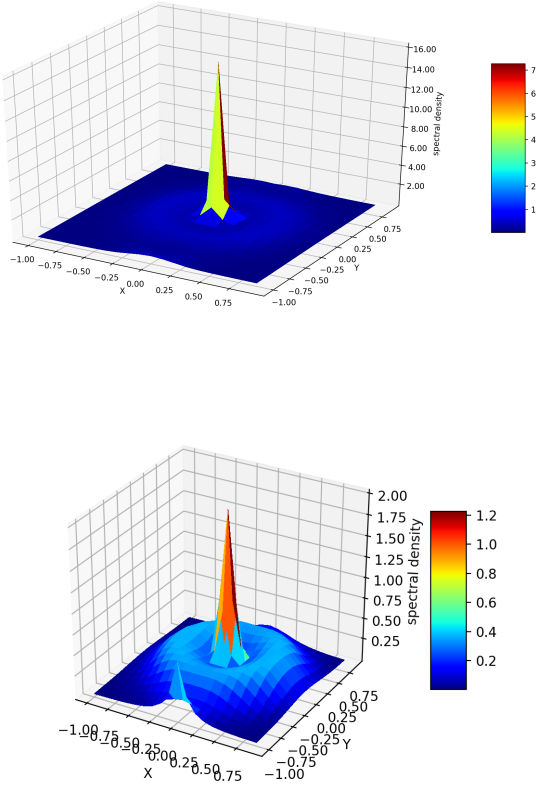

b)

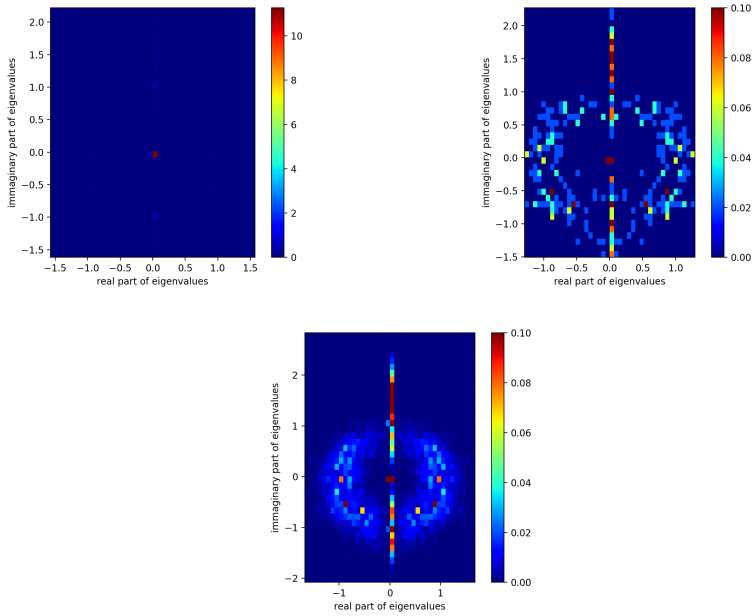

Figure 3.3: Fig.a shows the results obtained by the implementation of the cavity method for the spectral density of asymmetric Poissonian graphs with unitary edge weights and average connectivity $c = 2$. The edges are drawn uniformly from the circle of radius $1/\sqrt{c}$. Fig.b shows the results of the direct diagonalization where the top figures represent the bi-dimensional histograms for an ensemble of 50 matrices of size $S = 20$. The image at the bottom shows the results obtained averaging over 1000 matrices.

Chapter 4

An application to the ecological communities

In the previous chapters, it has been shown that the cavity method is a helpful tool to study the statistical limit of an ensemble of large matrices built through parameters which characterize its randomness, average connectivity and the relation between its simmetrical elements. The close connection between the values of these parameters, the size of the matrices and the shape of distribution of the eigenvalues, captures a wide interest in the scientific community for a large range of applications, which includes epidemiology [33], neuroscience[34] and complex system in general[35].
A problem of particular interest in the ecological field is to study the effect of modularity on local stability of ecological dynamical systems. The goal of this research is to investigate how a block structure of the community matrix influences the dynamics of the system and to understand which parameter have effects on the stability of ecological networks. Unfortunately, a systematic classification of the different effects generated by the possible complexities of the matrix is still lacking, also because the analysis is made more complicated by the combination of many contributions. In literature there are opposite results which do not simplify the analysis of the issue.
In this context the cavity method has provided a valid contribution thanks to a slightly different notation of the cavity equations based on quaternions, rather than Pauli matrices [36].
This approach guarantees the correctness of the mathematical passages used to search the spectral density of large block-structured matrices because many entries are null and for sparse matrices the method is a good approximation of the statistical limit of spectral distribution.
In this thesis, thanks to the cavity method, it has been possible to study, in an alternative way, the spectrum of a random matrix. This has allowed to obtain an analytic result in two particular cases concerning the modular organization. The explicit solutions for the support of the spectrum of the matrix have permitted to justify the qualitative behavior of the simulations, giving a direct relation between the parameters of the construction and the information about the stability of the block-structured random matrix.

4.1 Building community matrices

The aim of this chapter is to study the stability of a community matrix M, describing a continuous-time, dynamical ecological system composed by S populations, resting at a feasible equilibrium point. The matrix is the result of the multiplication element-by-element between a matrix of interaction strengths W, in which its elements W_{ij} represent the influence of species j on species i around equilibrium, and the adjacency matrix of an undirected graph K. In symbolic term $M = W \circ K$.
It can be demostrated that setting $M_{ii} = 0$ the investigated qualitative results do not change. Since the diagonal elements of M are nothing but the self-interactions, the study can be restricted to the inter-species effects.
The pair of elements (W_{ij}, W_{ji}) is drawn from a bivariate distribution, with identical marginals, determined by the mean $\mu = \mathbb{E}[W_{ij}] = \mathbb{E}[W_{ji}]$, the variance $\sigma^2 = \mathbb{E}[(W_{ij}-\mu)^2] = \mathbb{E}[(W_{ji}-\mu)^2]$ and the correlation $\rho = (\mathbb{E}[W_{ij}W_{ji}]-\mu^2)/\sigma^2$. The range of the possible values of these parameters covers all types of interactions between the species from preponderantly predator-prey to predominated by competition or mutualism[37].
The matrix K is composed by elements equal to 1 or 0, depending on whether the species i and j are connected by an interaction or not. So, the interactions in W are active for a pair of elements in symmetrical positions with respect the diagonal if $K_{ij} = K_{ji} = 1$.
In this study it has been assumed that K is a particular block-structured matrix: there are two subsystems (this means that the S populations are grouped in two ecological communities) of sizes αS and $(1 - \alpha)S$ respectively (with $\alpha \leq 1/2$). The species which are in the same subsystem interact with probability C_w, called within-subsystem connectance, while the species which are in different subsystems interact with probability C_b, called between-subsystem connectance.
Hence, the values of C_w and C_b define how much the structure is modular or anti-modular. For example, it is defined modular (or anti-modular) structure whenever $C_w > C_b$ (or $C_b > C_w$) and are expected more (or less) interactions between species of the same group than of different groups.
It is intuitive to understand that $C_w = C_b$ falls into the well-studied case of random ecological community that is the 'unstructured' system analyzed by May et al.[38][37]. With this parameterization it is possible to distinguish easily between two extreme cases: $C_b = 0$ for a perfectly modular network (the interactions accur exclusively within the same subsystem) and $C_w = 0$ for a perfectly anti-modular or bipartite network (only interactions between species belonging to different subsystems are present). See figure 4.1.

It is convenient to define a parameter which incorporates the degree of modularity associated to a network [39][40] as follows:

$$Q = \frac{L_w - \mathbb{E}[L_w]}{L_w + L_b} \tag{4.1}$$

where L_w is the observed number of interactions within the subsystems, L_b the observed number of between-subsystem interactions and $\mathbb{E}[L_w]$ is the number of interactions between species belonging to the same subsystems in an unstructured random network. Values of $Q > 0$ ($Q < 0$) indicate that more (less) interactions within-subsystem are observed than expected by chance. To calculate $\mathbb{E}[L_w]$ it is necessary to select a reference model for network structure and it has been chosen the Erdős-Rényi random graph[41]. The range of acceptable values for Q depends on the reference model, on α and on the overall connectance C (that is the overall density of interactions in K).

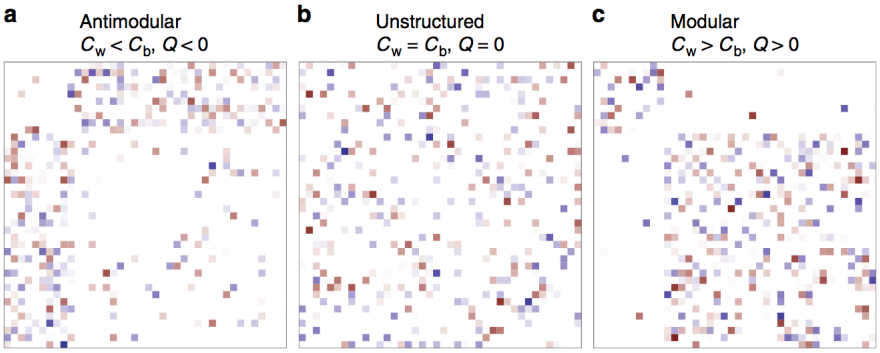

Figure 4.1: The modularity parameter incorporates the effects, on the network structure, of the within-group connectance C_w and the between-group connectance C_b. It is possible to obtain different community matrices by changing the modularity: matrices where the interactions occur mostly between species in different groups ($Q < 0, \mathbf{a}$), completely randomly ($Q = 0, \mathbf{b}$) or mostly within the same subsystem ($Q > 0, \mathbf{c}$). The colours represent, in this example, the type of interactions distinguishing between negative coefficients (red) and positive coefficients (blue). The intensity of the colour is proportional to the coefficient values, that have been drawn in pairs from a bivariate distribution with similar marginal defined by $\mu = 0$, $\sigma = 1/2$ and correlation $\rho = -3/4$.

In order to study the effect of the stability on a community matrix it is necessary to distinguish from the effect on the stability of a block structure (described by K through α, C and Q) and the effect due to the interaction strengths (modelled by W). The case $Q = 0$ has been greatly studied and for this type of random matrices the stability can be gotten analytically.

4.2 Effect of modularity on stability

The stability parameter, associated to a community matrix, is described by the real part of the 'rightmost' eigenvalue of M that must to be compared with the same value found for $\tilde{M}$, a matrix with exactly the same coefficients but re-arranged to create a random network structure($Q = 0$). $\mathrm{Re}(\lambda_{M,1})$ is a measure of stability, since it expresses the amount of self-regulation necessary to stabilize the equilibrium[38][37].
The effect of the modularity Q on the community stability can be measured as the ratio:

$$\Gamma = \frac{\mathrm{Re}(\lambda_{M,1})}{\mathrm{Re}(\lambda_{\tilde{M},1})}, \tag{4.2}$$

for a given choice of α, ρ and C and without loss of generality σ^2 has been set equal to 1. Values $\Gamma < 1$ are obtained when the block structure helps stabilizing the community, while $\Gamma > 1$ means a destabilizing effect. A study on how the modularity influences the stability was shown in [42] in which the same modularity Q, with the parameters α, ρ, σ^2 and overall connectance C fixed, can have a completely different effect on the stability, depending on the value of μ.
The analytical approach, used to understand how the stability depends on the construction parameters of the block-structured matrix, is based on the study of the distribution of

eigenvalues in the complex plane. If there are two subsystems, the spectrum of M is composed of a "bulk" of eigenvalues and up to two 'outlier' real eigenvalues.
The presence of the outliers depends on the sign of the interaction strength. In the following sections it will be shown the locations of these outliers in the particular case of $\alpha = 1/2$. Anyway, the considerations about these approximate positions are valid for every $\alpha < 1/2$. Despite this, the others parameters affect in different ways the resultant stability according to the combination of the values of α, ρ and μ.
This important consideration, that has emerged from both simulations and mathematical analysis, has brought to consider that the relantionship between network structure and local stability is much more complex than previously hypothesized[38][43]. A given structure is not stabilizing or destabilizing *per se* but it is so only under certain specific conditions.

4.3 Methods

In the community matrix M the elements are functions of the population densities of an unknown dynamical system around a feasible equilibrium point. Let us consider the case of random ecological networks with block structure. The pairs (W_{ij}, W_{ji}) are drawn independently from a bivariate normal distribution with means $(\mu, \mu)^T$ and covariance matrix:

$$\Sigma = \sigma^2 \begin{pmatrix} 1 & \rho \\ \rho & 1 \end{pmatrix}.$$

The matrix K is characterized by four parameters: S, α, C e Q. What we aim for is to have the pair (K_{ij}, K_{ji}) to be (1,1) with probability C_w if $\gamma_i = \gamma_j$ and with probability C_b if $\gamma_i \neq \gamma_j$ in function of α , Q and C (density of the nonzero elements). The overall connectance C is:

$$C = \frac{2L}{S(S-1)} = \frac{2(L_w + L_b)}{S(S-1)} \tag{4.3}$$

which is then associated to a matrix with a fixed number of non null entries.
The type of *random graph* in which is fixed only the number of vertices(S) (in this context correspondent to the number of populations) and the number of edges (L) is indicated by its mathematical name $G(S, L)$. Another entirely equivalent definition of the model is obtained when the network is created by choosing uniformly random among the set of simple graphs with exactly n vertices and L edges.
The model used to describe the ensemble of matrices with $Q = 0$ is the "Erdős-Rényi random graph" which is called $G(S, p)$. In $G(S, p)$ is fixed the probability, rather than the number, of the edges between vertices. Again there are S vertices, but now an edge is placed between each distinct pair with independent probability p.
When $S \to \infty$ the two type of ensembles are the same if $p = \frac{2L}{S(S-1)} = C \to 2L/S^2$. With n_w is indicated the total number of matrix elements which can be linked with another element of the same group and with n_b is indicated the number of species, belonging to a different species, that can interact. In this limit:

$$n_w = \frac{S^2\alpha^2 + S^2(1-\alpha)^2}{2}, \quad n_b = S^2\alpha(1-\alpha) \tag{4.4}$$

Knowing that $\mathbb{E}(L_w) = Cn_w$ and $\mathbb{E}(L_b) = Cn_b$, and using the definition of modularity, can be obtained as follow:

$$C_w = \frac{L_w}{n_w} = \frac{C(\frac{QS^2}{2} + n_w)}{n_w} = C\left(1 + \frac{Q}{\alpha^2 + (1-\alpha)^2}\right) \tag{4.5}$$

$$C_b = \frac{L_b}{n_b} = \frac{L - Cn_w - \frac{QCS^2}{2}}{n_b} = C\left(1 - \frac{Q}{2\alpha(1-\alpha)}\right) \tag{4.6}$$

which represent the probability to find a link within the diagonal blocks for C_w and the probability to find a link within the non-diagonal blocks for C_b. Note that, given the Erdős-Rényi reference model, the values of Q that are attainable depend on both α and C:

$$\frac{\max(C - 2\alpha(1-\alpha), 0) - C(\alpha^2 + (1-\alpha)^2)}{C} \leq Q \leq \frac{\min(C, \alpha^2 + (1-\alpha)^2) - C(\alpha^2 + (1-\alpha)^2)}{C}$$

4.3.1 Spectrum of block-structured matrices

In this section it is presented the mathematical treatment about the preliminary preparation of the spectrum study of block-structured matrices.
To do the subsequent derivations it has been adopted a slightly more general notation. The matrix M is considered, with the diagonal coefficients $M_{ii} = 0$ and the off-diagonal coefficients independently sampled in pairs as:

$$(M_{ij}, M_{ji}) \sim \begin{cases} \mathcal{Z}_w\left(\begin{pmatrix}\mu_w\\ \mu_w\end{pmatrix}, \sigma_w^2\begin{pmatrix}1 & \rho_w\\ \rho_w & 1\end{pmatrix}\right) & \text{if} \quad \gamma_i = \gamma_j \\ \mathcal{Z}_b\left(\begin{pmatrix}\mu_b\\ \mu_b\end{pmatrix}, \sigma_b^2\begin{pmatrix}1 & \rho_b\\ \rho_b & 1\end{pmatrix}\right) & \text{if} \quad \gamma_i \neq \gamma_j \end{cases} \tag{4.7}$$

Equation4.7 shows that the pairs (M_{ij}, M_{ji}) have been taken by two different distribution: $\mathcal{Z}_w$ when i and j belong to the same subsystem and $\mathcal{Z}_b$ when i and j belong to different subsystems, instead of considering, as done previously, that the pairs (M_{ij}, M_{ji}) are zero with probability $1 - C_w$ (case $\gamma_i = \gamma_j$) or probability $1 - C_b$ (case $\gamma_i \neq \gamma_j$) and that the nonzero pairs are sampled from a bivariate distribution defined by the parameters μ, σ^2 and ρ.
It is not necessary to specify the entire form of the distributions $\mathcal{Z}_w$ and $\mathcal{Z}_b$ because of the 'universality' property[9][44]: once fixed the mean and the covariance matrices of $\mathcal{Z}_w$ and $\mathcal{Z}_b$, and provided that the fourth moment of each distribution is bounded, any choice of distributions yields the same result for $S \to \infty$.
The parameters of these distributions can be calculated in relation to the parameters of the originary parameterization and the connectances between and within subsystems [10]:

$$\begin{aligned}
\mu_w &= C_w\mu \\
\mu_b &= C_b\mu \\
\sigma_w^2 &= C_w(\sigma^2 + (1-C_w)\mu^2) \\
\sigma_b^2 &= C_b(\sigma^2 + (1-C_b)\mu^2) \\
\rho_w &= \frac{\rho\sigma^2 + (1-C_w)\mu^2}{\sigma^2 + (1-C_w)\mu^2} \\
\rho_b &= \frac{\rho\sigma^2 + (1-C_b)\mu^2}{\sigma^2 + (1-C_b)\mu^2}.
\end{aligned} \tag{4.8}$$

With these replacements the 'effective' parameters have been obtained. These dictate the distribution shape of the eigenvalues of M because the connectances are absorbed. For the pairs (W_{ij}, W_{ji}) it is chosen a bivariate normal distribution.
The next goal is to obtain the distribution of the eigenvalues of M when S is very large. Following the study of Allesina *et al.*[45], the matrix M can be written as a sum of two matrices, $M = A + B$, where A is a matrix with block structure whose elements are

$$A_{ij} = \begin{cases} \mu_w & \text{if} \quad \gamma_i = \gamma_j \\ \mu_b & \text{if} \quad \gamma_i \neq \gamma_j \end{cases}$$

and B is obtained as the difference $B = M - A$. The diagonal elements of B are $B_{ii} = \mu_w$, while the off-diagonal elements are characterized by $\mathbb{E}[B_{ij}] = 0$, and $\mathbb{E}[B_{ij}B_{ji}] = \rho_w\sigma_w^2$ (when $\gamma_i = \gamma_j$) or $\mathbb{E}[B_{ij}B_{ji}] = \rho_b\sigma_b^2$ (when $\gamma_i \neq \gamma_j$).
This separation of the matrix M permits to obtain a bulk of eigenvalues from the spectrum of B, while the outlier eigenvalues of M are given by the nonzero eigenvalues of A modified by a small correction[46]. Based on the values of S, α, μ_w, μ_b the only two eigenvalues that can be different from zero, are easily computed (for more details refer to the C.1):

$$\lambda_{A,1-2} = \frac{S}{2}\Big(\mu_w \pm \sqrt{(1-4\alpha(1-\alpha))\mu_w^2 + 4\alpha(1-\alpha)\mu_b}\Big) \tag{4.9}$$

They are both zero when $\mu = 0$ and thus the stability is determined, independently by Q, by rightmost eigenvalue(s) in the bulk. They are one zero and the other nonzero when $Q = 0$ and then $\mu_w = \mu_b = \mu \neq 0$ (if $\mu < 0$ the outlier lies to the left of the bulk and has limited effects on stability; if $\mu > 0$ the outlier lies to the right of the bulk and therefore it determines stability).
In the case $Q > 0$ the spectrum presents two outliers, both lie either to the right ($\mu > 0$) or the left ($\mu < 0$) of the bulk.
In the bipartite case, for any $\mu \neq 0$ there is an outlier to the right and one to the left of the bulk.
Then these are the approximate locations of the two outlier eigenvalues of M. Since the exact location depends also on B, the spectrum of B has been studied in full generality using the cavity method.

4.4 Spectral distribution of B

The aim of this section is to find the spectral density of B characterized by the parameters specified above in an analytic form and then to understand how the distribution of eigenvalues

is influenced by the variations of these parameters. In the context of large S and high connectivity, the cavity solution is expected to be exact. The advantage of the application of this approach is to obtain a simple set of equations for the diagonal entries of Green's function of B through its quaternionic parameterization. Thanks to specific approximations, it is possible to get analytic expressions, for some particular cases, for the study of the spectral density.
The spectral density in the case of Non-Hermitian random matrices, can be defined (writing $\lambda = x + iy$) as:

$$\rho(x,y) = \frac{1}{S}\sum_{i=1}^{S}\delta(x - \mathrm{Re}(\lambda_i))\delta(y - \mathrm{Im}(\lambda_i)) \tag{4.10}$$

While for Hermitian matrices the resolvent is a complex function since the eigenvalues are real values, in the non-Hermitian case the eigenvalues are complex and the resolvent is a quaternion function:

$$\mathcal{G}(\mathbf{q}) = \frac{1}{S}\sum_{i}(\lambda_i - \mathrm{q})^{-1} \tag{4.11}$$

where $\mathbf{q}$ is a quaternion (for more details about the quaternions refers to C.2). The resolvent can be expressed in terms of the spectral density:

$$\mathcal{G}(\mathbf{q}) = \int dxdy\ \rho(x,y)(x + iy - \mathbf{q})^{-1} \tag{4.12}$$

and the spectral density can be easily obtained from the resolvent (the proof of this procedure is in C.3):

$$\rho(x,y) = -\frac{1}{\pi}\lim_{\epsilon\to 0^+}\mathrm{Re}\left(\frac{\partial}{\partial\bar{\lambda}}\mathcal{G}(\lambda + \kappa j)\right)\Bigg|_{\lambda = x+iy} \tag{4.13}$$

where it has been used the notation:

$$\frac{\partial}{\partial\bar{\lambda}} := \frac{1}{2}\left(\frac{\partial}{\partial x} + i\frac{\partial}{\partial y}\right) \tag{4.14}$$

In order to prepare the framework for the mapping between Pauli matrices and quaternions, it has been introduced the resolvent matrix:

$$\mathbf{G} = (\mathbf{B} - \mathbf{q})^{-1} \tag{4.15}$$

where $\mathbf{q}$ is the quaternion in the matricial rapresentation:

$$\mathbf{q} = \lambda + \kappa\mathbf{j} = \begin{pmatrix} \lambda & i\kappa \\ i\kappa & \bar{\lambda} \end{pmatrix} \tag{4.16}$$

which derives from a more general matricial representation:

$$\mathbf{q} = z + w\mathbf{j} = \begin{pmatrix} z & iw \\ +i\bar{w} & \bar{z} \end{pmatrix} \tag{4.17}$$

Meanwhile $\mathbf{B}$ is a $2SX2S$ block-matrix with structure:

$$\mathbf{B}_{ij} = \begin{pmatrix} B_{ij} & 0 \\ 0 & B_{ji} \end{pmatrix} \tag{4.18}$$

In the end, the resolvent can be written as:

$$\mathcal{G}(\mathbf{q}) = \frac{1}{S}\sum_i \mathbf{G}_{ii}(\mathbf{q}). \tag{4.19}$$

The entries $\mathbf{G}_{ii}$ can be connected, in their quaternionic form, to the covariance cavity matrices 3.4 which provide a solution to the recursive set of equations 3.44 and 3.54. The following mapping between Pauli matrices and quaternions has been used (see the matricial representation in 4.17):

$$\begin{cases} \mathbf{i} : i\sigma_x \\ \mathbf{j} : i\sigma_y \\ \mathbf{k} : i\sigma_z \end{cases}$$

and with these substitutions it is possible to make the identification:

$$\kappa \mathbf{1}_2 + i(x\sigma_x - y\sigma_y) = \begin{pmatrix} \kappa & i\lambda \\ i\bar{\lambda} & \kappa \end{pmatrix} \equiv \kappa + \lambda \mathbf{j} \tag{4.20}$$

and by using the identity:

$$\kappa + \lambda \mathbf{j} = \mathbf{i}(\lambda + \kappa \mathbf{j})\mathbf{j} \tag{4.21}$$

the equations 3.44 and 3.54 become:

$$C_i^{(j)} = \Big[\sum_{l\neq i,j} \begin{pmatrix} 0 & A_{il} \\ A_{li} & 0 \end{pmatrix} C_l^{(i)} \begin{pmatrix} 0 & A_{li} \\ A_{il} & 0 \end{pmatrix} + \mathbf{i}\,\mathbf{q}\,\mathbf{j}\Big]^{-1} \tag{4.22}$$

where $A_{li} = \bar{A_{li}} = A_{il}^h - iA_{il}^s$ due to the fact that in this case the community matrix has real entries. The equation 4.22 can be rewritten in the following form:

$$C_i^{(j)} = \left[\mathbf{i}\Big\{\sum_{l\neq i,j} \mathbf{i}\begin{pmatrix} 0 & A_{il} \\ A_{li} & 0 \end{pmatrix} C_l^{(i)} \begin{pmatrix} 0 & A_{li} \\ A_{il} & 0 \end{pmatrix}\mathbf{j} + \mathbf{q}\Big\}\mathbf{j}\right]^{-1} \tag{4.23}$$

and by noting that:

$$\begin{pmatrix} 0 & A_{il} \\ A_{li} & 0 \end{pmatrix} = -i\,\mathbf{i}\begin{pmatrix} A_{il} & 0 \\ 0 & A_{li} \end{pmatrix}\mathbf{j} \tag{4.24}$$

it becomes:

$$C_i^{(j)} = \left[\mathbf{i}\Big\{\sum_{l\neq i,j} \mathbf{B}_{il}\,\mathbf{j}\,(-C_l^{(i)})\,\mathbf{i}\,\mathbf{B}_{li} + \mathbf{q}\Big\}\mathbf{j}\right]^{-1} = \mathbf{j}^{-1}\left[\sum_{l\neq i,j} \mathbf{B}_{il}\,\mathbf{j}\,(-C_l^{(i)})\,\mathbf{i}\,\mathbf{B}_{li} + \mathbf{q}\right]^{-1}\mathbf{i}^{-1} \tag{4.25}$$

Finally, leading $\mathbf{i}$ and $\mathbf{j}$ to the first member of equation and multiplying all for -1 , the final expression is obtained:

$$-\,\mathbf{j}\,C_i^{(j)}\,\mathbf{i} = -\Big[\sum_{l\neq i,j} \mathbf{B}_{il}\,(-\mathbf{j}\,C_l^{(i)}\,\mathbf{i})\,\mathbf{B}_{li} + \mathbf{q}\Big]^{-1}. \tag{4.26}$$

The direct connection between the diagonal entries of $\mathbf{G}^{(i)}$, resolvent of the matrix obtained by removing row and column i from B, and the covariance matrix is:

$$\mathbf{G}_{ii}^{(j)} = -\mathbf{j}\, C_i^{(j)}\, \mathbf{i}. \tag{4.27}$$

By solving iteratively:

$$\mathbf{G}_{ii}^{(j)} = -\Big(\mathbf{q} + \sum_{l\neq i,j} \mathbf{B}_{il}\mathbf{G}_{ll}^{(i)}\mathbf{B}_{li}\Big)^{-1} \tag{4.28}$$

the diagonal entries of $\mathbf{G}$ of the matrix B can be obtained:

$$\mathbf{G}_{ii} = -\Big(\mathbf{q} + \sum_{l\neq i} \mathbf{B}_{il}\mathbf{G}_{ll}^{(i)}\mathbf{B}_{li}\Big)^{-1} \tag{4.29}$$

and, finally through 4.13, it is possible to evaluate the spectral density.

4.5 Cavity equations for block-structured matrices

In the large S limit several semplifications of the equations 4.28 and 4.29 can be considered. In this way, the calculation of the diagonal entries of $\mathbf{G}$ becomes analytical, in the meaning that it is possible to get a closed equation and, therefore, equation 4.28 is not necessary anymore.
These approximations are:

1. At the leading order in S the right side of 4.28 is identical for every l in the same group (because they are drawn by the same probability distribution) and, therefore, $\mathbf{G}_{ll} = \mathbf{G}_{\gamma_l}$ can be written.

2. By removing a single node i, the leading order behavior of the system does not change because its size is large and so the relations $\mathbf{G}_{ll}^{(i)} = \mathbf{G}_{ll} = \mathbf{G}_{\gamma_l}$ can be used.

3. By applying the law of large numbers, the terms of the sum in 4.29 can be approximated by the mean value:
$$\sum_{l\neq i} \mathbf{B}_{il}\mathbf{G}_{ll}^{(i)}\mathbf{B}_{li} \approx \mathbb{E}\Big(\sum_{l} \mathbf{B}_{il}\mathbf{G}_{\gamma_l}\mathbf{B}_{li}\Big) \tag{4.30}$$

By using these approximations and the matrix representation of quaternions with the notation $\mathbf{G}_\gamma = r_\gamma + \beta_\gamma\, j$, it can be obtained:

$$\mathbf{B}_{il}\mathbf{G}_{\gamma_l}\mathbf{B}_{li} = \begin{pmatrix} B_{il} & 0 \\ 0 & B_{li} \end{pmatrix}\begin{pmatrix} r_{\gamma_l} & \beta_{\gamma_l} \\ \bar{\beta}_{\gamma_l} & \bar{r}_{\gamma_l} \end{pmatrix}\begin{pmatrix} B_{li} & 0 \\ 0 & B_{il} \end{pmatrix} = \begin{pmatrix} B_{il}B_{li}r_{\gamma_l} & B_{il}^2\beta_{\gamma_l} \\ B_{li}^2\bar{\beta}_{\gamma_l} & B_{il}B_{li}\bar{r}_{\gamma_l} \end{pmatrix}. \tag{4.31}$$

In the case of two blocks, γ_l can assume only two values and according to the membership to the first group ($\gamma_l = 1$) or the later group ($\gamma_l = 2$), the element B_{il} represents the interaction between species belonging to the same group or to different groups. In order to simplify the evaluation of the mean values of the elements in the matrix 4.31, it can be considered an arbitrary vector with components z_{γ_l}, which encodes r_{γ_l} and β_{γ_l} . This vector can have only two distinct values z_1 and z_2 depending on the membership of the species taken into account.

$$\mathbb{E}\Big(\sum_l B_{il}^2 z_{\gamma_l}\Big) = \sum_l \mathbb{E}(B_{il}^2) z_{\gamma_l} = \sum_l \Big(\delta_{\gamma_i,\gamma_l}\sigma_w^2 z_{\gamma_l} + (1-\delta_{\gamma_i,\gamma_l})\sigma_b^2 z_{\gamma_l}\Big) \tag{4.32}$$

Considering $\gamma_i = 1$, the result is:

$$\mathbb{E}\Big(\sum_l B_{il}^2 z_{\gamma_l}\Big) = S\ \alpha\ \sigma_w^2 z_1 + S\ (1-\alpha)\sigma_b^2 z_2 \quad \text{if} \quad \gamma_i = 1 \tag{4.33}$$

where α is the fraction of elements belonging to the first block. For $\gamma_l = 2$ it can, instead, be obtained:

$$\mathbb{E}\Big(\sum_l B_{il}^2 z_{\gamma_l}\Big) = S\ (1-\alpha)\sigma_w^2 z_2 + S\alpha\sigma_b^2 z_1 \quad \text{if} \quad \gamma_i = 2. \tag{4.34}$$

Similarly, knowing the expectation value of $B_{il}B_{li}$, it can be found:

$$\begin{aligned}
\mathbb{E}\Big(\sum_l B_{il}B_{li} z_{\gamma_l}\Big) &= S\alpha\rho_w\sigma_w^2 z_1 + S(1-\alpha)\rho_b\sigma_b^2 z_2 \quad \text{if} \quad \gamma_i = 1, \\
\mathbb{E}\Big(\sum_l B_{il}B_{li} z_{\gamma_l}\Big) &= S(1-\alpha)\rho_w\sigma_w^2 z_2 + S\alpha\rho_b\sigma_b^2 z_1 \quad \text{if} \quad \gamma_i = 2.
\end{aligned} \tag{4.35}$$

By making use of these informations, the expectation value of the sum over l of equation 4.31 elements, can be written as:

$$\mathbb{E}\Big(\sum_l \mathbf{B}_{il}\mathbf{G}_{\gamma_l}\mathbf{B}_{li}\Big) = S\alpha\sigma_w^2\begin{pmatrix}\rho_w r_1 & \beta_1 \\ \bar{\beta}_1 & \rho_w\bar{r}_1\end{pmatrix} + S(1-\alpha)\sigma_b^2\begin{pmatrix}\rho_b r_2 & \beta_2 \\ \bar{\beta}_2 & \rho_b\bar{r}_2\end{pmatrix} \quad \text{if} \quad \gamma_i = 1 \tag{4.36}$$

By introducing the relations:

$$\mathbf{\Sigma}_w = S\sigma_w^2(\rho_w + \mathbf{j}) \quad \text{and} \quad \mathbf{\Sigma}_b = S\sigma_b^2(\rho_b + \mathbf{j}) \tag{4.37}$$

where $\rho_w + \mathbf{j}$, and similarly $\rho_b + \mathbf{j}$, corresponds to a quaternion with matricial form:

$$\begin{pmatrix}\rho_w & 1 \\ 1 & \rho_w\end{pmatrix}$$

the previous expression can be written in a compact way by using the Hadamard product (element by element product) between matrices:

$$\mathbb{E}\Big(\sum_l \mathbf{B}_{il}\mathbf{G}_{\gamma_l}\mathbf{B}_{li}\Big) = \alpha\mathbf{\Sigma}_w \circ \mathbf{G}_1 + (1-\alpha)\mathbf{\Sigma}_b \circ \mathbf{G}_2 \quad \text{if} \quad \gamma_i = 1. \tag{4.38}$$

A similar expression can be obtained in the case of $\gamma_i = 2$:

$$\mathbb{E}\Big(\sum_l \mathbf{B}_{il}\mathbf{G}_{\gamma_l}\mathbf{B}_{li}\Big) = (1-\alpha)\mathbf{\Sigma}_w \circ \mathbf{G}_2 + \alpha\mathbf{\Sigma}_b \circ \mathbf{G}_1 \quad \text{if} \quad \gamma_i = 2 \tag{4.39}$$

These calculations and simplifications lead the equation 4.29 to:

$$\mathbf{G}_1 = -(\mathbf{q} + \alpha\boldsymbol{\Sigma}_w \circ \mathbf{G}_1 + (1-\alpha)\boldsymbol{\Sigma}_b \circ \mathbf{G}_2)^{-1} \tag{4.40}$$
$$\mathbf{G}_2 = -(\mathbf{q} + \alpha\boldsymbol{\Sigma}_b \circ \mathbf{G}_1 + (1-\alpha)\boldsymbol{\Sigma}_w \circ \mathbf{G}_2)^{-1}. \tag{4.41}$$

The resolvent is then given by $\mathcal{G} = \alpha\,\mathbf{G}_1 + (1-\alpha)\mathbf{G}_2$ and through this, the spectral density can be obtained by using equation 4.13. G_1 and G_2 are quaternions that can be written in the general form:

$$\mathbf{G}_1 = r_1 + \beta_1\mathbf{j} \quad , \quad \mathbf{G}_2 = r_2 + \beta_2\mathbf{j} \tag{4.42}$$

where $r_1, r_2, \beta_1, \beta_2$ are generally complex numbers by definition.
The study of the spectral density, in terms of quaternions, demonstrates that the region where the spectral distribution is defined depends on the existence of a solution with real and positive values of β_1 and β_2. Following this analysis is possible to extrapolate the maximum real part of the eigenvalues of B. In the general case, the equations 4.40 and 4.41 can not be solved, but there are particular cases where this is allowed. The case of $\alpha = 1/2$ is studied in details in the next section and an explicit solution for the support of the spectrum of B is obtained.

4.6 An explicit solution

When the size of the subgroups is equal, an analytical solution can be obtain. In this particular case, the equations 4.40 and 4.41 correspond to a single equation where:

$$\mathbf{G}_1 = \mathbf{G_2} =: \mathbf{G} = r + \beta\mathbf{j} \tag{4.43}$$

with $\mathbf{G}$ solution of:

$$\mathbf{G} = -\Big(\mathbf{q} + \frac{\boldsymbol{\Sigma}_w + \boldsymbol{\Sigma}_b}{2} \circ \mathbf{G}\Big)^{-1}. \tag{4.44}$$

To simplify the notation, is suitable to introduce:

$$\tilde{\boldsymbol{\Sigma}} := \frac{\Sigma_w + \Sigma_b}{2} = S\tilde{\sigma}^2(\tilde{\rho} + \mathbf{j}) \tag{4.45}$$

where

$$\tilde{\sigma}^2 = \frac{\sigma_w^2 + \sigma_b^2}{2}, \quad \tilde{\rho} = \frac{\rho_w\sigma_w^2 + \rho_b\sigma_b^2}{\sigma_w^2 + \sigma_b^2}. \tag{4.46}$$

The equation 4.44 can now be rewritten as:

$$\mathbf{G}(-\mathbf{q} - \tilde{\boldsymbol{\Sigma}} \circ \mathbf{G}) = 1 \quad , \tag{4.47}$$

By setting $\epsilon = 0$ and using the equivalence:

$$\mathbf{q} = \lambda \quad , \text{and} \quad \mathbf{G} = r + \beta\mathbf{j}$$

the following equation can be obtain:

$$(r + \beta\mathbf{j})(-\lambda - S\tilde{\sigma}^2(\tilde{\rho}r + \beta\mathbf{j})) = 1 \tag{4.48}$$

This can be reduced to two equations by separating the factor multiplied by **j** from the other part:

$$r(-rS\tilde{\rho}\tilde{\sigma}^2 - \lambda) + S|\beta|^2\tilde{\sigma}^2 = 1 \tag{4.49}$$

and

$$\beta(-rS\tilde{\rho}\tilde{\sigma}^2 - \lambda - S\bar{r}\tilde{\sigma}^2) = 0. \tag{4.50}$$

The spectral density is then given by:

$$\rho(\lambda) = -\frac{1}{\pi}\mathrm{Re}\frac{\partial r}{\partial\bar{\lambda}}. \tag{4.51}$$

If $\beta = 0$ the equation 4.49 is reduced to:

$$r(-\lambda - rS\tilde{\sigma}^2\tilde{\rho}) = 1 \tag{4.52}$$

and by taking the derivative of both sides in respect to $\bar{\lambda}$, the equation is solved by $\partial r/\partial\bar{\lambda} = 0$. The solution $\beta = 0$ corresponds to values of λ outside the support of the spectral density. In the case of $\beta \neq 0$ by subtracting the complex conjugate of the eq. 4.50 with the eq. 4.50 itself , the result for r is:

$$r = \frac{1}{S\tilde{\sigma}^2}\Big(-\frac{x}{1+\tilde{\rho}} + \frac{iy}{1-\tilde{\rho}}\Big). \tag{4.53}$$

By substituting this solution inside eq.4.49, it can be found the solution for $|\beta|^2$:

$$|\beta|^2 = \frac{1}{S\tilde{\sigma}^2}\left(1 - \frac{x^2}{S(1+\tilde{\rho})^2\tilde{\sigma}^2} - \frac{y^2}{S(1-\tilde{\rho})^2\tilde{\sigma}^2}\right). \tag{4.54}$$

Since $|\beta|^2$ is a positive real value, a solution for $\beta \neq 0$ exists only if the right side of the previous equation is positive. Then, it is necessary to impose:

$$\frac{x^2}{S(1+\tilde{\rho})^2\tilde{\sigma}^2} + \frac{y^2}{S(1-\tilde{\rho})^2\tilde{\sigma}^2} < 1, \tag{4.55}$$

which represents the equation of an ellipse in the complex plane. Only in this region the spectral density is different from zero, and it can be obtained from eq. 4.51. The result is:

$$\rho(\lambda) = -\frac{1}{\pi}\mathrm{Re}\frac{\partial r}{\partial\bar{\lambda}} = \frac{1}{\pi S\tilde{\sigma}^2(1-\tilde{\rho}^2)}. \tag{4.56}$$

In the case of $\alpha = 1/2$, the spectral density is, therefore, uniform inside an ellipse with semi-axis:

$$r_x = \frac{\sqrt{S}}{2}\tilde{\sigma}(1+\tilde{\rho}) \quad , \quad r_y = \frac{\sqrt{S}}{2}\tilde{\sigma}(1-\tilde{\rho}). \tag{4.57}$$

Note that this would also be the limiting distribution for the eigenvalues of the unstructured matrix with -μ_w on the diagonal, and with the others entries sampled indipendently in pairs from the bivariate normal distribution with mean $(0,0)^T$, correlation equal to a weighted average of the correlations in B and variance equal to the arithmetic mean of the variances in B(4.46). These relations are a generalization of the case studied in the first section of Chapter 3 in which the variance has been choosed equal to $1/S$.

In order to make more clear the role of modularity in controlling the stability, it is convenient to express $\tilde{\sigma^2}$ and $\tilde{\rho}$ in terms of μ, σ^2, ρ, C and Q. In this case the relations can then be written as:

$$C_w = C(1+2Q) \quad \text{and} \quad C_b = C(1-2Q) \tag{4.58}$$

and by using the relations 4.8, the final result is:

$$\begin{aligned} \tilde{\rho} &= \frac{\rho\sigma^2 + (1-C-4CQ^2)\mu^2}{\sigma^2 + (1-C-4CQ^2)\mu^2} \\ \tilde{\sigma^2} &= C(\sigma^2 + (1-C-4CQ^2)\mu^2). \end{aligned} \tag{4.59}$$

The goal of this analysis is to understand the qualitative behavior of the numerical simulations and then to have an explanation on how the stability is affected by the values of the system parameters, in particular the modularity. In order to study the case $\alpha = 1/2$, it has been set $S = 100$, $C = 0.2$, $\sigma = 1$ and $\mu = 0$ (green), $\mu = -1$ (red) and $\mu = 1$ (blue) for three different values of ρ : -0.75, 0 and 0.75 . The parameter Q is varied in ten equally sized from -0.50 to 0.50. For each set of parameters, 50 block-structured matrices M and 50 unstructured matrices $\tilde{M}$, obtained in the case $Q = 0$ (considering an ensemble of Erdős-Rényi matrices), have been considered. Figure 4.2 shows the ratio $\Gamma = \mathrm{Re}(\lambda_{M,1})/\mathrm{Re}(\lambda_{\tilde{M},1})$ obtained by computing the average over the replicates. The implemented code is reported in Appendix D and can be used to obtain general results for every α.
When $\mu < 0$ there are no effects of modularity on stability; when $\mu \geq 0$ a bipartite structure is highly destabilizing, while a modular structure is moderately stabilizing. Both effects are more evident in the case of negative correlation.

From the equations in 4.59, it is clear that the radius of B is always lower or equal than the one that it would find by setting $Q = 0$. As a matter of fact, $\tilde{\sigma^2}$ is smaller than that the one without the term $-4CQ^2$ and $\tilde{\rho}$ is a strictly decreasing function of $4CQ^2$ when $\rho \leq 1$.
For $\mu = -1$ the stability changes according to the sign of Q and this means that to define it there are eigenvalues of different nature for $Q > 0$ and $Q < 0$ (as the bulk of B is independent by the sign of Q).
The two outlier eigenvalues for $\alpha = 1/2$ are:

$$\begin{aligned} \lambda_1 &= S\mu C \\ \lambda_2 &= 2S\mu CQ \end{aligned} \tag{4.60}$$

For $\mu < 0$ and $Q > 0$ it is valid $\lambda_2 > \lambda_1$. In the definition range of Q both values lie on the left of the bulk of B and, therefore, the stability is determined by the rightmost eigenvalues of the bulks (in the unstructured network there are only outlier eigenvalues which lie to the left of the bulk if $\mu < 0$). In this case the stability is justified. This stabilizing effect is stressed when ρ is negative because $\tilde{\rho}$ decreases faster at the increase of Q.
For $\mu < 0$ and $Q < 0$ the greatest outlier of B is positive and lies on the right of the bulk in the unstructured case. Therefore, the destabilizing effect in this case has been clarified. In the case of $\mu > 0$, if $Q > 0$ both λ_1 and λ_2 are positive and they lie on the right of the bulk of B. If $Q < 0$, λ_2 lies on the left the bulk and λ_1 on the right.
These considerations about the effect of the stability, obtained varying Q, tell that large effect of Q on stability are found when varying Q changes the type of eigenvalues determing

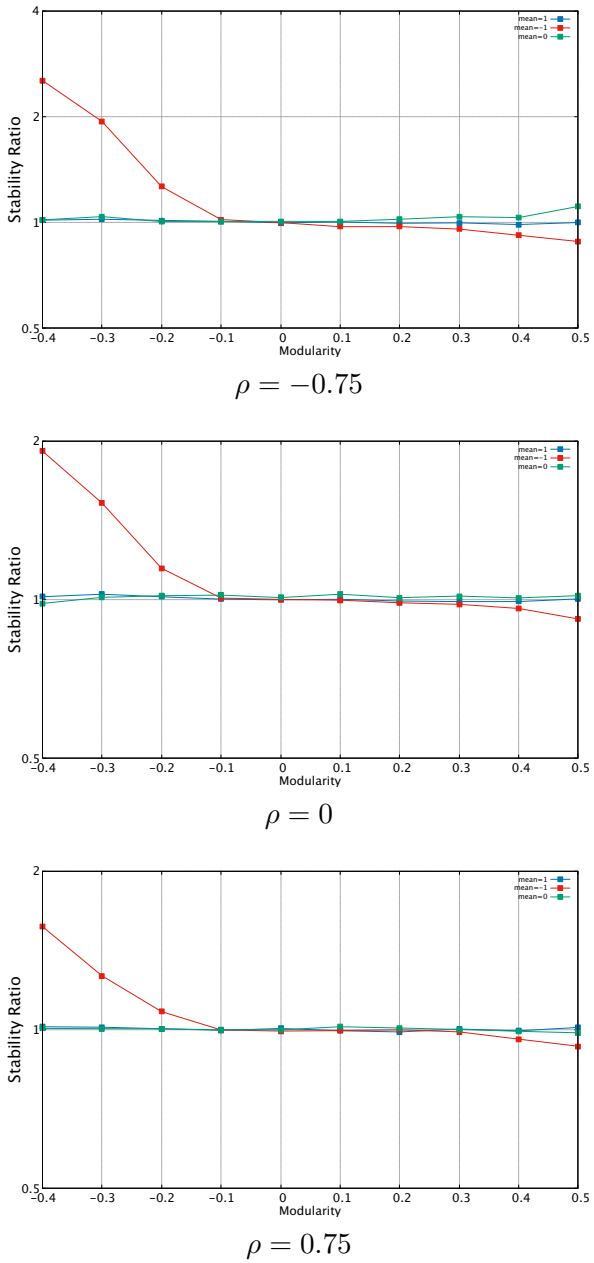

$\rho = -0.75$

$\rho = 0$

$\rho = 0.75$

Figure 4.2: Effects of modularity on stability for matrices of size S=100, C=0.2 and $\sigma^2 = 1$ averaged over 50 matrices at different values of ρ. In each figure $\mu = 0$ corresponds to green line, $\mu = -1$ to one red and $\mu = 1$ to one blue. The y-axis is the $\log_2$ of the ratio $\mathrm{Re}(\lambda_{M,1})/\mathrm{Re}(\lambda_{\tilde{M},1})$.

the stability (case $\mu < 0$). While when these eigenvalues does not depend on Q the effect will be moderate (case $\mu > 0$).

The case $\mu \approx 0$ is characterized by the absence of outliers in all cases and the stability is determined by the rightmost eigenvalues in the bulk. The parameters of spectrum of B are,

then, reduced to:

$$\tilde{\rho} = \rho, \quad \tilde{\sigma^2} = C\sigma^2 \tag{4.61}$$

Therefore, the dependence by Q is eliminated and it is expected that the structured network is slightly more stable than the unstructured, because $\tilde{\sigma^2} < \sigma^2$. These analytic considerations are in good agreement with the result in figure 4.2.
An more general numerical analysis which takes in consideration also others values of α can be found in [42]. In fig. 4.3 it is shown the results of this analysis. An analytic explanation

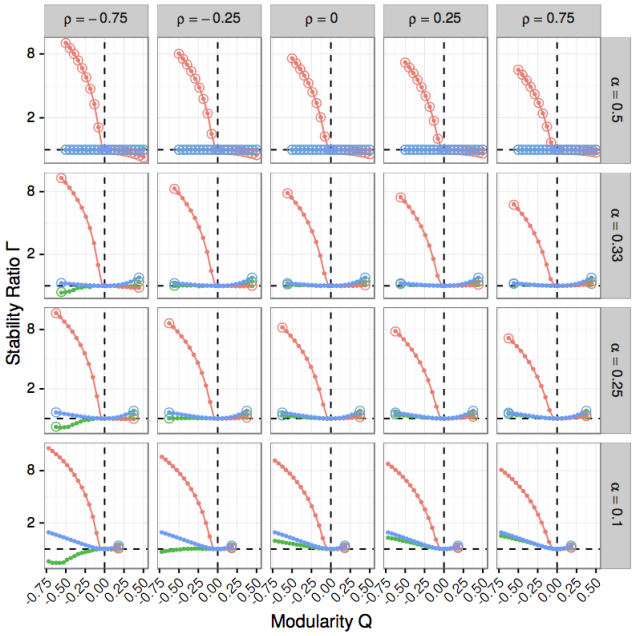

Figure 4.3: For each value of α and ρ, varying Q it has been obtained the ratio Γ. 20 equally spatially points between the minimum and maximum Q have been considered for each configuration. It has been set $C = 0.2$, $S = 1000$ and $\sigma^2 = 1$. The case $\mu = 0$ corresponds to the green line, $\mu = -1$ to the red one and $\mu = 1$ to the blue one. The dots represent numerical simulations, obtained by averaging over 50 replicates. The open circles are the corresponding analytic predictions.

for all the possible cases it is not yet accessible but the qualitative behavior of these system can be understood quite simply remembering the distribution of the eigenvalues of the block-structured matrices in the complex plane, explained in the Methods section.
The strong destabilizing effect of a bipartite structure when $\mu < 0$ is understood by the fact that the stability of the unstructured network is determined by the bulk of eigenvalues, while that of the block-structured network by the outlier to the right of the bulk.
When both $\mathrm{Re}(\lambda_{M,1})$ and $\mathrm{Re}(\lambda_{\tilde{M},1})$ are determined by the bulk (for example, modular case with $\mu < 0$ or any structure with $\mu \approx 0$), the either stabilizing or destabilizing effect is going to be moderate. Moderate effects are also observed when both $\mathrm{Re}(\lambda_{M,1})$ and $\mathrm{Re}(\lambda_{\tilde{M},1})$ are associated with an outlier lying to the right of the bulk ($\mu > 0$). Furthermore when both $\mathrm{Re}(\lambda_{M,1})$ and $\mathrm{Re}(\lambda_{\tilde{M},1})$ are determined by the same type (bulk, outlier) of eigenvalue, the

precise stabilizing or destabilizing effects depends non-linearly on the parameters $\alpha, C, Q, \mu, \sigma$ and ρ.
In the fig.4.3 it is evident this last consideration for $\mu \approx 0$ when the structure is bipartite and the correlation is negative the stability increases when decreasing α. But for positive correlations this stability effect disappears and the system can be also destabilizing. Also when the structure is modular and $\mu < 0$, the stabilizing effect presents for $\alpha = 1/2$ could change for small α or for a positive ρ. For all the other cases, the effect of a block structure ranges from neutral to highly destabilizing.

Chapter 5

Conclusion

In this thesis, it has been analytically and numerically developed a statistical approach for the study of the mean spectral density associated to sparse random matrices. This method is the cavity approach, introduced in this context of random matrices by Timothy Rogers [47].
The sparsity (property of the matrix with many entries equal to zero) complicates enormously the mathematical tools used to obtain an analytic form of the mean spectral density. The idea of this method is to move the problem from the search of the spectral density to a problem of interacting particles in statistical mechanics. The number of these particles is equal to the matrix size and they are located in nodes on a weighted graph. The interaction between the pair of particles (i, j) depends on the elements of the matrix (A_{ij}). An appropriate Gibbs-Boltzmann distribution has been introduced. Therefore, the randomness of the non-null entries of the matrix A represent the coupling strength between stochastic variables of the probability distribution, associated to each node. The problem is reduced to find the mean value of some object related to the marginal probability of these variables. When the matrix has an underlying *treelike* structure, the method leads to exact results.
It has been extended the May's work about the stability of a large ecological system, to more complex cases by introducing some basic tools of Random Matrix Theory (RMT).
The cavity approach to the spectral density of sparse symmetric random has been developed. Furthermore, the numerical results of the computational implementation has been compared with the results obtained by the direct diagonalization. The agreement is very good even for relatively small matrix like these considered. The method provides the statistical limit of the spectral density just considering an ensemble much more small than that necessary to direct diagonalization to obtain comparable results.
This approach has been extended to Non-Hermitian sparse random matrices, through more complex mathematical tools. Similarly to the Hermitian case, a simple closed set of equations is uncovered, whose solution characterizes the spectral density of a given matrix. Also in this case the numerical analysis has been very satisfactory.
For small matrices it is more convenient to use the direct diagonalization but when the matrix size is about 10^4 the current practical size limit for numerical diagonalization is close. Then an efficient implementation of belief propagation can handle matrices many orders of magnitude larger using the same hardware.
The cavity approach provides an analytic derivation of the spectral density for sparse random Hermitian and non-Hermitian matrices and this has allowed to develop a specific analysis by using the quaternionic parametrization of the cavity method. This study has provided valid

results which justify numerical simulations of how the modularity influences the stability in ecological communities.
The cavity method is applicable to more realistic systems, such as technological, social, biological and information networks. By varying the weights associated to the interactions, this method can analyze the spectral properties of different type of networks. In this way it is possible to extrapolate more information from the results, which can then be directly connected with the type of interactions and topological characteristics of the network.

Appendix A

The determinant of a symmetric matrix as Fresnel integral

To begin it is necessary to do a consideration about how to write the determinant of a general matrix as gaussian integrals: in the case of an $N \times N$ symmetric real positive definite matrix A is linear to obtain the following relation:

$$(\det A)^{-\frac{1}{2}} = (2\pi)^{-N/2} \int_{\mathbb{R}^N} \prod_{i=1}^{N} dx_i e^{-\frac{1}{2}\sum_{i,j=1}^{N} x_i A_{ij} x_j} \tag{A.1}$$

because this integration is convergent if all eigenvalues of A are strictly positive. In the case of a symmetric, but not real, matrix, its eigenvalues are not in general positive and real, hence it is not straightforward to demonstrate a similar formula in terms of Fresnel integrals. The problem is that the convergence is not guaranteed for complex eigenvalues. For this reason, it can be used a convenient integral of exponentials with an imaginary unit. The condition that $z = \lambda - i\epsilon$ has negative imaginary part is important for the convergence because in the considered integral is the real part of the exponential.
The goal is to resolve the following integral and demonstrate that for a matrix of form $(z\mathbf{1} - A)_N$, with A symmetric and real matrix, it is possible to write a similar expression to A.1.

$$I = \int \prod_i \frac{dx_i}{\sqrt{2\pi}} e^{-\frac{i}{2}\sum_{i,j} x_j((\lambda - i\epsilon)\mathbf{1} - A)_{ji} x_i} \tag{A.2}$$

By making an orthogonal transformation, the matrix $(z\mathbf{1} - A)_N$ is diagonalized and the result is:

$$I = \int \prod_k \frac{dy_k}{2\pi} e^{-\frac{1}{2}y_k^2(\epsilon + i(\lambda - \lambda_k))}$$

with $\vec{y} = S^T\vec{x}$, where S is the matrix of the transformation.
Considering the expression $\epsilon + i(\lambda - \lambda_k) = \rho_{\epsilon k} e^{i\theta_\epsilon(k)}$, it can be done a variables substitution in order to move the axis of integration from real to that of $z_k = y_k e^{i\theta_\epsilon(k)/2}$, and the integral is given by:

$$I = \prod_{z_k=1}^{N} e^{-i\theta_\epsilon(k)/2} \int_{\nwarrow\nearrow} \frac{dz_k}{\sqrt{2\pi}} e^{-\frac{1}{2}\rho_{\epsilon k} z_k^2}$$

The different directions of the arrows indicate that the line of integration depends on the sign of $\theta_\epsilon(k)/2$ and, therefore, of $(\lambda - \lambda_k)$. In both cases, the demonstration leads to the same result and the steps to get to the solution are similar.
So, it will be demostrated only the case $\theta_\epsilon(k)/2 < 0$.
The fig.A.1 shows the simple closed path of a simply-connected region where the Chauchy

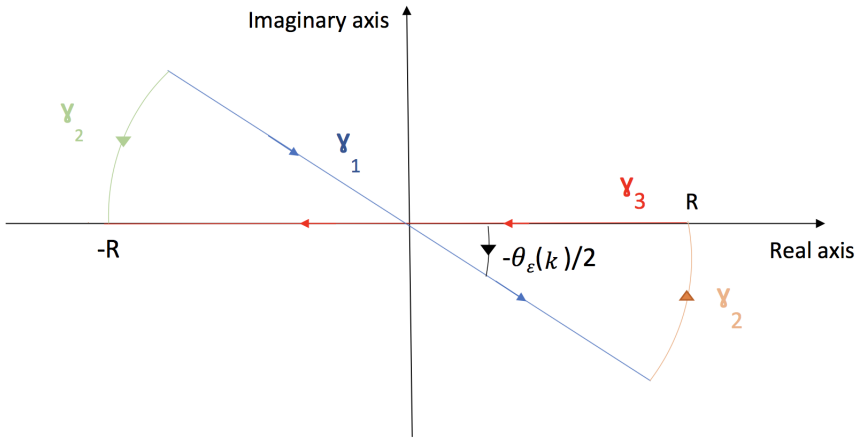

Figure A.1: The lines $\gamma_1, \gamma_2, \gamma_3$ and γ_4 compose the path along which it is performed the line integration.

theorem is applicable for the analytical function in I. To demostrate that the line integral on γ_2 and γ_4 are null, the parameterization $\gamma_2 : z = Re^{+i\phi_\epsilon(k)}$ with $\phi_\epsilon(k) \in [0; -\theta_\epsilon(k)/2]$ is used and the steps are the following:

$$I_2 = \int_{\gamma_2} e^{-\frac{1}{2}\rho_{\epsilon k} z_k^2}\, dz_k = -i \int_0^{-\theta_\epsilon(k)/2} Re^{i\phi_\epsilon(k)} e^{-\frac{1}{2}\rho_{\epsilon k} R^2 e^{2i\phi_\epsilon(k)}}\, d\phi_\epsilon(k)$$

$$\implies |I_2| \leq \int_0^{-\theta_\epsilon(k)/2} Re^{-\frac{1}{2}\rho_{\epsilon k} R^2 \cos(2\phi_\epsilon(k))}\, d\phi_\epsilon(k) \leq \int_0^{-\theta_\epsilon(k)/2} Re^{-\frac{1}{2}\rho_{\epsilon k} R^2 \cos(\theta_\epsilon(k))}\, d\phi_\epsilon(k)$$

$$= R(-\theta_\epsilon(k)/2) e^{-\frac{1}{2}\rho_{\epsilon k} R^2 \cos(\theta_\epsilon(k))} \qquad R \to \infty$$

$$= 0$$

The same is valid for the line γ_4 integration. Hence the line integral on γ_1 is minus the line integral on γ_3 and the axis of integration becomes the real one:

$$I = -\prod_{k=1}^{N} \int_{-R}^{+R} \frac{1}{\sqrt{2\pi}} e^{-i\theta_\epsilon(k)/2} e^{-\frac{1}{2}\rho_{\epsilon k} z_k^2} dz_k = {}_{R\to\infty}$$

$$= \prod_{k=1}^{N} e^{-i\theta_\epsilon(k)/2} \int_{-\infty}^{+\infty} \frac{1}{\sqrt{2\pi}} e^{-\frac{1}{2}\rho_{\epsilon k} z_k^2}\, dz_k = \prod_{k=1}^{N} e^{-i\theta_\epsilon(k)/2} \frac{1}{\sqrt{\rho_{\epsilon k}}}$$

$$= \prod_{k=1}^{N} e^{-i\theta_\epsilon(k)/2} \frac{e^{i\theta_\epsilon(k)/2}}{\sqrt{\rho_{\epsilon k} e^{i\theta_\epsilon(k)}}} = \prod_{k=1}^{N} \frac{1}{\sqrt{\epsilon + i(\lambda - \lambda_k)}} = \prod_{k=1}^{N} e^{-i\frac{\pi}{4}} \frac{1}{\sqrt{z - \lambda_k}} = e^{-i\frac{\pi N}{4}} \frac{1}{\sqrt{\det(z\mathbf{1} - A)}}$$

Therefore, the equation 2.7 has been demostrated.

Appendix B

Iterative equations for the cavity variances

The Gaussian cavity distributions is substituted in equation 2.19:

$$
\begin{aligned}
e^{-\frac{x_i^2}{2\Delta_i^{(j)}}} &= e^{\frac{-zx_i^2}{2}} \int d\boldsymbol{x}_{\partial i/\ j} \prod_{l\in\partial i/\ j} \frac{1}{\sqrt{2\pi\Delta_l^{(i)}}} \exp\left[x_i \sum_{l\in\partial i/\ j} A_{il}x_l - \frac{x_l^2}{2\Delta_l^{(i)}}\right] \\
&= e^{-\frac{zx_i^2}{2}} \prod_{l\in\partial i/\ j} \frac{1}{\sqrt{2\pi\Delta_l^{(i)}}} \left\{ \int dx_l \exp\left[x_i A_{il} x_l - \frac{x_l^2}{2\Delta_l^{(i)}}\right]\right\}
\end{aligned}
$$

by completing the square in the exponential, it is added and subtracted the term $\frac{-A_{il}^2 x_i^2 \Delta_l^{(i)}}{2}$:

$$
= e^{-\frac{zx_i^2}{2}} \prod_{l\in\partial i/\ j} \frac{1}{\sqrt{2\pi\Delta_l^{(i)}}} \left\{ e^{\frac{A_{il}^2 x_i^2 \Delta_l^{(i)}}{2}} \int dx_l \exp\left[-\left(\frac{x_l}{\sqrt{2\Delta_l^{(i)}}} - \sqrt{\frac{\Delta_l^{(i)}}{2}} A_{il}x_i\right)^2\right]\right\}.
$$

The variable substitution $x_l \longmapsto y_l = \frac{x_l}{\sqrt{2\Delta_l^{(i)}}} - \sqrt{\frac{\Delta_l^{(i)}}{2}} A_{il}x_i$ leads to the easy integrals:

$$
\begin{aligned}
&= e^{-\frac{zx_i^2}{2}} \prod_{l\in\partial i/\ j} \frac{1}{\sqrt{2\pi\Delta_l^{(i)}}} \left\{ e^{\frac{A_{il}^2 x_i^2 \Delta_l^{(i)}}{2}} \sqrt{2\Delta_l^{(i)}} \int dy_l e^{-y_l^2}\right\} \\
&= e^{-\frac{zx_i^2}{2}} \prod_{l\in\partial i/\ j} \frac{1}{\sqrt{2\pi\Delta_l^{(i)}}} \left\{ e^{\frac{A_{il}^2 x_i^2 \Delta_l^{(i)}}{2}} \sqrt{2\pi\Delta_l^{(i)}}\right\} \\
&= e^{-\frac{zx_i^2}{2}} \prod_{l\in\partial i/\ j} e^{\frac{A_{il}^2 x_i^2 \Delta_l^{(i)}}{2}}
\end{aligned}
$$

$$
\implies \quad \frac{1}{\Delta_i^{(j)}} = z - \sum_{l\in\partial i/\ j} A_{il}^2 \Delta_l^{(i)}(z) \quad \implies \quad \Delta_i^{(j)}(z) = \frac{1}{z - \sum_{l\in\partial i/\ j} A_{il}^2 \Delta_l^{(i)}(z)}
$$

Appendix C

Supplementary notes

C.1 Search of eigenvalues of A matrix

The entries of the matrix A can be written as:

$$A_{ij} = \mu_w(v_i v_j + w_i w_j) + \mu_b(v_i w_j + w_j v_i), \tag{C.1}$$

where $\vec{v}$ is a vector in the S-dimensional space with the first αS components equals to 1 and the $(1-\alpha)S$ remaining components equals to 0, while for the vector $\vec{w}$ the first αS components are equal to 0 and the others equals to 1.
By considering a vector ϕ orthogonal to the plane defined by the vectors $\vec{v}$ and $\vec{w}$, it is easy to verify that:

$$A\,\vec{\phi} = 0$$

then the matrix A has $S-2$ degenerate eigenvalues equal to 0 associated to the orthogonal complement subspace of the bidimensional space $\{\vec{v}, \vec{w}\}$. The search of the non-null eigenvalues occurs in this space by using the eigenvalues equation and by considering as a generic eigenvector $\psi = a\vec{v} + b\vec{w}$: (for semplicity it has been used the redefinitions : $\alpha S = n$ and $(1-\alpha)S = m$)

$$A\,\vec{\psi} = \mu_w\, a\, n\, \vec{v} + \mu_w\, b\, m\, \vec{w} + \mu_b\, b\, m\, \vec{v} + \mu_b\, b\, n\, \vec{w} = \lambda\, a\, \vec{v} + \lambda\, b\, \vec{w} \tag{C.2}$$

This equation is solved by the system:

$$\begin{cases} a(\mu_w\, n - \lambda) + \mu_b\, b\, m = 0 \\ b(\mu_w\, m - \lambda) + \mu_b\, a\, n = 0 \end{cases}$$

which admits solutions for a and b when:

$$\begin{vmatrix} \mu_w\, n - \lambda & \mu_b\, m \\ \mu_b\, n & \mu_w\, m - \lambda \end{vmatrix} = 0$$

Finally, the equation to be solved in λ is:

$$\lambda^2 - \mu_w\, \lambda\, S - \mu_b^2\, n\, m + \mu_w^2\, n\, m = 0 \tag{C.3}$$

which admits the solutions:

$$\lambda_{1-2} = \frac{S}{2}\Big(\mu_w \pm \sqrt{\mu_w^2 - 4\,\alpha(1-\alpha)\mu_w^2 + 4\alpha(1-\alpha)\mu_b^2}\Big). \tag{C.4}$$

C.2 Quaternions

The quaternions are a number system that extends the complex number. The quaternion units which represent basis elements are i,j and k satisfying the relation:

$$i^2 = j^2 = k^2 = ijk = -1. \tag{C.5}$$

A quaternion can be specified by the linear combination $q = \alpha + \beta i + \gamma j + \delta k$, where $\alpha, \beta, \gamma, \delta \in \mathbb{R}$ As $k = ij$ the generic quaternion may just as well be specified by a pair of complex numbers a and $b \in \mathbb{C}$ by $q = a + bj$. Operations on quaternions have a close relation to those of matrices, in fact, there is an isomorphism between the algebra of quaternions and a certain group of $2x2$ matrices. For a generic quaternion $q = a + bj$ can be introduced the matrix representation:

$$M(q) = \begin{pmatrix} a & ib \\ i\bar{b} & \bar{a} \end{pmatrix}$$

and this matrix can be written in terms of certain products of Pauli matrices:

$$M(q) = \begin{pmatrix} \alpha + i\beta & i(\gamma + i\delta) \\ i(\gamma - i\delta) & \alpha - i\beta \end{pmatrix} = \alpha I + \beta\sigma_x\sigma_y + \gamma\sigma_y\sigma_z + \delta\sigma_x\sigma_z.$$

Therefore, the algebra of quaternions is isomorphic to that generated by real linear combinations of the matrices $I, (\sigma_x\sigma_y), (\sigma_y\sigma_z)$ and $(\sigma_x\sigma_z)$.

C.3 Spectral density from the resolvent

The relation 4.13 is a general result which holds for any matrix A. It can written in a more clear form:

$$\rho(\lambda; A) = -\frac{1}{\pi}\frac{\partial}{\partial\bar{\lambda}} G(\lambda; A) \tag{C.6}$$

Proof. To prove the claim it can be introduced the generalised function:

$$D_\mu(\lambda) = -\frac{1}{\pi}\frac{\partial}{\partial\bar{\lambda}}(\mu - \lambda)^{-1}$$

and it is necessary to demonstrate that $D_\mu(\lambda)$ is the Dirac delta $\delta(\mu - \lambda)$. For this scope it suffices to show the following:

1.$D_\mu(\lambda) = 0$ for all $\lambda \neq \mu$

2. For any $a \in \mathbb{R}^+$, over the μ-centred square $S(a) = \{x + iy : x, y \in [\mu - a, \mu + a]\}$, it is verified:

$$\int_{S(a)} D_\mu(\lambda) d\lambda = 1$$

For point 1, let us take $\lambda = x + iy$ and $\mu = u + iv$. By assuming $\lambda \neq \mu$, the derivative can be easily calculated:

$$\begin{aligned}\frac{\partial}{\partial\bar{\lambda}}(\mu-\lambda)^{-1} &= \frac{1}{2}\Big(\frac{\partial}{\partial x}+i\frac{\partial}{\partial y}\Big)\frac{1}{(u-x)+i(v-y)}\\ &= \frac{1}{2((u-x)+i(v-y))^2}+i\Big(\frac{i}{2((u-x)+i(v-y))^2}\Big)=0.\end{aligned}$$

For point 2, it can be made the variables substitution $\tilde{x}=x-u$, $\tilde{y}=y-v$ and it is then possible to compute:

$$\begin{aligned}\int_{S(a)} D_\mu(\lambda)d\lambda &= -\frac{1}{2\pi}\int_{u-a}^{u+a}\int_{v-a}^{v+a}\Big(\frac{\partial}{\partial x}+i\frac{\partial}{\partial y}\Big)\frac{1}{(u-x)+i(v-y)}dxdy\\ &= \frac{1}{2\pi}\int_{-a}^{+a}\int_{-a}^{+a}\Big(\frac{\partial}{\partial\tilde{x}}+i\frac{\partial}{\partial\tilde{y}}\Big)\frac{1}{\tilde{x}+i\tilde{y}}d\tilde{x}d\tilde{y}\\ &= \frac{1}{2\pi}\int_{-a}^{a}\Big[\frac{1}{\tilde{x}+i\tilde{y}}\Big]_{\tilde{x}=-a}^{\tilde{x}=a}d\tilde{y}+i\frac{1}{2\pi}\int_{-a}^{a}\Big[\frac{1}{\tilde{x}+i\tilde{y}}\Big]_{\tilde{y}=-a}^{\tilde{y}=a}d\tilde{x}\\ &= \frac{1}{\pi}\int_{-a}^{a}\frac{2a}{a^2+\tilde{x}^2}d\tilde{x}\\ &= 1\end{aligned}$$

Appendix D

Python Codes

The Python codes implemented to obtain the numerical results inserted in this thesis are reported.

Code for the spectral density of symmetric random matrices

In this section is reported the code which implements the belief propagation algorithm for ensemble of Poissonian graphs with a bimodal and Gaussian distribution of nonzero edge weights. Additionally, it has been implemented the regularized function for the distributions of eigenvalues obtained by computational found numerically through code of a python library.

```
import numpy as np
import matplotlib.pyplot as plt
import scipy as sc
import sys
import random
import math
import pylab

S = int(sys.argv[1])
#S=size of the matrix
c = int(sys.argv[2])
#c=average connectance
E = int(sys.argv[3])
#number of matrices in the ensemble

#the idea of the implementation of the method is to consider one matrix of
    size S
#where each element(i,j) corresponds to cavity variance for the node pair(i,j)
    .

Delta_old = (np.zeros(S * S)).reshape(S, S) + 0j
Delta_new = (np.zeros(S * S)).reshape(S, S) + 0j
eigenvalues = []
def rhocavity(x):
    Delta_tot = []
    ensemble1 = []
    rho_ensemble = []
    #building of the ensemble of matrices
    while len(ensemble1) < E:
        """
```

```
        #poissonian ensemble with bimodal distribution
        A = np.zeros(S * S).reshape(S, S)
        for i in range(S):
            for j in range(S):
                if j < i:
                    if random.uniform(0, 1) <= c /S:
                        if random.uniform(0, 1) <= 0.5:
                            A[i, j] = 1
                        else:
                            A[i, j] = -1
                    else:
                        A[i, j] = 0
        for i in range(S):
            for j in range(S):
                A[i, j] = A[j, i]
        """"""
        # gaussian poissonian ensemble of symmetric matrices with mean=0 and
    variance=1/c
        A = np.zeros(S * S).reshape(S, S)
        for i in range(S):
            for j in range(S):
                if j < i:
                    if random.uniform(0, 1) <= c / S:
                            A[i, j] = random.normalvariate(0,np.sqrt(1./c))
        for i in range(S):
            for j in range(S):
                A[i, j] = A[j, i]
        vals, vecs = (np.linalg.eig(A))
        vals = vals.real
        eigenvalues.extend(vals)
        ensemble1.append(A)

    for e in range(E):
        Delta_old = (np.zeros((S * S),dtype=np.complex)).reshape(S, S)
        Delta_new = (np.zeros((S * S),dtype=np.complex)).reshape(S, S)

        # we construct a vector which has for elements vectors(one vector
        # for each row) which element are the positions of columns non null.

        v=[]
        for i in range(S):
             v_i=[]
             for j in range(S):
                 if ensemble1[e][i,j]!= 0:
                     v_i.append(j)
             v.append(v_i)

        epsilon = 0.005j
        errore_max = 0.1
        confronto = 10*errore_max*S*S
        ciclo = 0
        Delta_sum_init = (np.zeros((S * S),dtype=np.complex)).reshape(S, S)

        #ciclo while for the iteraction
        while confronto>errore_max:
            Delta_sum = np.copy(Delta_sum_init)
            for l in range(S):
                for j in range(S):
```

```
                    if j != l:
                      #we do the sum along one row only for the positions of the matrix different from zero
                        for k in range(len(v[l])):
                            if v[l][k] != j:
                                Delta_sum[l, j] = Delta_sum[l, j] + Delta_old[l, v[l][k]] * abs(ensemble1[e][l, v[l][k]]) ** 2
            for l in range(S):
                for j in range(S):
                    if j!= l:
                        Delta_new[l, j] = 1. / (-x - epsilon - Delta_sum[j, l])

            confronto = sum(sum(abs((Delta_new) - (Delta_old))))
            Delta_old = np.copy(Delta_new)

        Delta_s = 0.
        for i in range(S):
            Delta_i = (((-x - epsilon - sum(Delta_new[i, :] * abs(ensemble1[e][i, :]) ** 2)) ** -1).imag) / E
            Delta_s = Delta_s + Delta_i
        Delta_tot.append(Delta_s)
        Delta_finale = sum(Delta_tot)
    return 1. / (math.pi * S) * Delta_finale

#search of eigenvalues through direct diagonalization
eigenvalues1 = []

for i in range(100*E):
    """
    #poissonian ensemble with bimodal distribution
    A = np.zeros(S * S).reshape(S, S)
    for i in range(S):
            for j in range(S):
                if j < i:
                    if random.uniform(0, 1) <= c /S:
                        if random.uniform(0, 1) <= 0.5:
                            A[i, j] = 1
                        else:
                            A[i, j] = -1
                    else:
                        A[i, j] = 0
        for i in range(S):
            for j in range(S):
                A[i, j] = A[j, i]
        """
    # gaussian poissonian ensemble of symmetric matrices with mean=0 and variance=1/c
    A = np.zeros(S * S).reshape(S, S)
    for i in range(S):
        for j in range(S):
            if j < i:
                if random.uniform(0, 1) <= c / S:
                    A[i, j] = random.normalvariate(0,np.sqrt(1./c))
    for i in range(S):
        for j in range(S):
            A[i, j] = A[j, i]
    vals1, vecs = (np.linalg.eig(A))
```

```
    vals1 = vals1.real
    eigenvalues1.extend(vals1)


#define the regularized function for the distribution of eigenvalues
epsilon = 0.005
def rho_regolarizzata(x):

    rho = 0
    for j in range(100*E*S):
            rho_new=(epsilon/(epsilon**2+abs(x-eigenvalues1[j])**2))/(100*E)
            rho= rho + rho_new
    return rho/(math.pi*S)

#code to plot
X=range(-30,30)
t = []
t1= []
y = []
y1= []
for z in X:
    temp=z/10
    t.append(temp)
    t1.append(temp)
    y1.append(rhocavity(temp))
    y.append(rho_regolarizzata(temp))

fig = plt.figure()
pylab.plot(t1,y1)
pylab.plot(t,y)
plt.xlabel("$\lambda$",fontsize=10)
plt.ylabel("$\\rho(\lambda)$",fontsize=10)
plt.show()
```

Listing D.1: symmetric matrices

Code for the spectral density of non-Hermitian random matrices

In this section is reported the code which implements the set of recursive equations 3.53 and 3.58.

```
import numpy as np
import sympy
from sympy import *
from sympy import I
from sympy.physics.matrices import msigma
from numpy.linalg import inv
import scipy.sparse.linalg
import sys
import random
import cython
from scipy.sparse import csr_matrix
import math
import pylab
from IPython import get_ipython
```

```
get_ipython().magic('reset -sf')
import time
from mpl_toolkits.mplot3d import Axes3D
from numpy import exp,arange
from pylab import meshgrid,cm,imshow,contour,clabel,colorbar,axis,title,show
from matplotlib.ticker import LinearLocator, FormatStrFormatter

import matplotlib.pyplot as plt
from numba import jit, autojit
from joblib import Parallel, delayed
sigma_2 =np.array([[0,-1.j],[1.j,0]])
sigma_1 =np.array([[0,1],[1,0]])
S = int(sys.argv[1])
# S  matrices size
c = int(sys.argv[2])
# c  average connectivity
E = int(sys.argv[3])
start_time=time.time()
# E number of samples
M = np.array([[0, 0], [1.j, 0]])
r=1/np.sqrt(c)

PR=np.array([])
PI=np.array([])
ensemble1=[]
"""""
while len(ensemble1)<E:
    A = np.zeros(S * S).reshape(S, S)
    for k in range(S):
        for j in range(S):
            if k < j:
                if random.uniform(0, 1) <= c/S:
                    A[k, j] = random.normalvariate(0, sqrt(1./c))
                    A[j, k] = random.normalvariate(0, sqrt(1./c))
    vals, vecs = np.linalg.eig(A)
    PR = np.concatenate((PR, vals.real), axis=0)
    PI = np.concatenate((PI, vals.imag), axis=0)
    ensemble1.append(A)
"""""
#building of the ensemble
while len(ensemble1)<E:
    A = np.zeros(S * S).reshape(S, S)
    for k in range(S):
        for j in range(S):
            if j!=k:
                if random.uniform(0, 1) <= c/(S-1):
                    a = random.uniform(-r, r)
                    b = random.uniform(-r, r)
                    if a ** 2 + b ** 2 <= r ** 2:
                        A[k, j] = 1.
    ensemble1.append(A)



def nonherm2(x,y):
    Gamma_rho = 0
    Gamma_tot = []
    for e in range(E):
```

```
73          #initial condition for the iterations
74          k=0.07
75          C_old = np.empty((S, S), dtype=np.matrix)
76          Gamma_old = np.empty((S, S), dtype=np.matrix)
77          C_new = np.empty((S, S), dtype=np.matrix)
78          Gamma_new = np.empty((S, S), dtype=np.matrix)
79
80          #for each elements and each its neighbors, it is associated an array 2
    x2 which corresponds to the matrix C^{j}_i
81          for i in range(S):
82              for j in range(S):
83                  C_old[i, j] = np.array([[0., 0.], [0., 0.]], complex)
84                  C_new[i, j] = np.array([[0., 0.], [0., 0.]], complex)
85                  Gamma_old[i, j] = np.array([[0., 0.], [0., 0.]], complex)
86                  Gamma_new[i, j] = np.array([[0., 0.], [0., 0.]], complex)
87
88          A_h = np.zeros(S * S).reshape(S, S) + 0.j
89          A_s = np.zeros(S * S).reshape(S, S) + 0.j
90          for i in range(S):
91              for l in range(S):
92                  A_h[i, l] = (ensemble1[e][i, l] + ensemble1[e][l, i].conjugate
    ()) / 2.
93                  A_s[i, l] = 1.j * (ensemble1[e][l, i].conjugate() - ensemble1[
    e][i, l]) / 2.
94
95          A_h = np.asmatrix(A_h)
96          A_s = np.asmatrix(A_s)
97          A_sum = A_h + A_s
98          NZ_sum=[]
99          NZ_sum = A_sum.nonzero()
100
101
102         confr = 100
103         confr_ = 100
104         confr_prova=100
105         ciclo=0
106
107         #while confr > 0.001 or confr_ > 0.01 :
108         #cycle implemented to obtain the convergence of the set of recursive
    equations
109         for q in range(c):
110
111             F_sum = np.empty((S, S), dtype=np.matrix)
112             Gamma_sum = np.empty((S, S), dtype=np.matrix)
113             for i in range(S):
114                 for j in range(S):
115                     F_sum[i, j] = np.array([[0, 0], [0, 0]], complex)
116                     Gamma_sum[i, j] = np.array([[0, 0], [0, 0]], complex)
117             #build the matrix field F(C^{i}_{\partial i\j}) and field
    associated to the derivative partial of the cavity covariance matrices
118             confr1 = []
119             confr2 = []
120             for i in range(S):
121                 for j in range(S):
122                     for l in range(len(NZ_sum[1])):
123                         if NZ_sum[0][l] == i:
124                             if NZ_sum[1][l] != j:
```

```
125                                 F_sum[i, j] = np.add(F_sum[i, j], (np.subtract
    (np.multiply(A_h[i, NZ_sum[1][l]], sigma_1),np.multiply(A_s[i, NZ_sum[1][l
    ]], sigma_2))).dot(C_old[i, NZ_sum[1][l]]).dot(np.subtract(np.multiply(A_h[
    NZ_sum[1][l], i], sigma_1),np.multiply(A_s[NZ_sum[1][l], i], sigma_2))))
126                                 Gamma_sum[i, j] = np.add(Gamma_sum[i, j],(np.
    subtract(np.multiply(A_h[i, NZ_sum[1][l]],sigma_1),np.multiply(A_s[i,
    NZ_sum[1][l]], sigma_2))).dot(Gamma_old[i, NZ_sum[1][l]]).dot(np.subtract(
    np.multiply(A_h[NZ_sum[1][l], i], sigma_1),np.multiply(A_s[NZ_sum[1][l], i
    ], sigma_2))))
127             #build C^{i}_{\partial i \j}
128             for i in range(S):
129                 for j in range(S):
130                     if j != i:
131                         C_new[i, j] = np.linalg.inv(np.add(F_sum[j, i], np.add
    (np.multiply(k, np.identity(2)),np.multiply(1.j, np.subtract(np.multiply(x,
     sigma_1),np.multiply(y, sigma_2))))))
132                         Gamma_new[i, j] = np.multiply(-1, C_new[i, j].dot(np.
    add(M, Gamma_sum[j, i])).dot(C_new[i,j]))
133                     confr1.append((abs(np.subtract(C_new[i,j], C_old[i,j]))).
    max())
134                     confr2.append((abs(np.subtract(Gamma_new[i,j], Gamma_old[i
    ,j]))).max())
135
136             confr = max(confr1)
137             confr_ = max(confr2)
138             C_old = np.copy(C_new)
139             Gamma_old = np.copy(Gamma_new)
140
141
142         F_end = []
143         C_end = []
144         Gamma_end = []
145         F_gamma = []
146
147         # build the "true" covariance matrix and its partial derivatives
148
149         for i in range(S):
150             F_end.append(np.array([[0, 0], [0, 0]], complex))
151             F_gamma.append(np.array([[0, 0], [0, 0]], complex))
152             C_end.append(np.array([[0, 0], [0, 0]], complex))
153             Gamma_end.append(np.array([[0, 0], [0, 0]], complex))
154             for l in range(len(NZ_sum[1])):
155                 if NZ_sum[0][l] == i:
156                     F_end[i] = np.add(F_end[i],np.subtract(np.multiply(A_h[i,
    NZ_sum[1][l]],sigma_1), np.multiply(A_s[i,NZ_sum[1][l]], sigma_2)).dot(
    C_new[i,NZ_sum[1][l]]).dot(np.subtract(np.multiply(A_h[NZ_sum[1][l], i],
    sigma_1),np.multiply(A_s[NZ_sum[1][l], i], sigma_2))))
157                     F_gamma[i] = np.add(F_gamma[i], np.subtract(np.multiply(
    A_h[i,NZ_sum[1][l]],sigma_1),np.multiply(A_s[i, NZ_sum[1][l]],sigma_2)).dot
    (Gamma_new[i, NZ_sum[1][l]]).dot(np.subtract(np.multiply(A_h[NZ_sum[1][l],
    i], sigma_1), np.multiply(A_s[NZ_sum[1][l], i], sigma_2))))
158             C_end[i] = np.linalg.inv(np.add(F_end[i], np.add(np.multiply(k, np
    .identity(2)), np.multiply(1.j,np.subtract(np.multiply(x,sigma_1),np.
    multiply(y,sigma_2))))))
159             Gamma_end[i] = np.multiply(-1.j, C_end[i].dot(np.add(M, F_gamma[i
    ])).dot(C_end[i]))[1][0]
160
161         Gamma_mean = np.mean(Gamma_end)/E
```

```
            Gamma_rho+=Gamma_mean
    return (1./math.pi)*Gamma_rho.real

# Make data.
X = np.arange(-1., 1., 0.1)
Y = np.arange(-1.,1., 0.1)

f=open('20circle1.txt','w')
Z=[]
Z = Parallel(n_jobs= -1, backend="multiprocessing")\
(delayed(nonherm2)(i,j) for i in X for j in Y)
for i in range(len(Z)):
    f.write(str(Z[i])+'\n')
f.close()
```

Listing D.2: Non-hermitian matrices

Stability

In this section is reported the code used to find the Γ values of the stability for different values of the modularity Q.

```
import numpy as np
import matplotlib.pyplot as plt
import scipy as sc
import sys
import random
import math as mt

S = int(sys.argv[1])
C = float(sys.argv[2])
ro = float(sys.argv[3])
mu = float(sys.argv[4])
a = float(sys.argv[5])
E = int(sys.argv[6])

# 1 Step: buind the matrix with a fixed modularity

# define the interval of Q
Q_MIN = (float(max(C - 2 * a * (1 - a), 0)) - C * (a ** 2 + (1 - a) ** 2)) / C
Q_MAX = (float(min(C, a ** 2 + (1 - a) ** 2)) - C * (a ** 2 + (1 - a) ** 2)) /
    C
Q_TOT = np.linspace(Q_MIN, Q_MAX, 20)

Q =0.50

#fill the matrix with fixed connectance associated to diagonal blocks(C_W) and
    those not diagonal (C_b) according to a probability

C_W = C * (1 + Q / (a ** 2 + (1 - a) ** 2))
C_B = C * (1 - Q / (2 * a * (1 - a)))

ensemble=[]
while len(ensemble)< E:
    A = np.zeros(S * S).reshape(S, S)
    riga_W = []
    colonna_W = []
```

```
    riga_B = []
    colonna_B = []
    for i in range(0, S):
        if i < S * a:
            for j in range(0, S):
                if j < i:
                    riga_W.append(i)
                    colonna_W.append(j)
        if i >= S * a:
            for j in range(0, S):
                if S * a <= j < i:
                    riga_W.append(i)
                    colonna_W.append(j)
                if j <= S * a:
                    riga_B.append(i)
                    colonna_B.append(j)

    coppie_W = [[R, C] for R, C in zip(riga_W, colonna_W)]
    coppie_B = [[R, C] for R, C in zip(riga_B, colonna_B)]

    # coppie= the total interaction in the matrix
    # build two array of size Link_W e Link_B (number of total links in the
    diagonal blocks and these out diagonal)
    N_W = (S * a * (S * a - 1) + S * (1 - a) * (S - S * a - 1)) / 2
    N_B = S ** 2 * a * (1 - a)
    Link_W = []
    while len(Link_W) < C_W * N_W:
        r = random.uniform(0, 1) * N_W
        t = int(r)
        if t not in Link_W:
            Link_W.append(t)
    mean = (mu, mu)
    cov = [[1, ro], [ro, 1]]

    for k in Link_W:
        RO = np.random.multivariate_normal(mean, cov, 1)
        A[coppie_W[k][0], coppie_W[k][1]] = RO[0][0]
        A[coppie_W[k][1], coppie_W[k][0]] = RO[0][1]

    #the blocks of the matrix have been filled according C_W and the
    correlation
    Link_B = []
    while len(Link_B) < C_B * N_B:
        r = random.uniform(0, 1) * N_B
        t = int(r)
        if t not in Link_B:
            Link_B.append(t)

    mean = (mu, mu)
    cov = [[1, ro], [ro, 1]]

    for k in Link_B:
        RO = np.random.multivariate_normal(mean, cov, 1)
        A[coppie_B[k][0], coppie_B[k][1]] = RO[0][0]
        A[coppie_B[k][1], coppie_B[k][0]] = RO[0][1]

    ensemble.append(A)
vals,vecs = np.linalg.eig(ensemble)
```

```
Lamba=[]
for K in (ensemble):
    vals,vecs = np.linalg.eig(K)
    Lamba.append(max(vals).real)
#Lamba is the vector of maximum real part of eigenvalues for each matrix of
    the ensemble with a certain modularity
#building the ensemble of Erdos-Renyi  matrix
ensembleER = []
while len(ensembleER) < E:
    B=np.zeros(S*S).reshape(S,S)
    riga = []
    colonna = []
    for i in range(0, S):
        for j in range(0, S):
            if j < i:
                colonna.append(j)
                riga.append(i)
    coppie = [[R, C] for R, C in zip(riga,colonna)]

    L=[]
    while len(L) < (np.fabs(C) * S*(S-1)/2) :
         r = random.uniform(0, 1) *(S*(S-1)/2)
         t = int(r)
         if t not in L:
            L.append(t)


    for k in L:
        RO = np.random.multivariate_normal(mean, cov, 1)
        B[coppie[k][0], coppie[k][1]] = RO[0][0]
        B[coppie[k][1], coppie[k][0]] = RO[0][1]


    for i in range(S):
     B[i,i]=0
    ensembleER.append(B)

LambaER=[]
for K in (ensembleER):
    vals,vecs = np.linalg.eig(K)
    LambaER.append(max(vals).real)
#build an array of Gamma values and computed the mean

RATIO=[]
for i in range(E):
    R=Lamba[i]/LambaER[i]
    RATIO.append(R)

GAMMA = sum(RATIO)/len(RATIO)

print(GAMMA)
```

Listing D.3: Stability and Modularity

Bibliography

[1] ML Mehta. *Randon matrices and the statistical theory of energy level*. Academic Press, 1967.

[2] HJ Sommers, A Crisanti, Haim Sompolinsky, and Y Stein. Spectrum of large random asymmetric matrices. *Physical review letters*, 60(19):1895, 1988.

[3] Robert M May. Will a large complex system be stable? *Nature*, 238(5364):413–414, 1972.

[4] Robert McCredie May. *Stability and complexity in model ecosystems*, volume 6. Princeton university press, 2001.

[5] Richard Levins. *Evolution in changing environments: some theoretical explorations*. Number 2. Princeton University Press, 1968.

[6] Zhidong Bai and Jack W Silverstein. *Spectral analysis of large dimensional random matrices*, volume 20. Springer, 2010.

[7] Greg W Anderson, Alice Guionnet, and Ofer Zeitouni. *An introduction to random matrices*, volume 118. Cambridge university press, 2010.

[8] Eugene P Wigner. On the distribution of the roots of certain symmetric matrices. *Annals of Mathematics*, pages 325–327, 1958.

[9] Terence Tao, Van Vu, Manjunath Krishnapur, et al. Random matrices: Universality of esds and the circular law. *The Annals of Probability*, 38(5):2023–2065, 2010.

[10] Stefano Allesina and Si Tang. The stability–complexity relationship at age 40: a random matrix perspective. *Population Ecology*, 57(1):63–75, 2015.

[11] Si Tang, Samraat Pawar, and Stefano Allesina. Correlation between interaction strengths drives stability in large ecological networks. *Ecology letters*, 17(9):1094–1100, 2014.

[12] Tim Rogers, Isaac Pérez Castillo, Reimer Kühn, and Koujin Takeda. Cavity approach to the spectral density of sparse symmetric random matrices. *Physical Review E*, 78(3):031116, 2008.

[13] Tim Rogers and Isaac Pérez Castillo. Cavity approach to the spectral density of non-hermitian sparse matrices. *Physical Review E*, 79(1):012101, 2009.

[14] TA Brody, J Flores, J Bruce French, PA Mello, A Pandey, and Samuel SM Wong. Random-matrix physics: spectrum and strength fluctuations. *Reviews of Modern Physics*, 53(3):385, 1981.

[15] S F Edwards and R C Jones. The eigenvalue spectrum of a large symmetric random matrix. *Journal of Physics A: Mathematical and General*, 9(10):1595–1603, 1976.

[16] G Biroli and R Monasson. A single defect approximation for localized states on random lattices. *Journal of Physics A: Mathematical and General*, 32(24):L255, 1999.

[17] Taro Nagao and Toshiyuki Tanaka. Spectral density of sparse sample covariance matrices. *Journal of Physics A: Mathematical and Theoretical*, 40(19):4973, 2007.

[18] Michel Bauer and Olivier Golinelli. Random incidence matrices: moments of the spectral density. *Journal of Statistical Physics*, 103(1):301–337, 2001.

[19] O Golinelli. Statistics of delta peaks in the spectral density of large random trees. *arXiv preprint cond-mat/0301437*, 2003.

[20] Reimer Kühn. Spectra of sparse random matrices. *Journal of Physics A: Mathematical and Theoretical*, 41(29):295002, 2008.

[21] Yan V Fyodorov and AD Mirlin. On the density of states of sparse random matrices. *Journal of Physics A: Mathematical and General*, 24(9):2219, 1991.

[22] GJ Rodgers and Cyrano De Dominicis. Density of states of sparse random matrices. *Journal of Physics A: Mathematical and General*, 23(9):1567, 1990.

[23] Marc Mézard and Giorgio Parisi. The bethe lattice spin glass revisited. *The European Physical Journal B-Condensed Matter and Complex Systems*, 20(2):217–233, 2001.

[24] GJ Rodgers and AJ Bray. Density of states of a sparse random matrix. *Physical Review B*, 37(7):3557, 1988.

[25] Guilhem Semerjian and Leticia F Cugliandolo. Sparse random matrices: the eigenvalue spectrum revisited. *Journal of Physics A: Mathematical and General*, 35(23):4837, 2002.

[26] H. J. Sommers, A. Crisanti, H. Sompolinsky, and Y. Stein. Spectrum of large random asymmetric matrices. *Physical Review Letters*, 60(19):1895–1898, 1988.

[27] Joshua Feinberg and Anthony Zee. Non-hermitian random matrix theory: Method of hermitian reduction. *Nuclear Physics B*, 504(3):579–608, 1997.

[28] Joshua Feinberg, R Scalettar, and A Zee. "single ring theorem" and the disk-annulus phase transition. *Journal of Mathematical Physics*, 42(12):5718–5740, 2001.

[29] Romuald A Janik, Maciej A Nowak, Gabor Papp, Jochen Wambach, and Ismail Zahed. Non-hermitian random matrix models: Free random variable approach. *Physical Review E*, 55(4):4100, 1997.

[30] John R Silvester. Determinants of block matrices. *The Mathematical Gazette*, 84(501):460–467, 2000.

[31] Boris Khoruzhenko. Non-hermitian random matrices, 2001.

[32] Jean Zinn-Justin. Quantum field theory and critical phenomena. 2002.

[33] Marcel Salathé and James H. Jones. Dynamics and control of diseases in networks with community structure. *PLoS Computational Biology*, 6(4), 2010.

[34] Johnatan Aljadeff, Merav Stern, and Tatyana Sharpee. Transition to chaos in random networks with cell-type-specific connectivity. *Physical Review Letters*, 114(8), 2015.

[35] Evan A. Variano, Jonathan H. McCoy, and Hod Lipson. Networks, dynamics, and modularity. *Physical Review Letters*, 92(18):188701–1, 2004.

[36] Jacopo Grilli, Tim Rogers, and Stefano Allesina. Modularity and stability in ecological communities. *Nature Communications*, 7:12031, 2016.

[37] Stefano Allesina and Si Tang. Stability criteria for complex ecosystems-supp mat. *Nature*, 2012.

[38] R M May. Will a large complex system be stable? *Nature*, 238:413–414, 1972.

[39] Mark EJ Newman and Michelle Girvan. Finding and evaluating community structure in networks. *Physical review E*, 69(2):026113, 2004.

[40] Mark EJ Newman. Modularity and community structure in networks. *Proceedings of the national academy of sciences*, 103(23):8577–8582, 2006.

[41] Paul Erdos and Alfréd Rényi. On the evolution of random graphs. *Publ. Math. Inst. Hung. Acad. Sci*, 5(1):17–60, 1960.

[42] Jacopo Grilli, Tim Rogers, and Stefano Allesina. Modularity and stability in ecological communities. *Nature communications*, 7, 2016.

[43] Andrew R Solow, Christopher Costello, and Andrew Beet. On an early result on stability and complexity. *The American Naturalist*, 154(5):587–588, 1999.

[44] Hoi H Nguyen and Sean O'Rourke. The elliptic law. *International Mathematics Research Notices*, 2015(17):7620–7689, 2015.

[45] Stefano Allesina, Jacopo Grilli, György Barabás, Si Tang, Johnatan Aljadeff, and Amos Maritan. Predicting the stability of large structured food webs. *Nature communications*, 6, 2015.

[46] Sean O'Rourke, David Renfrew, et al. Low rank perturbations of large elliptic random matrices. *Electron. J. Probab*, 19(43):1–65, 2014.

[47] Timothy Rogers. *New results on the spectral density of random matrices.* PhD thesis, King's College London, 2010.

[48] E Brezin. *Applications of Random Matrices in Physics.* 2006.

[49] Sergey N Dorogovtsev, Alexander V Goltsev, José FF Mendes, and Alexander N Samukhin. Spectra of complex networks. *Physical Review E*, 68(4):046109, 2003.

[50] Mark Newman. *Networks: an introduction.* Oxford university press, 2010.